Ministry of Science and Higher Education of the Republic of Kazakhstan
Al-Farabi Kazakh National University

UDC 621.182.243 (043)
Manuscript

MAGZHAN ORYNBASAR

Energy and ecological efficiency of plasma-coal burners: numerical simulation and experiment

8D07106 – Thermal Power Engineering

Dissertation submitted to qualify for
the degree of Doctor of Philosophy (PhD)

Scientific consultant:
Doctor of Technical Sciences,
Professor Messerle V.E.,
Almaty, Kazakhstan

Foreign scientific consultant:
Senior Researcher,
PhD Slavinskaya N.A.,
Munich, Germany

The Republic of Kazakhstan
Almaty, 2025

CONTENT

DESIGNATIONS AND ABBREVIATIONS 3
INTRODUCTION 4
1 EXISTING TECHNOLOGIES FOR BURNING AND GASIFICATION OF THERMAL COALS 10
1.1 The problem of the efficiency of the use of thermal coals at thermal power plants 10
1.2 Existing technologies of ignition of thermal coals at thermal power plants 20
1.3 Mathematical modeling of plasma ignition of thermal coals 31
1.4 Statement of the problem of numerical and experimental investigation of a plasma-coal burner 34
2 THERMODYNAMIC MODELING OF PLASMA IGNITION OF THERMAL COALS 49
2.1 Description of the universal thermodynamic calculation software TERRA 49
2.2 Methods for determining the initial composition of the thermodynamic system, specific energy consumption for the plasma ignition process, and the degree of gasification of thermal coals 52
2.3 Results of calculations of plasma ignition of thermal coals 59
3 KINETIC MODELING OF THE PROCESSES OF HEATING AND IGNITION OF THERMAL COALS IN A PLASMA-COAL BURNER 65
3.1 Description of the mathematical model and the PlasmaKinTherm software for kinetic calculations of heating and ignition of thermal coals in a plasma-coal burner 65
3.2 Results of kinetic calculations of plasma heating and ignition of thermal coals in a plasma-coal burner according to the PlasmaKinTherm software 72
3.3 Results of experimental studies of plasma ignition of thermal coal in a plasma-coal burner 80
3.4 Comparison of the results of calculations using TERRA and PlasmaKinTherm software packages with the results of an experimental study of plasma ignition of thermal coals 84
CONCLUSION 87
REFERENCES 89
APPENDIX A – An example of a listing of thermodynamic calculations of plasma ignition of thermal coal using the TERRA software 102
APPENDIX B – An example of a listing of kinetic calculations of heating and plasma ignition of thermal coal using the PlasmaKinTherm software 105
APPENDIX C – Act on the use of work results 108

DESIGNATIONS AND ABBREVIATIONS

G	Consumption, kg/s
I_i	Enthalpy, kJ/kg
Q_{sp}	Specific energy consumption, kW·h/kg
P_{arc}	Electrical arc energy, kW
P	Pressure, Pa
S_i	Entropy, kJ/kg
T	Temperature, K
U_i	Internal energy, kJ/kg
V	Specific volume, m^3/kg
X_c	Gasification degree, %
P	Density, kg/m^3
W^w	Moisture content per working mass
A^d	Ash content per dry mass
V^{daf}	Volatile matter per combustible mass
C_i	Concentration of products
T_{HRDF}	Temperature of high reactive dual-component fuel
DC	Direct current
PCB	Plasma-coal burner
TPP	Thermal power plant
HRDF	High reactive dual-component fuel
PICS	Plasma ignition and combustion stabilization
ETCPF	Electrothermochemical fuel preparation
NMR	Nuclear magnetic resonance
EU	European union
CIS	Commonwealth of Independent States
USSR	Union of Soviet Socialist Republics
IEA	International Energy Agency

INTRODUCTION

General characteristics of the work

The dissertation is devoted to the study and optimization of a plasma-coal burner (PCB) for ignition and combustion stabilization of low-grade coal. For numerical studies, software packages for thermodynamic and kinetic calculations were used: TERRA and PlasmaKinTerm, respectively. Experimental studies were carried out on a plasma-coal burner and the results obtained were compared with the results of numerical studies.

Relevance of the research work

At present, pulverized coal thermal power plants in Kazakhstan and Commonwealth of Independent States (CIS) nations predominantly utilize low-grade, high-ash coal, which is primarily obtained through open-pit mining methods. Such coals have a high ash content and a low yield of volatile substances. The direct combustion of these low-grade fuels in conventional firing systems poses considerable challenges, including poor ignition and incomplete burnout, as well as elevated emissions of harmful particulates and gases such as ash, nitrogen oxides (NO_x), and sulfur oxides (SO_x) into the atmosphere.

There are various traditional methods for improving the ignition and combustion stabilization of low-grade thermal coals in thermal power engineering. One of the widely used technologies for many thermal power plants in the world is fuel oil kindling of boilers and combustion stabilization of a pulverized coal flare, which is ineffective from an environmental, energy and economic point of view. This technology requires substantial amounts of scarce fuel oil (approximately 25 million tons annually across the CIS) and is associated with the release of environmentally hazardous gases. When fuel oil is burned, harmful gases are released - nitrogen and sulfur oxides, the use of which is restricted by the world community. Existing technologies for heating boilers and stabilizing the combustion of a pulverized coal torch worsen the energy and environmental safety of countries [1].

Coal is an attractive option for energy producers because it is relatively cheap and widely available. In addition to being a major energy resource, coal plays a significant role in multiple industrial sectors. It is utilized in metallurgy, the production of phosphate-based fertilizers, and the manufacturing of cement. Moreover, byproducts derived from coal contribute to the creation of various advanced materials, including activated carbon for filtration systems, carbon fiber for aerospace and automotive applications, metallic silicon used in lubricants, and rare earth elements extracted through chemical processing. These examples highlight coal's continued relevance, as it remains a fundamental component of the global energy mix and cannot be entirely phased out as a fuel source. Addressing today’s global challenges requires a multifaceted approach that combines various energy sources and technological innovations. Despite shifts toward alternative energy, coal remains a vital part of the global energy mix (owing not only to its widespread availability, but also to its essential role in supporting numerous strategic

industrial domains). Furthermore, coal contributes to the development and stabilization of infrastructure essential for the deployment and reliable operation of renewable energy systems. Therefore, research should be focused on finding new technological advances in the efficient use of coal.

A promising technology in the field of thermal power engineering is plasma ignition and combustion stabilization of pulverized coal using PCB. The PCB eliminates the need for additional highly reactive fuels (such as natural gas or fuel oil) during boiler startup and for maintaining stable ignition and combustion of pulverized coal. This technology is based on the concept of electrothermochemical fuel preparation for combustion (ETCPF), which involves the use of an electric arc plasma to heat the air–coal mixture to temperatures that trigger the release of volatile compounds and partially gasify the remaining coke. Through this process, the PCB transforms the original solid coal into a highly reactive, dual-component fuel (HRDF), consisting of combustible gases and solid carbon residue. Upon exiting the PCB, the HRDF undergoes rapid ignition due to its effective mixing with air in the furnace chamber.

A substantial body of research on plasma-assisted ignition and stabilization of pulverized coal combustion has been published globally. Notably, the most extensive implementation of this technology is observed in China, where approximately 45% of coal-fired boilers are equipped with PCBs. Experimental investigations into the ignition and combustion behavior of low-grade coal with ash content as high as 45% have demonstrated that such high-ash fuels can be effectively ignited and sustained using PCB technology [2].

Connection of the thesis topic with the plan of scientific projects

The dissertation work was completed in accordance with the approved research plan of the Ministry of Science and Higher Education of the Republic of Kazakhstan, as well as within the framework of grant funding for scientific research on the topics: «Obtaining energy gas and neutral inorganic material by plasma gasification of carbon-containing waste, including polyethylene terephthalate» (AP19674754, 2023-2025); «Development and testing of technologies for new functional materials using plasma-chemical, mechanochemical and self-propagating high-temperature synthesis processes» (BR18574084, 2023-2025); «Ecological and energy efficiency of plasma technology: numerical modeling and experiment» (AP22687016, 2024-2026).

The aim of the dissertation is to assess the environmental and energy efficiency of using a plasma-coal burner at pulverized coal thermal power plants.
To achieve these goals, it was necessary to solve the following **tasks:**

1 To perform thermodynamic and kinetic modeling of the products formed during the electrothermochemical preparation of low-rank, high-ash fuel for combustion, using the TERRA and PlasmaKinTherm software packages, in order to obtain a highly reactive dual-component fuel at the outlet of the plasma-coal burner;

2 To conduct experimental studies of plasma ignition and combustion stabilization (PICS) processes within the burner volume;

3 To determine the optimal parameters ensuring the efficient progress of plasma ignition and partial gasification processes of pulverized coal fuel within the volume of the plasma-coal burner.

The object of the study is plasma-coal burners.

The subject of the research is a process of electrothermochemical preparation for combustion of Ekibastuz coal in a plasma-coal burner.

Research methods

Numerical analyses were performed using the TERRA and PlasmaKinTerm software packages, which are designed for thermodynamic and kinetic calculations, respectively. To analyze the results, experimental studies were conducted using a plasma-coal burner and compared with the numerical results.

The scientific novelty of this research is reflected in the following original findings:

1 Numerical simulation was performed for the first time, confirming the possibility of producing highly reactive dual-component fuel from high-ash, low-grade energy coal using a plasma-coal burner;

2 Experimental data were obtained for the first time, confirming the formation of synthesis gas ($CO + H_2$) with a total concentration of 37.1% during the plasma ignition and partial gasification of high-ash Ekibastuz coal in the plasma-coal burner chamber;

3 Optimization of plasma ignition and partial gasification processes of high-ash Ekibastuz coal in the volume of burner was carried out and optimal parameters were determined.

Statements for defence

1 Electrothermochemical preparation of pulverized low-grade Ekibastuz coal for combustion enables the production of a highly reactive dual-component fuel (comprising combustible gases and coke residue) with elevated concentrations of CO (26.5%) and H_2 (15.2%), ensuring rapid ignition at the outlet of the plasma-coal burner;

2 The highly reactive dual-component fuel obtained at the outlet of the experimental setup, with a specific calorific value of 12,550 kJ/kg, ensures stable and intensive ignition when mixed with secondary air;

3 The optimal parameters of the plasma-coal burner are an average mass temperature of 1880 K, pressure of 0.1 MPa, plasmatron power of 60 kW with its length of 3 m and diameter of 0.15 m.

Theoretical significance of the research

The identified general patterns of the distribution of temperatures, velocities, and concentrations of products in the electro-thermochemical preparation for coal combustion along a plasma-coal burner allow for the improvement of the efficiency and stability of such systems. The obtained results can be used to develop new methods for enhancing the energy efficiency of coal combustion, optimizing combustion processes, and reducing the environmental impact.

Practical significance of the research

The optimal parameters of plasma ignition for high-ash Ekibastuz coal have been experimentally confirmed, ensuring increased efficiency and reliability of plasma-coal burners in pulverized coal-fired thermal power plants and boiler systems. The developed approach was applied on the TPE-215 boiler at the Gusinoozersk State District Power Station, in collaboration with the Industry Center for Plasma Energy Technologies of RAO "UES of Russia." This confirms the applicability, efficiency, and industrial relevance of the technology for improving the ignition and combustion stability of low-grade, high-ash coal in thermal power generation.

Reliability and validity of the obtained results

The dissertation uses widely known and verified thermodynamic and kinetic mathematical models TERRA and PlasmaKinTherm. The reliability and validity of the research findings are supported by a consistent correlation between the results of numerical modeling and experimental studies. Additionally, the scientific credibility of the work is confirmed through its dissemination in peer-reviewed international journals with a non-zero impact factor, in publications recommended by the Committee for Quality Assurance in the Sphere of Science and Higher Education of the Ministry of Science and Higher Education of the Republic of Kazakhstan (CQASSHE MSHE RK), as well as in the proceedings of international scientific conferences held both in neighboring and distant countries.

The personal contribution of the author consists in independently solving the tasks and performing numerical calculations of the plasma ignition and combustion stabilization processes. The author took an active part in the bench experimental studies of the plasma-coal burner for plasma ignition and combustion stabilization processes of solid fuel. The formulation of research tasks, the choice of methods and the discussion of the results were carried out jointly with the scientific supervisors.

Approbation of dissertation work and publications

The main results of the dissertation research were published in 14 scientific printed works, including: 1 article in a journal indexed by Scopus and Web of Science, 7 articles in publications recommended by the Committee for Quality Assurance in the Sphere of Science and Higher Education of the Ministry of Science and Higher Education of the Republic of Kazakhstan, 1 publication in a collective monograph recommended by the Academic Council of the Institute of Combustion Problems of the National Academy of Sciences of the Republic of Kazakhstan, and 5 papers in the proceedings of international scientific conferences.

Scientific publications with non-zero impact factor indexed by Scopus and Web of Science

- Messerle V.E., Lavrichshev O.A., Ustimenko A.B., Orynbasar M.N. Plasma-chemical waste processing: numerical analysis and experiment. Part 3. Rubber of used tires // Thermophysics and Aeromechanics. - 2023. - Vol. 30. - P. 595–599.

Scientific publications recommended by the CQASSHE MSHE RK for publishing the main results of scientific activity:

- Messerle V.E., Mossé A.L., Orynbasar M.N., Ustimenko A.B. Plasma ignition of solid fuel: Mathematical simulation and experiment // Journal of Engineering Physics and Thermophysics. - 2024. - Vol. 97. - No. 3. - P. 116–125.
- Orynbasar M., Messerle V., Ustimenko A. Modeling and experiments on plasma ignition of Ekibastuz coal in the form of dust // Combustion and Plasma Chemistry. - 2024. - Vol. 22. - No. 3. - P. 179–186.
- Messerle V., Orynbasar M., Ustimenko A. Efficiency of plasma technology for preparing solid fuels for combustion [Effektivnost' plazmennoy tekhnologii podgotovki tverdykh topliv k szhiganiyu] // Combustion and Plasma Chemistry. - 2024. - Vol. 22. - No. 3. - P. 169–178. (in Russian)
- Messerle V.E., Orynbasar M.N., Ustimenko A.B. Simulation and experiment of plasma ignition of low-grade coal // Combustion and Plasma Chemistry. - 2024. - Vol. 22. - No. 1. - P. 27–36.
- Messerle V., Orynbasar M., Umbetkaliev K., Ustimenko A. Gasification of carbon–containing waste in a plasma–chemical reactor [Gazifikatsiya uglerodsoderzhashchikh otkhodov v plazmokhimicheskom reaktore] // Combustion and Plasma Chemistry. - 2023. - Vol. 21. - No. 3. - P. 191–200. (in Russian)
- Orynbasar M.N. The clean combustion of solid fuel using a plasma-coal burner // Combustion and Plasma Chemistry. - 2022. – Vol. 20. - No. 1. - P. 83–91.
- Messerle V., Orynbasar M. Ecological efficiency of utilization solid fuel plasma technology // Combustion and Plasma Chemistry. - 2021. - Vol. 19. - No. 4. - P. 289-298.

Publication in the collective monograph recommended by the Academic Council of the Institute of the Committee of Science, Ministry of Higher Education and Science of the Republic of Kazakhstan:

- Messerle V.E., Orynbasar M.N., Ustimenko A.B. Ecological efficiency of plasma technology for using solid fuels [Ekologicheskaya effektivnost' plazmennykh tekhnologiy ispol'zovaniya tverdogo topliva] // In the collective monograph “Some problems of decarbonization and alternative energy [Nekotoryye problemy dekarbonizatsii i al'ternativnoy energetiki]” edited by Z.A. Mansurov. – Almaty: Daryn, 2024. - P. 130–147. (in Russian)

Publications in books of abstracts of international scientific conferences:

- Messerle V.E., Orynbasar M.N. Ecological efficiency of plasma-coal burners // XII International Symposium “Combustion and Plasmochemistry. Physics and Chemistry of Material Science” dedicated to the 125th anniversary of Academician N.N. Semenov and the 30th anniversary of independence of the Republic of Kazakhstan. 12-13 October 2021. - P. 11-12.
- Orynbasar M.N., Messerle V.E. The utilization of plasma technology in thermal power plants for technical modernization and environmental safety // XIV Konferencja “Młodzi w energetyce”. - Wroclaw, 2022. – P. 48.
- Lavrichshev O.A., Messerle V.E., Mosse A. L., Paskalov G., Orynbasar M.N., Ustimenko A.B. Plasma-Chemical Processing of Agricultural Waste:

Numerical Analysis and Experiment // Proceedings SARDINIA. 19th International Symposium on Waste Management and Landfilling. - 2023. – P. 4.

- Kaltay T.D., Orynbasar M.N. Utilization of plasma technology to minimize emissions of hazardous substances // XV Konferencja “Młodzi w energetyce”. - Wroclaw, 2023. – P. 101.

- Messerle V.E, Orynbasar M.N., Pawlak-Kruczek H., Ustimenko A.B. Plasma ignition of coal: numerical simulation and experiment // XV Konferencja “Młodzi w energetyce”. - Wroclaw, 2023. – P. 105.

Scope and structure of the dissertation:

The dissertation work consists of an introduction, three chapters, a conclusion and a list of references. The work includes 26 figures, 9 tables, 153 sources in the bibliography, 108 pages and 3 appendices.

1 EXISTING TECHNOLOGIES FOR BURNING AND GASIFICATION OF THERMAL COALS

1.1 The problem of the efficiency of the use of thermal coals at thermal power plants

During millions of years, chemical changes, pressure, and heat compacted decayed plant material into a solid form, which is coal. Due to its carbon content, coal holds a significant amount of energy, which is released as heat during combustion when exposed to oxygen or air. A variety of conversion methods are available for turning this energy into other useful forms, such as electricity. It is generally considered that coal used for generating electricity is thermal coal [3].

Over the last three decades, coal has consistently served as the predominant energy source for electricity production on a global scale. In 2023, coal-fired power plants worldwide generated approximately 10,500 terawatt-hours of electricity. The total amount of electricity produced worldwide that year was approximately 60 percent derived from coal, natural gas, and other fossil fuels. There is no question that fossil fuels remain the world's primary source of electricity generation. A global power mix dominated by coal accounted for about 35.5% of the global energy mix for 2023, followed by natural gas at 23%. Globally, there are 2,435 coal-fired power plants operating as of July 2023. China is home to nearly half of all coal-fired power plants in the world. There has been an increase in coal power generation capacity around the world, which has almost doubled in the period 2005-2022, reaching roughly 2.27 terawatts [4]. Gao Yuhe, a project leader for Greenpeace, said energy security has become a code word for coal in recent years [5].

Coal is one of the most energy-dense sources available: a single metric ton of coal produces as much electricity as 1,927 kilowatt-hours. The equivalent amount of electricity produced by natural gas is only 99 watts per 1,000 cubic feet, and the equivalent amount of electricity produced by fuel oil is 578 watts per barrel. Clean coal is a term that refers to numerous practices, including washing the coal before it is burned as well as removing pollutants such as sulfur dioxide from its emissions. Also known as carbon capture and storage (CCS), this technology involves pumping CO_2 deep underground or removing it from the atmosphere in some other way. It is still not possible to offset the harm caused by coal consumption with these technologies, despite the fact that they are able to make a difference [6]. Fortunately, the development of new 'clean coal' technologies is addressing this challenge, allowing the vast coal resources worldwide to be utilized responsibly for future generations. However, several obstacles must be overcome to commercialize these technologies and ensure that coal remains economically viable, despite the high costs associated with achieving low, and eventually 'near-zero', emissions. With a growing number of coal-fired power stations approaching retirement, 'cleaner' electricity can become available through their replacements [7].

This type of fossil fuel, is responsible for just over one-third of global electricity production. Although many countries are progressively moving away from its use, coal continues to play a significant role in both metallurgy and power

generation. Coal-fired power generation continues to rise in 2022, and southern power stations emit more than 2% more CO_2 than last year. The Net Zero scenario requires a 10% annual reduction of coal power plants by 2030. For the second consecutive year, coal-fired power generation reached approximately 10,400 terawatt-hours, setting a new record for the sector.

In the Asia-Pacific region, elevated natural gas prices combined with severe weather conditions have driven a rise in coal consumption for electricity generation, which increased by nearly 3% relative to 2021. Currently, China has 11 GW of coal-fired power plants, with new plants being added to the grid annually. This strategy in the energy sector has been driven by concerns over energy security, economic factors, and the growing trend of integrating variable renewable energy sources with reliable power generation options. A sharp increase in electricity demand has driven coal generation in India to record levels due to extreme heat. There was an increase of more than 8.5% in coal-fired power in 2022. Due to low levels of hydropower and nuclear power in the EU, coal-fired electricity production grew by almost 7%. Consequently, coal accounted for about 36 percent of global electricity production.

Coal has become the preferred source of energy for the EU and the UK as a result of geopolitical instability in the world. Despite limited gas markets and low levels of fuel supply, the EU has had to take measures to improve the security of supply due to the ongoing energy crisis and geopolitical instability in the world. Some EU countries, including the UK, have decided to return to maximum capacity on the market or to push back the closure date. A coal capacity addition of about 10 GW is planned for the winter of 2022 and 2023 in Germany. The approved plan increases coal generation capacity by approximately 15% (19 GW) and amounts to 146 GW in the EU and UK [8].

A significant effort was made to increase thermal efficiency and power during the last phase of power plant development. The thermal efficiency of thermal power plants has increased by around 5 – 45% over the last century. Efficiency improvements have always been driven by reducing the cost of power generation. Increasing concerns about CO_2 emissions have led to further improvements in thermal efficiency. Direct combustion of coal produces electricity by converting its chemical energy into heat, which is converted into electricity. Improved thermal efficiency has been achieved through reducing the irreversibility of coal's chemical energy conversion into heat, minimizing low-temperature heat losses, and maximizing heat-to-energy conversion [9].

To reduce carbon emissions in power generation, more efficient technologies for utilizing low-emission coal must be developed. Despite significant progress in renewable energy technologies and energy storage, fossil fuels are expected to maintain a dominant position in the global energy mix. According to the International Energy Agency (IEA), by 2040, coal-fired electricity generation is projected to surpass all renewable sources except for hydropower.

The IEA estimates that 730 GW of new coal-fired power plants with high efficiency and low emissions will be built by 2040, mostly in developing countries.

Globally, coal power plants are on average 33 percent efficient, according to World Coal Association, a strong supporter of HELE. It is possible to reach 45% for modern plants, and 40% for «ready» plants. A mere 1% improvement in the efficiency of coal-fired power plants can lead to a 2-3% reduction in CO_2 emissions [10].

As the world's most highly demanded and advanced energy resource, coal was the first fossil fuel used by mankind. Coal was first utilized in the early 17th century for smelting iron, and by the late 18th century, it was used to produce gas for lighting lamps [11]. The pulverized coal combustion technology was pioneered in the 1920s and, by 1930, had established itself as the leading technique for coal burning in thermal power stations.

Natural coal is formed through the slow decomposition of organic matter, predominantly of plant origin, under natural environmental conditions [12]. Russia and CIS countries distinguish brown coals, bituminous coals, anthracites, and graphites according to their metamorphic stage (carbonization). There has been an interesting distinction made in the United States and the European Union among lignite, bituminous coal, subbituminous coal, graphites, and anthracites. A comparison of the characteristics of the main types of solid fuels used in thermal power plants can be found in Table 1.1 [13 – 15].

There is little heat of combustion in brown coal because it contains up to 43% moisture and 50% volatile substances. At a depth of about 1000 meters, they form from dead organic residues under the pressure of dead organic residues. The heat of combustion of hard coals is higher. They contain up to 12% moisture, which is 3-4% internal, and 32% volatile substances, so they ignite easily. Brown coal is formed at depths of about 3000 meters.

Anthracites have the highest heat of combustion among coals because the organic mass consists almost entirely of carbon up to 96%, but they are poorly ignited. At depths of about 6000 meters, anthracites are formed when pressure and temperature of coal increase.

Table 1.1 – Thermal Characteristics of Solid Fuels

Type of coal	W^w	A^d	V^{daf}	Q_l^w
Petrocoke	1-2	2-3	3-4	8800-9700
Anthracite	5-8	25-35	4-10	4300-6200
Hard coal	5-12	20-56	15-40	4000-5000
Brown coal	25-35	15-20	35-50	3000-3800
Lignite	32-40	28-35	23-27	1900-2100
Shale	40-50	75-80	48-50	1600-2000
Coal mixture	10.4	48.5	38.2	3150

Designations: W^w – moisture content per working mass, A^d – ash content per dry mass, V^{daf} – volatile yield per combustible mass, Q_l^w – lower heating value of combustion of coal per working mass

During the refining of oil and oil sands, petroleum coke or petrocox is produced as a solid fuel. Petrocox is made up of carbon, ash, and resin, and it has a high heat of combustion (up to 9700 kcal/kg). Its low mechanical strength and high resin content make its direct use difficult. A promising way to utilize this solid fuel is through plasma gasification in steam or air atmospheres, which produces high-calorie synthesis gas (CO + H_2) ensuring combustion with zero sulfur and nitrogen oxide output.

Coal is a naturally formed fossil fuel consisting predominantly of carbon, accompanied by varying amounts of oxygen, hydrogen, nitrogen, and sulfur. There are proven methods for determining the elemental composition of coals and their thermal properties using this simple formula: carbon (C) + ash content (Ac) + volatile (V) + moisture (W).

The formula for determining the heat of combustion of coal [16]:

$$Q_L = 4.19(81C + 246H - 26(O - S) - 6W), \quad (1.1)$$

where C, H, O, S, and W are the content of carbon, hydrogen, oxygen, sulfur, and moisture (mass. %) in the working mass of coal. In the Table 1.2 below, coal composition changes as metamorphism increases.

Table 1.2 – Dependence of Coal Composition on the Degree of Metamorphism

Composition of coal	Content	Process
Carbon	65-91%	Increase
Hydrogen	8-4%	Decrease
Oxygen	30-2%	Decrease
Nitrogen	0.5 – 2%	Increase
Sulfur	0.5 – 3%	Increase
Inorganic components	varying between a few percent and several tens of percent	Decrease

Coal comprises three main categories of organic substances: bitumens, humic acids, and the carbon-rich matrix referred to as residual coal. Bitumens can be isolated from coal through solvent extraction, whereas humic acids are soluble in alkaline solutions. In alkalis, residual carbon cannot be extracted or dissolved. Humic acids are found in the highest concentration in brown coal, and they are found in the lowest concentration in hard coal.

Coal is predominantly composed of organic compounds with high molecular weights. While brown coal predominantly contains aliphatic compounds, higher-rank coals are distinguished by the presence of aromatic structures integrated into larger, more complex molecular frameworks. In hard coals, the proportion of

aromatic carbon atoms increases with metamorphism, ranging from 80% in flaming coals to 100% in anthracites. Anthracite has a C:H ratio of 2:1 (low molecular weight hydrocarbon coronene $C_{24}H_{12}$) rather than 1:1 (benzene, methylnaphthalene as a result of low metamorphism).

In addition to studying the detailed composition of coal products following hydrolysis (steam treatment), halogenation (halogenation treatment), oxidation, and thermal destruction, much information can be obtained about coal structure. Methods of mass spectroscopy, infrared spectroscopy (IR), X-ray diffraction analysis, nuclear magnetic resonance (NMR), electron paramagnetic resonance (EPR), and various physical and physicochemical methods are employed in coal research. Until recently, the structural analysis of coal using NMR spectroscopy was primarily conducted on liquid fractions derived from coal through processes such as extraction, pyrolysis, and hydrogenation. Indirect information about coal structure was provided by these studies. Until recently, solid coal samples were analyzed by NMR H^1 and C^{13} spectra using special equipment. Different coals were analyzed using the C^{13} NMR method to determine the ratios of aromatic ring carbons and total carbons (C_{ar}/C_{tot}); aromatic α- and β- aliphatic hydrogens were estimated using NMR H^1 spectroscopy. Hydroxide atoms, aliphatic hydrogen atoms, and aromatic hydrogen atoms can also be determined using Fourier transform infrared spectroscopy on hard carbon samples [17].

The following ideas regarding the chemical structure of codes have been developed based on the research conducted by scientists. Organic matter in coal is primarily a rigid, three-dimensional polymer with an irregular structure. Furthermore, it contains monomolecular or low-polymerized ones that are immobilized in pores or associated with polymer frameworks through donor-acceptor interactions [18]. Coal consists of fragments connected by ether, aliphatic, thioether, and imine bridges in the mobile and hard phases.

Figure 1.1 illustrates the approximate structure of a molecule of coal's organic mass [19]. There are many parts to a coal molecule, and this picture illustrates only a part of its complexity. It is estimated that coal molecules contain more than 1,000 fragments.

Each structural fragment consists of an aromatic nucleus surrounded by an aliphatic periphery. As coal undergoes metamorphism, the aromatic core becomes increasingly condensed. At a carbon content of 78%, the core typically includes two aromatic rings; at 82%, three rings; and at 90%, four. In extensively metamorphosed coal varieties such as anthracite, the aromatic structures may contain up to twelve fused rings. Heteroatoms including oxygen, sulfur, and nitrogen are commonly incorporated within these aromatic rings. The aliphatic segments of these molecular fragments consist of short chains and bridging groups.

Aromatic rings undergo hydrogenation to form hydroaromatic structures. The number of methyl groups (CH_3) is less than that of methylene groups (CH_2). As a result, hydroaromatic structures are mainly composed of non-aromatic C and H atoms. In coal, there are no double bonds made up of ethylene, except for those

formed by the radicals of the type $R_1R_2C = CR_3R_4$, in which R_i are hydrocarbon radicals.

Oxygen in coal is primarily found in phenolic hydroxyl groups, carbonyl groups, and carboxyl groups. As the carbon content of coal rises, the concentration of phenolic hydroxyl groups decreases, becoming particularly low even at 89% carbon content.

Sulfur in coal is typically present as iron disulfide (FeS_2) (pyritic sulfur), iron sulfate (Fe_2SO_4), and organic sulfur. The amount of organic sulfur in the total is 30-50%. Hydrogen sulfide (H_2S) is released when pyrite and organic groups decompose during coal processing. There are a variety of interactions that occur between the released hydrogen sulfide and organic substances as well as ash components of coal, as well as various reactions between hydrogen sulfide and pyrite in this case [20].

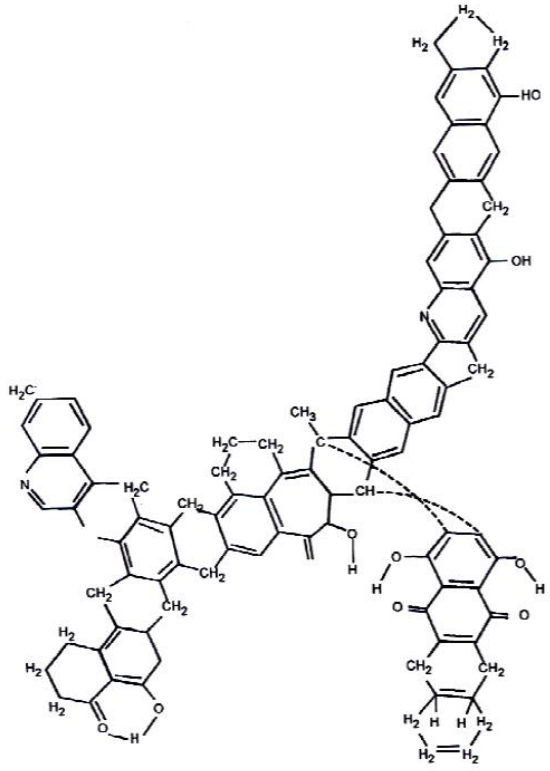


Figure 1.1 – Chemical structure of a coal molecule, C – 82% ($C_{100}H_{76}O_{10}N_2$) [19]

Only organic matter in coal contains nitrogen, not ash. Extraction, pyrolysis, and hydrogenation products determine the composition of nitrogen-containing structures. When coal undergoes pyrolysis at temperatures ranging from 770 to 1370 K, the liquid products include pyridine (C_5H_5N) and its derivatives, aniline ($C_6H_5NH_2$), pyrrole (C_4H_5N), nitriles (RCN), carbazoles, quinolines, acridine, indole and their derivatives. These compounds are formed through the pyrolysis of amines and substituted amine groups, which are converted into gaseous ammonia (NH_3). According to coal hydrogenation studies, nitrogen is predominantly present in heterocyclic rings or as bridges linking two carbocyclic rings. About 10% of volatile

substances are released from coal before nitrogen-containing compounds are released. There is a large amount in aromatic rings and a very small amount in side chains.

The main nitrogen-containing compounds of coal pyrolysis resins are pyridines, pyrroles, nitriles, carbosols, quinolines, and indoles. The amount of nitrogen released depends on the temperature, heating rate, and type of coal. Thus, with an increase in temperature from 770 to 1170 K, the amount of nitrogen released in the form of volatiles increases from 20 to 80%. The nitrogen remaining in the coke is held in very strong bonds that are not destroyed during pyrolysis at high temperatures. This nitrogen can only be converted into volatiles by complete gasification of the coke with steam or by combustion with oxygen. Volatiles released during coal pyrolysis are in the form of NH_3, HCN, N_2 and compounds included in the resin [18].

Among coal's structural features is its porous structure; according to [18], coal has three types of pores: micropores (0.0012 – 0.03 microns), mesopores (0.03 – 0.3 microns), and macropores (0.3 – 3 microns). As a result of the large surface area of micropores, the majority of decomposition products are formed when heated, and the reagents diffuse during the adsorption process. For reagents and products to enter the gas phase, mesopores are the primary channels. Macropores are relatively few in number. By not interfering with free mass transfer, they effectively reduce particle size.

Although coal has been used for a long time, it still poses a challenge for efficient and environmentally safe combustion [21]. In spite of these disadvantages, coal continues to be actively used due to its complex structure and properties that change with the type of coal. Coal is a multifaceted fuel with diverse applications in the chemical industry, where it can be combusted, subjected to pyrolysis, incinerated, gasified, or employed as a feedstock [22]. The extraction, transportation, storage, and use of coal, including dust, is convenient [23].

Because it is compact and has a high energy density (about 30 MJ/kg), combustion is enhanced [24]. In contrast to fuel oil and gas, other fossil fuels do not leak or splash, and explosions and spontaneous combustion are less dangerous [12]. Prices of coal are stable and attractive due to the availability of coal and abundant reserves [25]. Coal finds extensive application in today’s world, fulfilling diverse roles such as electricity generation (thermal coal), serving as a critical raw material in metallurgical processes (coking coal), supporting the chemical industry, facilitating the extraction of rare earth elements, and contributing to graphite production. Globally, coal reserves are estimated to exceed 14.8 trillion tons, with economically recoverable reserves surpassing 1 trillion tons, making coal the most abundant energy resource compared to others [13]. In contrast to the oil and gas sectors, the coal market is characterized by greater competition due to the widespread geographical distribution of coal deposits, which are present on nearly every continent, in the majority of countries, and across numerous regions worldwide. At current consumption rates, coal supplies are projected to last around 250 years, compared to 65 years for natural gas and just 45 years for oil.

Additionally, global coal demand is experiencing steady growth, increasing by roughly 2% annually [26].

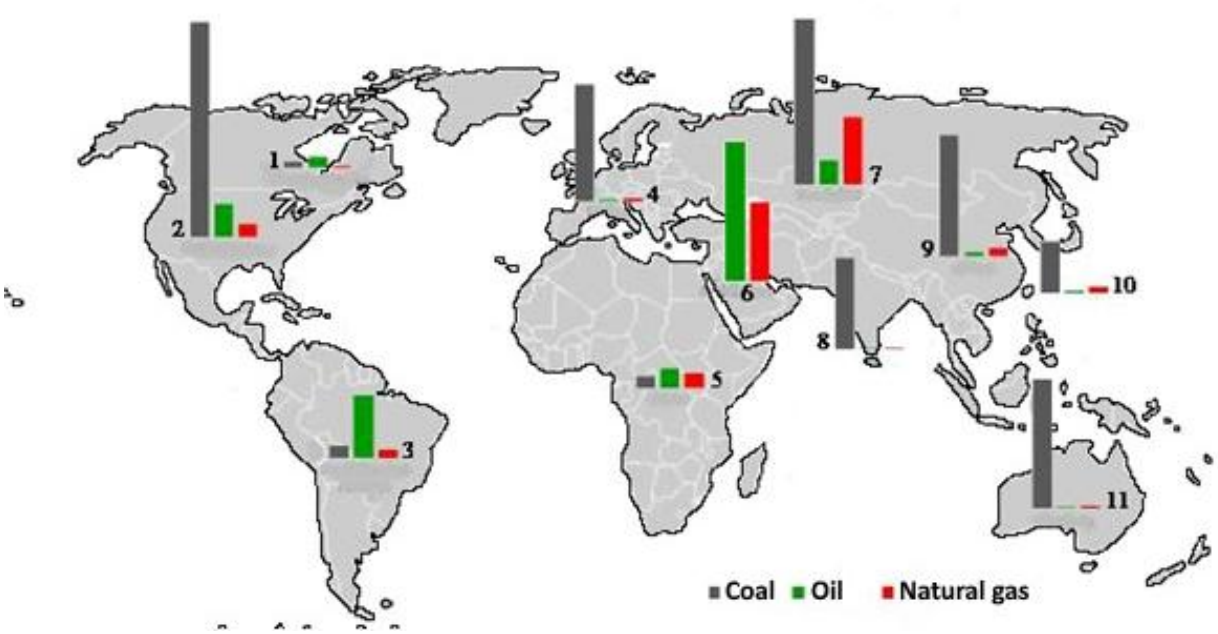
By millions of years of chemical change, pressure, and heat, coal is formed from decayed plant material that has been compacted into a solid state. When coal undergoes combustion in the presence of air or oxygen, its high carbon content allows it to release a significant amount of energy in the form of heat. This thermal energy can then be converted into a usable form, such as electricity. Coal used specifically for this purpose is known as *thermal coal* [27]. For the past 30 years, coal has remained the dominant fuel for electricity generation on a global scale. As of July 2023, there were 2,435 coal-powered electricity plants operating worldwide, with China accounting for almost half of these facilities [28].

Electricity is an important part of modern life, and coal is the world's most common source of electricity, contributing over 36.4% to global electricity generation. Coal-fired thermal power plants account for a significant share of electricity generation in various countries: accounting for roughly 25% in the United States, 30% in Russia, 50% in India, and reaching up to 85% in both China and Kazakhstan. Worldwide, many energy consumers continue to depend on coal-fired power due to its cost-effectiveness and reliability. In regions with limited access to modern and clean energy technologies, coal remains an indispensable energy source. Its broad availability, which is more evenly distributed globally than oil and natural gas, further underscores its role as an accessible energy resource, as depicted in Figure 1.2.

Beyond its use as a fuel, coal supports a variety of industrial applications. It serves as a critical raw material in metallurgy, phosphate fertilizer production, and cement manufacturing. Coking coal, in particular, is vital for these sectors, especially in phosphate processing. Furthermore, coal and its derivatives are employed in the production of activated carbon filters essential for air and water purification. Coal-based materials also contribute to the manufacture of carbon fiber, which is extensively used in the aerospace and automotive industries. Additionally, coal serves as a source of silicon metal utilized in lubricants, and specific chemical processes enable the extraction of rare earth elements from coal

Coal plays a vital role in alleviating energy poverty by providing a reliable and accessible source of energy, particularly in regions lacking modern energy infrastructure. Around 2.6 billion people live without electricity around the world. Each year, approximately 1.5 million people around the world die as a result of household air pollution, primarily caused by burning biomass such as wood and animal dung, along with inadequate access to basic sanitation.

Completely removing coal from the global energy mix is not a practical option. Addressing today’s complex energy challenges requires a diverse range of fuels and technologies. Coal will continue to be essential, not only because it remains widely accessible across various markets, but also because, for many industrial applications, it is currently the only viable option. Furthermore, coal supports the development and functioning of renewable energy infrastructure, making it a key component in the broader energy transition [29, 30].



1 – Canada and Mexico, 2 – USA, 3 – North and Central America, 4 – Europe, 5 – Africa, 6 – Middle East, 7 – Russia and the CIS, 8 – India, 9 – China, 10 – Asia-Pacific region, 11 – Australia

Figure 1.2 – Global distribution of fossil fuel reserves [29]

To increase coal's share in the energy mix, the development and adoption of energy-efficient and environmentally sustainable technologies for coal utilization will be essential. Around 75% of the world's coal reserves are concentrated in countries of the former USSR (including Kazakhstan, Ukraine, and Russia), as well as in China and the US. Additionally, Australia possesses substantial reserves of high-quality coking coal along with significant thermal coal deposits, characterized by favorable geological and mining conditions.

Electricity is primarily generated by coal. Coal accounts for over 40% of global electricity production. In the United States alone, coal-fired power plants have a combined installed capacity of 250 gigawatts. It is estimated that 950 million tons of coal were burned at these thermal power plants in 2008, which accounted for 57% of the coal used in electricity generation. In China, coal is burned on an annual basis in the amount of 1.5 billion tons.

However, a significant challenge has been the declining quality of coal supplied to power plants. Increases in ash and moisture content have corresponded with reductions in calorific value. For example, Table 1.3 presents data from TPPs demonstrating variations in ash content and the lower heating value of Ekibastuz coal. Such abrupt fluctuations in fuel properties adversely affect the operational efficiency of power plants. Additionally, a substantial amount of fuel oil is required to stabilize the combustion process in pulverized coal burners due to the rapid fuel decomposition within the plants. Furthermore, the ongoing increase in global energy demand, combined with the progressive depletion of the most valuable hydrocarbon fuels (primarily oil and gas) and their reserves, has compelled researchers to

reconsider the importance of coal, whose proven reserves far surpass those of oil and gas.

Table 1.3 – Variations in the Properties of Ekibastuz Coal

Year	1960	1965	1970	1975	1990	2000
A^d, %	37,4	39,9	41,3	41,7	43,8	43,8
Q_l^w, kJ/kg	17400	16900	16800	16600	16200	15900

Current combustion and thermal treatment technologies for solid fuels and their blends fall short of meeting contemporary standards for fuel efficiency, environmental impact, and economic viability. Pulverized coal boilers, in particular, face considerable challenges when burning low-grade coals that do not conform to design specifications. TPPs generate harmful gases (NO_x, SO_x, CO) and fly ash emissions that are negatively affected by poor fuel quality (such as ignition behavior, flame stability, and combustion properties of the fuel [31].

The situation is further aggravated by the declining quality of thermal coal, which increases the reliance on supplementary fuels such as fuel oil or natural gas in pulverized coal-fired thermal power plants. These additional fuels are required for boiler ignition, flame stabilization, and ensuring continuous liquid slag discharge in furnaces equipped with slag-tapping systems [32]. In countries like Kazakhstan, Russia, and Ukraine, coal-fired power plants collectively consume over 15 million tons of fuel oil annually, resulting in substantial economic inefficiencies.

Fuel and energy balances are progressively shifting toward the utilization of lower-grade fuels, particularly in CIS countries. In Kazakhstan, significant reserves of thermal coal are available and can be efficiently extracted through surface mining methods. The Ekibastuz coal basin serves as a prominent example, with coal seams favorably positioned for open-pit mining and total estimated reserves of approximately 8 billion tons across the region [33]. Kazakhstan’s energy resource base is sufficient not only to meet domestic energy demand but also to support electricity exports to neighboring states. Although Kazakhstan occupies roughly 1.8% of the global land area, it accounts for about 0.5% of the world’s mineral fuel reserves and 3.3% of global industrial coal reserves. Within the Commonwealth of Independent States, Kazakhstan ranks third in coal production, following Russia and Ukraine. Hard coal dominates Kazakhstan's energy resources, followed by brown coal to a lesser extent. The volatile yield of hard coals with the appropriate moisture content of the ash-free mass can reach 15% and the calorific value can reach more than 24,000 kJ/kg (5,740 kcal/kg). The calorific value of brown coal is below 24,000 kJ/kg, and its moisture content is around 30 – 40%. There are 24.3 billion tons of hard coal in reserves, of which 6.1 billion tons (about 25%) are suitable for coking.

In Kazakhstan, coal reserves are substantial, but 90% of the coal balance is high-ash Ekibastuz coal, which has a high moisture content and is more expensive to transport, emits CO_2, and spontaneously combusts. Kazakhstan currently

possesses over 100 coal deposits, with total geological reserves estimated at 176.7 billion tons. Of these, around 40 deposits have been explored, revealing commercially viable resources amounting to 34.1 billion tons. The three largest coal deposits are Karagandy (9.3 billion tons), Turgay (5.8 billion tons), and Ekibastuz (12.5 billion tons), all located in northern and central Kazakhstan. Furthermore, open-pit mining operations in the region possess the potential to produce over 400 million tons of coal per year. The industrial coal reserves are concentrated primarily in the basins of Ekibastuz (51%), Turgai (26.4%), Maikuben (8.8%), and Shubarkol (7%), totaling approximately 21 billion tons.

Globally, low-rank coal represents roughly 50% of the total coal reserves. In spite of this, low-rank coals contain a high moisture content, which negatively affects their use in power plants, increases transportation costs, increases CO_2 emissions, and leads to spontaneous combustion as a result of storage. Low-rank coal presents a number of challenges when burned in traditional boilers or pulverized coal combustion systems. A number of issues arise from the use of such fuels, including the need for efficient combustion and the need to comply with environmental requirements that reduce emissions of fly ash particles, nitrogen oxides, and sulfur pollutants into the environment. Therefore, ongoing research and development efforts focus on advancing new technologies for solid fuel combustion to achieve both enhanced efficiency and improved environmental protection [34, 35].

1.2 Existing technologies of ignition of thermal coals at thermal power plants

The enduring presence of coal not only supports renewable energy during intermittent periods, but also ensures energy security, affordability, and reliability for coal-dependent nations, while ensuring the countries are able to select their own energy sources without losing control over the production process [36]. Keeping nature secure and conserving energy requires the application of the most successful technological and scientific advancements [37, 38, 39].

In general, current technologies for the thermal treatment and combustion of solid fuels and their blends fail to fully satisfy modern demands for improved fuel efficiency, sustainability, and the economic performance of energy facilities. Pulverized coal boilers face significant challenges when burning low-grade coals that do not meet design specifications, as poor-quality fuels negatively impact ignition, flame stability, and combustion completeness. Emissions of toxic gases such as NO_x, SO_x, CO, along with volatile ash, lead to considerable declines in both the environmental performance and economic efficiency of TPPs.

This challenge is exacerbated by the deteriorating quality of thermal coal, which compels pulverized coal-fired power plants to increasingly depend on auxiliary fuels such as fuel oil and natural gas. These are essential for boiler ignition, torch lighting, and maintaining stable slag flow in furnaces equipped with liquid slag removal systems. In countries like Russia, Kazakhstan, and Ukraine, such plants

collectively consume over 15 million tons of fuel oil annually, a practice that is economically inefficient.

Moreover, the continuous rise in global energy demand, coupled with the gradual depletion of hydrocarbon resources such as oil and natural gas, has reinforced the strategic importance of coal. Both the thermal power sector and the chemical industry increasingly depend on coal as a primary raw material, owing to its substantially larger reserves compared to oil and gas.

Low-grade fuels have increasingly become a significant component of the global fuel and energy mix, particularly within CIS countries. The Republic of Kazakhstan possesses substantial reserves of thermal coal that can be extracted cost-effectively through open-pit mining methods. For instance, the Ekibastuz coal basin contains exceptionally thick coal seams (with total reserves estimated at approximately 8 billion tons), making it especially well-suited for large-scale surface mining and thereby reducing extraction costs.

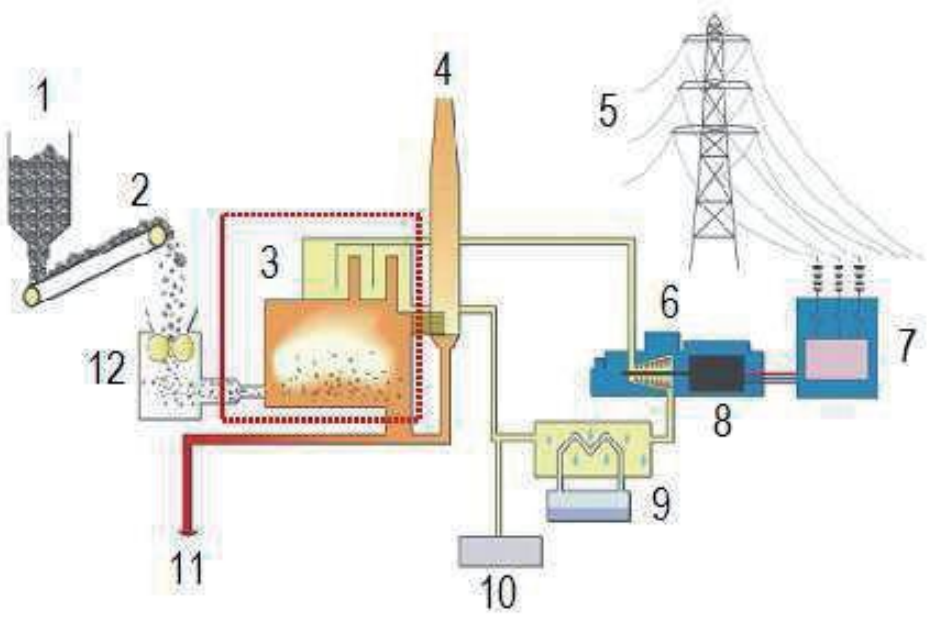
The main fuel for most thermal power plants in Russia and the CIS countries is low-grade coal, ballasted with ash, mined by open-pit methods. These coals are characterized by high moisture content, elevated ash levels, and low volatile matter yield. The direct combustion of such fuels in conventional thermal power systems poses significant challenges, including unstable ignition, incomplete combustion, and elevated emissions of hazardous pollutants such as particulate matter, nitrogen oxides, and sulfur oxide.

In conventional thermal power systems, various techniques are applied to improve ignition and stabilize the combustion of coal characterized by high ash content and low volatile matter. These approaches include enhancing the fineness of coal grinding (to R_{90} = 6-8%), preheating the primary air to 410 K and the secondary air to 673 K, delivering pulverized coal at elevated concentrations (up to 50 kg/kg), and employing thermal conditioning or co-firing with fuel oil. However, these approaches are not without significant limitations. Enhanced grinding fineness leads to substantial energy losses, thereby reducing the net efficiency of the boiler. Moreover, due to fire safety concerns, the temperatures of the primary and secondary airflows cannot be increased beyond 410 K and 673 K, respectively [40].

Pulverized coal thermal power plants consume approximately 25 million tons of liquid fuel annually for flare stabilization with fuel oil (accounting for over 12% of total thermal power generation). However, the widespread reliance on costly, high-sulfur heavy fuel oil fails to offer an effective solution to the broader issue of enhancing fuel efficiency. In addition, the co-combustion of coal with heavy fuel oil substantially worsens environmental pollution levels.

Despite its relatively low calorific value and poor environmental characteristics, coal is projected to play an increasingly important role in the global energy market. This is largely due to its abundance and the presence of various chemical elements and mineral components within its composition. Coal’s complex structure enables its broad utilization across multiple industries (including thermal power generation, chemical production, metallurgy, and construction) through integrated processing technologies.

The combustion of solid fuels has been the subject of sustained research and development for many decades, reflecting its continued relevance in both energy and industrial applications. The burning of coal has become one of the most common and dominant fuel combustion technologies. A pulverized coal thermal power plant utilizing this technology is shown in Figure 1.3.



1 – Raw coal bunker, 2 – conveyor, 3 – boiler, 4 – chimney, 5 – electricity, 6 – steam turbine, 7 – transformer substation, 8 – generator, 9 – condenser, 10 – water purification, 11 – ash disposal systems, 12 – pulverized coal mill

Figure 1.3 – Diagram of electricity generation at a thermal power plant using pulverized coal fuel [40]

In the coal-fired thermal power sector, "clean coal technologies" refer to methods aimed at enhancing both environmental performance and economic efficiency. These technologies are generally divided into two main categories. The first involves coal pretreatment, including processes such as coal beneficiation (enrichment), crushing, washing, drying, and the recovery or utilization of methane emitted during coal extraction. The second focuses on pollutant reduction, incorporating systems such as electric filters, low-emission burners, selective catalytic reduction, and flue gas desulfurization technologies. Desulfurization technologies, electro filters, and fabric filters can reduce the sulfur dioxide content in flue gases by 97% and remove ash by 99%. Construction can make use of the remaining particles after fly ash is effectively removed. Three known methods can reduce nitrogen oxide (NO_x) emissions by up to 90%: re-combustion, selective catalytic reduction, and the use of low-emission burners.

The adoption of advanced coal combustion technologies represents a key strategy for mitigating carbon dioxide emissions. Enhancing the efficiency of thermal power plants from 30% to 40% (primarily by reducing the amount of fuel

required per unit of energy output) can lead to an approximate 25% reduction in CO_2 emissions. However, a substantial portion of existing thermal power infrastructure remains outdated. For instance, over 60% of pulverized coal-fired power plants in Europe were commissioned more than three decades ago, with typical efficiencies reaching only up to 35%. In many developing countries, the average efficiency of thermal power plants remains even lower, at around 25%. By increasing parameters such as critical pressure and steam temperature, pulverized coal thermal power plants can increase efficiency based on subcritical operating parameters of the steam cycle. Nevertheless, the effectiveness of this technology may be constrained by the material quality employed in boiler design. A new generation of pulverized coal thermal power plants operating under supercritical and ultrasupercritical conditions has reached efficiency levels of approximately 45%, primarily due to advancements in high-performance materials, such as superalloys [11, 41].

As part of the second group of «clean technologies» there are a number of innovative technologies that are radically different from the technology of flaring pulverized coal in principle. One of the most important is intra-cycle gasification of coal and combustion in a circulating fluidized bed under pressure. These technologies have the advantage of reducing fuel oil consumption and improving the environment, but they are still being tested experimentally, and their use will be far in the future [42].

There has been a significant increase in the use of full or partial gasification processes in the coal processing industry in recent years. During coal gasification, both organic and ash masses of coal undergo thermochemical transformations, resulting in the production of the target products. As a more reactive fuel than coal, combustible gas obtained from partial gasification of low-grade fuels is used as a fuel for partially gasifying low-grade fuels. Coal gasification in the presence of air generates a mixture of combustible gases (including carbon monoxide (CO), hydrogen (H_2), methane (CH_4), carbon dioxide (CO_2), and nitrogen (N_2)—alongside an inert ash byproduct. After separating the solid residue, the resulting combustible gas can be utilized for combustion in furnaces or ignited using a pulverized coal torch. In contrast, steam or oxygen gasification of coal produces synthesis gas (syngas), primarily composed of carbon monoxide (CO) and hydrogen (H_2), along with inert ash. Syngas, once purified from ash, serves as an environmentally friendly fuel or reducing agent widely employed in metallurgy and chemical synthesis [43].

The gasification of solid fuels follows a systematic approach that is primarily determined by two fundamental parameters: the characteristics of the fuel and the method of energy provision required to sustain the process [44]. A solid fuel can be gasified in three ways, depending on the state of the fuel: the stationary (dense) layer is the Lurgi process, the boiling layer is the Winkler process, and the flow of pulverized fuel is the Kopers-Tozek process. Gasifiers can be classified as autothermal or allothermal, depending on how they receive their energy. The heat required for endothermic conversion is obtained in autothermal processes by burning part of the fuel injected into the gasifier. It is estimated that 35 – 40% of coal is spent on maintaining the thermal regime. Allothermic processes obtain heat from the

external environment (solid or gaseous fuel, by means of heat transfer through walls) or external energy sources (electric arcs, lasers, radiation heaters). At atmospheric pressure, these gasification methods have been extensively studied. In these methods (namely fixed-bed, fluidized-bed, and pulverized coal flow) a part of the fuel is oxidized to supply the thermal energy required for the gasification process. Coal, together with oxidizing agents such as air, oxygen, or steam, is fed into the gasifier and subjected to elevated temperatures ranging between 1200 and 1800 K [45].

Several factors contribute to the growing interest in intra-cycle coal gasification. It is possible to implement a binary cycle on solid fuel, reducing specific fuel consumption and increasing power plant efficiency. Moreover, TPPs utilizing integrated gasification systems are considered environmentally benign, as the design of the gasification process combined with advanced gas-cleaning technologies significantly minimizes emissions of sulfur oxides, nitrogen oxides, and particulate matter.

In [46], hydrogen was directly produced from coal using two fluidized bed reactors (gasifier and regenerator). Coal gasification yields a gas mixture composed predominantly of hydrogen (73 wt.%) along with methane, carbon monoxide, and carbon dioxide (27 wt.% combined). During this process, the organic content of coal is transformed into synthesis gas with an overall conversion efficiency of 92.6%. When hydrogen is used in a hybrid system with solid oxide fuel cells, it is possible to generate electricity at 61.9% efficiency with full CO_2 capture. The technology of producing hydrogen and electricity from coal in a circulating fluidized bed under pressure (CFB) is of interest [47]. A CFB power plant with a capacity of 255 MW will produce 260 tons of hydrogen each day with a purity of 99.99%.

According to the paper [48], hydrogen can be produced by electrolysis of a carbon-water-graphite mixture. The cost of electricity is 0.04 US dollars/kWh, coal is 32 US dollars/ton, and 1 ton of hydrogen costs 1700 US dollars, based on a theoretical energy cost of 5.6 kWh/kg for hydrogen. Hydrogen produced by electrolysis of water has a cost 50% lower than this value.

The process of steam gasification of coal is described in [49] using the heat generated in a tubular solid oxide fuel cell. A computer model was used to investigate the proposed installation. The operation of fuel cells releases heat as well as electricity. This is essential for the endothermic coal gasification reaction, occurring in an atmosphere of carbon dioxide and water vapor, which are also byproducts of fuel cell oxidation. The synthesis gas from the gasifier is fed into the fuel cell, where it is oxidized and heat is released. The described process has been confirmed by computer modeling. Magneto hydro generators and underground coal gasification are also available. Generally, these technologies increase fuel efficiency while reducing pollution emissions, but their widespread use is limited by high capital costs, operational risk, and unreliability [50].

In addition to flue gas recirculation technology, carbon dioxide recovery and burial underground have recently attracted attention [51]. In spite of this, CO_2 capture and storage technologies are not widely used due to their high cost and the danger associated with storage of CO_2 underground. All of these technologies,

however, will not solve the main problem of reducing carbon dioxide in the long run.

Consequently, coal faces several challenges within the energy sector, despite its significant potential for enhancing and optimizing combustion technologies. Among these challenges, two key issues stand out, one being the high sensitivity of the combustion process to variations in coal properties. In addition, the ignition and combustion of pulverized coal demand substantial quantities of supplementary fuel, amounting to approximately 50 million tons of fuel oil annually. In most cases, existing methods of improving fuel efficiency have reached their limits. New, environmentally friendly, and progressive technologies are being developed now. Additionally, the combustion of ETCPF is extensively utilized, notably through plasma technology, which is distinguished by its high efficiency, environmental compatibility, cost-effectiveness, and, importantly, its ability to address multiple challenges simultaneously. Furthermore, plasma technologies have demonstrated versatility across various applications, including the recycling and conversion of carbon-containing wastes, processing of rubber from discarded tires, and the disposal of agricultural residues [51, 53, 54].

During the thermochemical process, the molecular structure of coal undergoes varying degrees of disruption and rearrangement. These reactions, which are destructive in nature, involve both free and bound oxygen and water vapor. Various organic and inorganic compounds inherent to the coal, as well as externally introduced substances, act as catalysts facilitating these processes. Alternatively, ETCPF for combustion involves the combination of thermal energy and chemical reagents during its decomposition. As a result of the thermochemical transformation, only the organic component of coal is affected, whereas the mineral portion is practically unaffected.

In recent years, there has been a growing interest in technologies focused on carbon dioxide capture and storage in underground mines, alongside advancements in flue gas recycling methods. The high cost of carbon dioxide capture and the unpredictable environmental impacts of underground carbon dioxide storage, however, limit the widespread use of carbon dioxide capture and storage technologies [55, 56].

Methods for preparing pulverized coal using in-line pulverized coal technology can be categorized into two primary approaches: the first involves heating the entire air–coal mixture prior to its introduction with secondary air; the second consists of heat-treating a portion of the pulverized coal stream separately, which is then combined with the remaining coal dust and secondary air [25]. According to the first group of studies, volatile coal can be added to low-grade fuel to enhance its reactivity, i.e. its ability to ignite and oxidize, which is largely influenced by its volatile chemical composition. Coal's reactivity is affected by the developed method of ETCPF in order to increase combustion stability and intensity. In this context, low-reactivity fuels interact with the high-temperature combustion products produced by highly reactive fuels, such as gaseous fuels or fuel oils. The two-phase (solid-gas) fuel mixture consists of carbon monoxide (CO), hydrogen

(H_2), unreacted particulates, coke residues, and inert components such as water vapor (H_2O), carbon dioxide (CO_2), and nitrogen (N_2). Among the processes classified in the second group, pulverized coal is divided into two unequal parts, the smaller of which is then thermally prepared and the larger is then pulverized into powder. The stabilization of pulverized coal flames with highly combustible gaseous fuels was studied via both complete and partial gasification of low-grade coal.

The principal goals of the present study [26, 57] were to minimize fuel oil consumption during the combustion of low-grade coal and to mitigate the adverse effects associated with burning coal and fuel oil simultaneously within the same furnace chamber. Subsequent advancements in electrothermochemical preparation techniques enabled the development of a method that entirely eliminates the need for fuel oil by employing a plasmatron to heat and stabilize the combustion of the auxiliary fuel stream [12].

In many cases, electric arc plasma exhibits superior energy efficiency relative to traditional combustion methods. This enhanced efficiency is attributed to the plasma's elevated energy density and its rich composition of chemically active species (including atoms, radicals, ions, and electrons) which substantially facilitate the electrothermochemical reactions between coal and oxidizing agents. Consequently, this leads to a more rapid and comprehensive combustion process within the torch. Furthermore, electrical energy offers broad versatility in its applications. More importantly, it can be generated from both renewable and non-renewable energy sources, which guarantees an optimal energy consumption structure causing negligible harm to the environment. The utilization of electricity in fuel-electric processes preserves the inherent benefits of electrical energy while simultaneously imparting new characteristics to the natural coolant (most notably elevated enthalpy and enhanced chemical reactivity) attributes that are difficult to achieve through conventional techniques.

Plasma burners employ two distinct heat sources: the energy provided by low-temperature plasma to initiate ignition of the pulverized coal flame, and Joule heating produced either by an electric current flowing through carbon-containing materials within an electric fluidized bed or via ohmic resistance in resistor-type electric igniters. Numerous configurations of pulverized coal burners have been developed both domestically and internationally. The conversion of electrical energy into electric arc discharge energy can significantly enhance the ignition process and stabilize the combustion of solid fuels. Pioneering contributions to this field were made by researchers such as Blackburn P.R. and Reason I. from England, Cioffi P.L. and Tuppenny W.H. from the USA, as well as Duverger D. and Ashard I.L. from Canada [58, 59].

The preceding review of the current challenges in solid fuel recycling demonstrates that, in recent years, diverse methods of electrothermochemical preparation, gasification, and integrated fuel processing have been developed with the aims of enhancing combustion efficiency and minimizing environmental impact. An innovative plasma-coal burner (PCB) represents a highly effective alternative to conventional burners, utilizing coal dust as fuel. This system replaces traditionally

used highly reactive fuels (such as fuel oil or natural gas, with solid fuel). The operational principle of the PCB consists of heating the coal dust-air mixture with electric arc plasma to temperatures adequate for coal devolatilization and partial gasification of the remaining coke. As a result, the original coal is transformed into a highly reactive dual-component fuel (comprising combustible gases and coke residue) which facilitates stable ignition and sustained combustion within the boiler furnace.

When pulverized coal is burned with plasma guns, the devolatilization and ignition of coal are accelerated very quickly, resulting in little impact on the environment [60]. The electricity generated by the plasmatron is utilized as low-temperature plasma energy to ignite the pulverized coal flame. The transformation of electrical energy into electric arc discharge energy facilitates a more efficient ignition and stabilization of solid fuel combustion.

Examine the interaction dynamics between electric arc plasma and an air mixture within a confined cylindrical channel engineered to reduce energy dissipation. When a flow of relatively cool air-mixture (ambient temperature ranging from 350 to 400 K) encounters the plasma jet emitted by the plasma torch nozzle, both coal and air particles undergo simultaneous heating. Notably, only about 3 to 5% of the air mixture initially infiltrates the interaction zone, a restriction imposed by the inherent thermophysical limits of the compact plasma torch operating inside the burner chamber.

If the air is heated solely by the plasma source, coal particles up to 250 microns in size experience rapid thermal shock at heating rates of 10^3–10^4 K/s, resulting in thermal stresses within the particle volume. Consequently, the coal particles disintegrate into 8–10 fragments within 0.01–0.05 seconds. This fragmentation causes a sharp increase in the gas-solid interface area, thereby enhancing the reactivity of the air mixture. Volatile components released from coal fragments include gases such as N_2, H_2O, CO, CO_2, CH_4, and C_6H_6, along with nitrogenous compounds like pyrole (C_4H_5N) and pyridine (C_5H_5N), are released from these fragments.

Subsequently, atomic species such as oxygen (O), hydrogen (H), nitrogen (N), carbon (C), and sulfur (S) are generated in the gas phase, along with mineral alements including silicon (Si), aluminum (Al), and calcium (Ca), as well as reactive radicals like NH, CH, CN, and OH. The gas phase also contains free electrons (e), positive ions (C^+, H^+, N^+, CO^+, O^+, Si^+, K^+, etc.), and negative ions (O^-, H^-, N^{+2}). The swift thermal decomposition, often described as a thermal explosion, of pulverized coal particles markedly enhances the release of volatile compounds. This acceleration is attributed to the enlarged reactive surface area and the generation of ultra-fine particles (less than 5 μm), which heat up and emit volatiles at a much faster rate compared to larger particles measuring 50–100 μm.

Interactions between plasma and pulverized coal fuel enhance the energy efficiency of plasma-coal burners by a factor of three to four compared to conventional combustion processes [61]. Furthermore, the high temperatures generated by the plasma torch and the resulting temperature gradients within the

plasma-coal burner necessitate careful consideration of the behavior of the mineral matter present in the fuel.

Figure 1.4 demonstrates that the success of emerging plasma technologies largely depends on the advancement of computational methods capable of analyzing the processes and equipment involved. The progress in computational techniques is intrinsically linked to comprehensive investigations of thermophysical and thermochemical phenomena across theoretical, numerical, and experimental domains. Consequently, the development of plasma technologies necessitates sophisticated physical and chemical modeling based on the insights gained from these studies

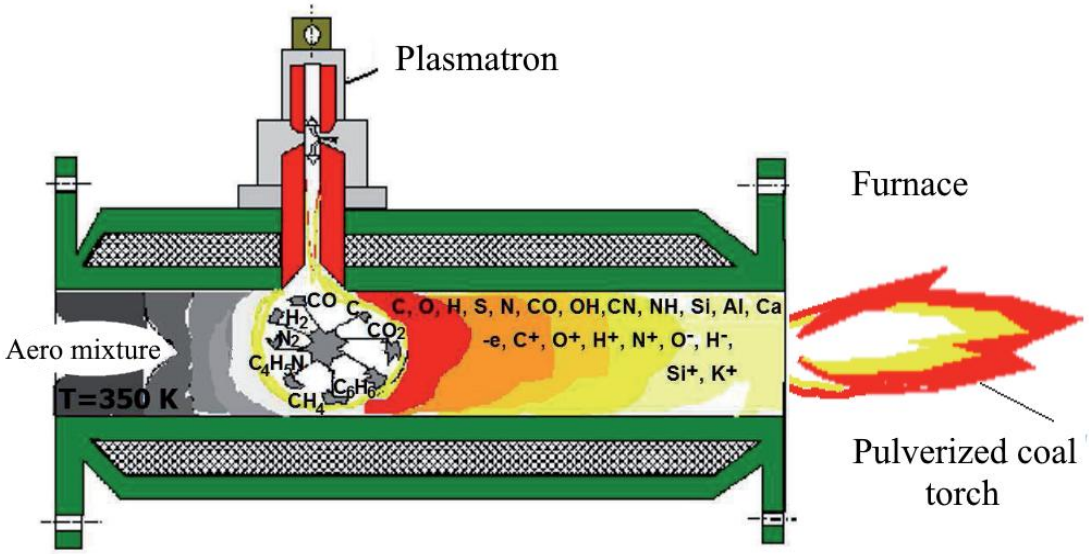


Figure 1.4 – Schematic representation of a plasma-coal burner (PCB) illustrating the stabilization process of ignition and combustion in a pulverized coal flame [61]

The operation of boilers using heavy oil burners adversely impacts the environment due to elevated emissions of heavy hydrocarbons and soot. Furthermore, they are more expensive than other fuels, which leads to high fuel prices. The installation and maintenance of heavy oil plants are also expensive and technically complex. Keeping the fuel oil fluid requires more energy in the latter case.

In boiler furnaces, heavy oil generates 30% of the total heat volume. The combustion of coal and heavy oil in the specified proportions leads to severe corrosion of boiler screen tubes at elevated temperatures, chemical underburning, and increased pollutant emissions (with fuel oil containing approximately twice the sulfur content of coal). This process causes a significant reduction in the burnout efficiency of solid fuel particles, resulting in unburned residues being discharged with flue gases and ash, and contributes to a higher incidence of superheater failures.

Table 1.4 presents a comparative analysis between conventional heavy fuel oil burners and innovative plasma-coal burner technologies used for fuel combustion in boilers.

Table 1.4 – Technical Specifications of the Plasma Torch

Fuel oil-based conventional technology	Plasma-based modern technology
1. Fuel oil consumption levels in TPPs across Kazakhstan and Russia	
Approximately 6.1 million t/year	0
2. Capital expenditures (Capex) for TPPs	
100%	5%
3. Operating expenditures	
100%	28 – 30%
4. Electricity consumed for in-house operations of TPPs	
3 – 5%	0.5 – 1.0%

With plasma technology, low-grade coals are ignited and burned efficiently, environmentally safely, and at a relatively low cost. In the heat treatment chamber, coal particles and air are mixed and heated by combustion with an electric arc plasma. Regardless of coal quality (different humidity, volatile matter output, and ash content), this technology ensures reliable operation. High-energy-density plasma is characterized by a high concentration of chemically active electrons, atoms, ions, and radicals. This promotes more complete and rapid combustion of the pulverized coal jet, thereby enhancing the electrothermochemical preparation of both the coal and the oxidizer.

An innovative plasma combustion technology for solid fuels, also known as fuel-free boiler ignition, was showcased at EXPO-2017 in Kazakhstan. The internal mechanisms of the plasma-coal torch involve rapid chemical and physical interactions between the plasma and pulverized coal. These interactions facilitate the thermal decomposition of coal particles, the release of volatile compounds, and ultimately the ignition of the coal fuel, resulting in a stable pulverized coal flame.

In a plasma coal burner, a plasmatron ensures the whole process of plasma ignition and combustion. When coal dust and air are mixed as a dual-component fuel, they do not lack oxygen when mixed together. Electric arc plasma serves as both an oxidizer and heat source, creating a chemically active environment at elevated temperatures. Consequently, coke residues are partially gasified and volatile substances are released.

The application of PCBs in TPPs offers multiple benefits. These include enhanced flame stabilization, oil-free ignition of pulverized coal boilers, and a significant reduction in both unburned carbon and nitrogen oxide emissions during combustion. Within PCBs, the fuel-air mixture is exposed to an electric arc plasma, which elevates the temperature to levels sufficient for coal devolatilization and partial gasification of the remaining carbonaceous material. This plasma-assisted thermochemical treatment facilitates the formation of a reactive mixture comprising combustible gases and highly reactive coke particles, regardless of coal quality. Furthermore, incorporating polyurethane foam into this process has demonstrated the potential to lower nitrogen oxide and unburned carbon emissions by around 50%, while carbon dioxide emissions are reduced by approximately 1–2%.

Plasmatrons generate low-temperature plasma, a medium characterized by a high concentration of electrons, ions, atoms, and radicals, enabling the release of significant energy within a confined volume. This unique environment enhances the physical and chemical reactions involved in coal dust combustion. This modern type of burner is specifically designed for fuel-free boiler ignition, wherein coal dust is ignited by ionized gas heated by low-temperature plasma to temperatures ranging from 3300 K to 5300 K.

There are a wide range of applications of plasma technologies in the field of energy that are limited by the lack of basic knowledge of physics. These include the interaction of plasma with coal particles and the potential negative impact plasma systems may have on the operation of municipal boilers [62].

The development and implementation of direct current (DC) plasmatrons for igniting boilers and pulverized coal flames were pioneered by Academician Mikhail Zhukov and Doctor of Technical Sciences Vladimir Messerle, who currently serves as a professor at al-Farabi Kazakh National University and leads the Plasma Chemistry Laboratory at the Institute of Combustion Problems. In the late 1990s and early 2000s, Professor Messerle designed and commissioned powerful DC plasma torches at thermal power plants across Kazakhstan, Russia, Ukraine, Mongolia, China, Korea, Slovakia, and Serbia. He holds several innovations in this field, including the introduction of a propane-butane gas mixture supplied to the plasma torch's interelectrode space to extend electrode service life. This process led to the formation of a nanostructured protective composite coating on the electrodes, significantly enhancing the reliability of the technology by protecting the plasmatron electrodes against erosion and high-temperature damage.

Over recent decades, plasma ignition technology for coal has seen significant global advancement. Today, DC plasma torches with power ratings of 250 kW, 300 kW, and above are widely and successfully employed in countries such as China and the USA. Meanwhile, Europe is gradually reverting to coal fuel amid the emerging gas crisis.

In plasma-assisted combustion systems, a mixture of air and pulverized coal is heated to temperatures between 1180 K and 1580 K, with the specific range depending on the quality of the coal used. At these elevated temperatures, thermochemical reactions lead to the generation of a highly reactive dual-component fuel composed of combustible gases and residual coke particles. This reactive mixture undergoes spontaneous ignition when it comes into contact with the secondary air stream, which functions as the oxidizing agent within the boiler environment [63].

Compared to coal combustion, fuel oil combustion generally occurs at higher temperatures and under conditions of excess air, largely due to the higher chemical reactivity of fuel oil. These conditions favor the formation of nitrogen oxides through both thermal and fuel-bound mechanisms. Furthermore, heavy fuel oil contains substantially more sulfur than coal, leading to increased sulfur oxide emissions. Another issue is the presence of vanadium in fuel oil, which can oxidize to vanadium pentoxide (a compound known for its carcinogenic properties).

Vanadium also accelerates high-temperature corrosion of heat-exchange surfaces, a problem that is rarely encountered in coal-fired systems due to the typically low vanadium content of coal.

Heavy fuel oil is generally more expensive than traditional coal fuel. Consequently, employing PCB for ETCPF allows for a rapid return on investment, as coal dust effectively replaces the previously utilized heavy fuel oil. On average, plasma-based systems designed for oil-free ignition of pulverized coal achieve payback within 12 to 24 months.

Multiple studies [64 – 66] have demonstrated that, when carbon is present in the fuel, the formation of carbon monoxide (CO) and nitric oxide (NO) predominantly takes place in the zone where the primary fuel jet exits the burner. However, the spatial distribution of NO concentrations within this area is not uniform, reflecting the complexity of NO formation mechanisms and the role of plasma activation in influencing these processes. In a highly reactive dual-component flow, the CO concentration tends to increase inversely with the intensity of the plasma-activated flow, reaching its peak across the burner's cross-sectional area as plasma activation intensifies. Overall, the use of plasma burners leads to a reduction in the total concentrations of both NO and CO at the exit of the combustion zone. An additional capacity utilization of the thermal power plant is used to reduce harmful CO emissions.

Professor Howarth noted that coal burning emits more carbon dioxide than natural gas burning, but methane emissions more than offset this difference. Considering that methane is more than 80 times more powerful as a greenhouse gas than carbon dioxide over a 20 – year period, even small methane emissions can play a significant role in climate change. The gas production process was characterized by leaks of methane at every step. A rapid transition away from fossil fuels, including natural gas, is increasingly being called for by climate policy leaders [67].

1.3 Mathematical modeling of plasma ignition of thermal coals

The ignition and combustion characteristics of fuel can be determined using a number of mathematical models as well as experiments. Each approach typically employs a highly simplified representation of the initial interaction between cold air (T = 290–300 K, consisting of primary air and coal particles) and the plasma torch. A broad body of research has proposed mathematical models capable of delivering both qualitatively and quantitatively accurate results, provided that suitable process parameters are applied. Nevertheless, the complexity and high computational cost of these models often limit their practicality for use in parametric numerical analyses. Typically, such computational models incorporate the following components:

- Governing equations for heat and mass transfer between coal particles and the surrounding gas phase;
- An Arrhenius-based formulation to estimate the release rate of volatile matter from coal particles;

- Equations describing the thermochemical interactions of species released into the gas stream.

The model describes a two-phase chemically reactive flow consisting of coal particles and air, with the optional inclusion of an internal heat source (such as an arc plasma torch, electric arc, or microwave plasma torch) distributed throughout the flow field. In the PICS processes, the gas and solid particles are uniformly mixed and pass through a cylindrical channel containing a plasma torch. The plasma heat source elevates the temperature of the gas, thereby transferring heat to the suspended coal particles. Once the particles reach their volatilization temperature, volatile components begin to transition into the gas phase according to their kinetic behavior.

The model operates under several simplifying assumptions: coal particles are assumed to be isothermal, while ash is modeled as an inert, non-reactive component; and the system is assumed to be quasi-stationarity and one-dimensional. Additionally, interactions between individual particles are neglected. The pulverized coal stream is heated through direct contact with the hot gas, which is itself heated by plasma interacting with the coal-air mixture.

The plasma-assisted combustion of coal in the presence of an oxidizer initiated by an electric arc is modeled through classical differential equations. The model utilizes one-dimensional differential equations to describe the conservation of momentum and energy for each fraction of coal particles as well as for the gas phase.

The equation governing momentum conservation in the gas phase is expressed as follows:

$$u\frac{d(\rho u)}{dx} = -\sum_{l=1}^{L} F_l, \tag{1.2}$$

where u and ρ denote the velocity and density of the gas phase, respectively. The term $F_l = C_{Dl}\frac{\rho(u-u_l)^2}{2}\pi R_l^2 N_l$ represents the aerodynamic drag force acting on particles of dimensional fraction *l*. In this expression, C_{Dl} is the drag coefficient for particles of fraction *l*, while R_l and N_l refer to the radius and the number of particles in that fraction, respectively.

The following equation represents the momentum conservation for coal particles in fraction *l*:

$$m_l u\frac{du_l}{dx} = F_l, \quad l = 1,2\ldots L, \tag{1.3}$$

where m_l and u_l represent the mass and velocity of particles belonging to a specific fraction, respectively.

Energy conservation in the gas phase can be expressed by the equation below:

$$\rho u\frac{dI}{dx} = \sum_{i=1}^{k} \rho u\frac{dn_i}{dx} I_i - \sum_{i=1}^{L} \Delta Q_l + \Delta Q_r + \Delta Q_p, \tag{1.4}$$

where the term $\Delta Q_l = \alpha_l(T_g - T_l) \cdot 4\pi R_l^2 N_l$ represents the heat transfer between the particles and the gas phase. Here, ΔQ_p and ΔQ_r are the contribution of energy from the electric arc of the plasmatron and the thermal effect of the volatile release reaction of coal, T_g and T_l are the temperatures of the gas and the particles of fraction l, respectively. Thus, n_i and I_i correspond to the gas phase concentration and enthalpy of the i-th component, α_l is the heat transfer coefficient for particles.

The energy conservation equation for coal particles of fraction l is formulated as follows:

$$\rho u \frac{dI_l}{dx} = \Delta Q_c + \Delta Q_l, \quad l = 1,2 \dots L, \tag{1.5}$$

where ΔQ_c denotes the heat released by the carbon combustion reaction.

Based on the drag force equation for spherical particles, the drag coefficient is defined as a function of the Reynolds number (Re), which quantifies the relative velocity between the particle and the fluid, and is given by the following expression [68, 69]:

$$C_{Dl} = \begin{cases} \frac{24}{\mathrm{Re}_l}\left(1 + 0.15\mathrm{Re}_l^{0,687}\right), & \mathrm{Re}_l = \frac{2(u-u_l)R_l}{\nu} < 1000 \\ 0.44 & \mathrm{Re}_l \geq 1000 \end{cases}. \tag{1.6}$$

The heat transfer coefficient $\alpha_l = \frac{Nu_l \lambda}{2R_l}$ is calculated using the Nusselt number correlation, which is applicable to laminar flow conditions around a spherical particle, and is given by:

$$Nu_l = 2 + 0.03\mathrm{Re}^{0.54}\mathrm{Pr}^{0.33} + 0.35\mathrm{Re}^{0.58}\mathrm{Pr}^{0.35}, \tag{1.7}$$

where Nu_l and Pr represent the Nusselt and Prandtl numbers, respectively, for particles of fraction l.

The equation governing the flow rates of the aeromixture and the plasma-forming gas is given by:

$$\frac{dm_{air}}{dt} + \frac{dm_{plasma}}{dt} = \frac{\rho u \pi d_c^2}{4}, \tag{1.8}$$

where $\frac{dm_{air}}{dt}$ and $\frac{dm_{plasma}}{dt}$ are aeromixture (primary air + coal) and plasma-forming gas (air) flow rates, accordingly, d_c is the diameter of the channel.

The term $\sum_{j=1}^{k} \rho u \frac{dn_j}{dx} I_j$ represents the main energy input responsible for heating the gas phase, originating from the combustion of volatiles in the oxygen present within the air mixture. This contribution is calculated through a stepwise determination of the equilibrium composition of combustion products along with the

incremental mass of coal volatiles. Such an approach considerably reduces complexity by eliminating the need to explicitly simulate numerous individual chemical reactions, thereby enabling more efficient parametric analysis.

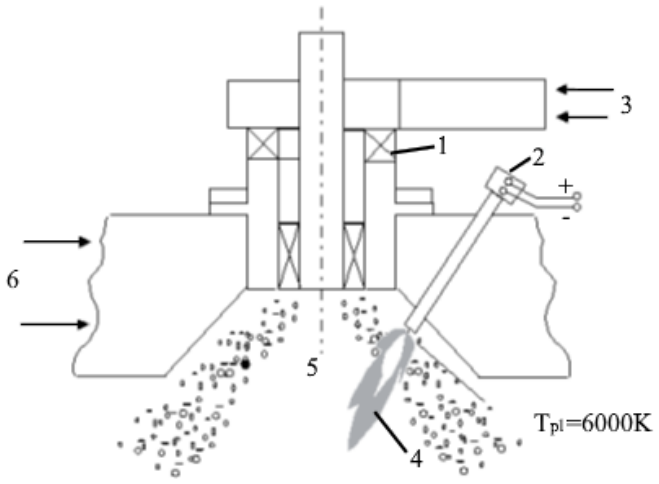
The release of volatile matter from coal can be modeled using a first-order Arrhenius-type expression as follows:

$$\frac{dn_j}{dt} = K_j C_j C_k, \text{ where } K_j = A_j \exp\left(-E_{ij}/(RT_l)\right), \quad (1.9)$$

where A_j represents the pre-exponential factor, E_{ij} denotes the activation energy (expressed in kJ/mol), T_l is the temperature of the particle *l*, and *R* corresponds to the universal gas constant [70].

1.4 Statement of the problem of numerical and experimental investigation of a plasma-coal burner

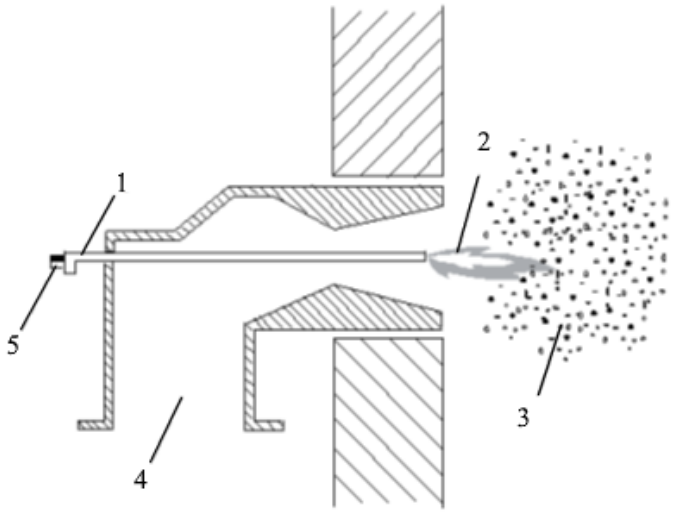
The first industrial test of plasma-assisted ignition of a pulverized coal torch was conducted by F. Blackburn in 1978 at a 200 MW unit at the Marietta TPP (USA) [71]. Blackburn's method utilizes a plasma jet with temperatures ranging from 5700 to 6000 K (Great Britain, 1978). In Figure 1.5, the plasma jet enters the combustion space at the root (base) of the pulverized coal fuel torch. In tests using a 200 MW unit (TPP «Marietta», USA), plasma ignition was six times more efficient than traditional fuel oil ignition. Coal ignition was successfully achieved using a plasma torch with a power of 109 kW at a mass flow rate of 0.4 kg/s and a calorific value of 25.4 MJ/kg. F. Blackburn estimated that for a 200 MW boiler, the required plasmatron power would be approximately 1 MW, compared to over 6 MW for a conventional oil igniter.



1 – Pulverized coal burner, 2 – plasma torch, 3 – air mixture, 4 – plasma jet, 5 – combustion space, 6 – air mixture

Figure 1.5 – Scheme of ignition of a pulverized coal torch by a plasma jet according to the F. Blackburn method [71]

As shown in Figure 1.6, Babcock-Wilcox modified Blackburn's method by using a plasma ignition system instead of an oil nozzle [72]. The plasma torch had a power of 125 kW. Lakewood Thermal Power Plant in Canada (1980) tested the system. Plasma torch operating costs are 28 percent lower than fuel oil combustion systems, and plasma torch energy efficiency is five to six times higher than fuel oil systems, according to tests.



1 – Plasma torch, 2 – plasma torch, 3 – pulverized coal torch, 4 – air mixture supply, 5 – electricity

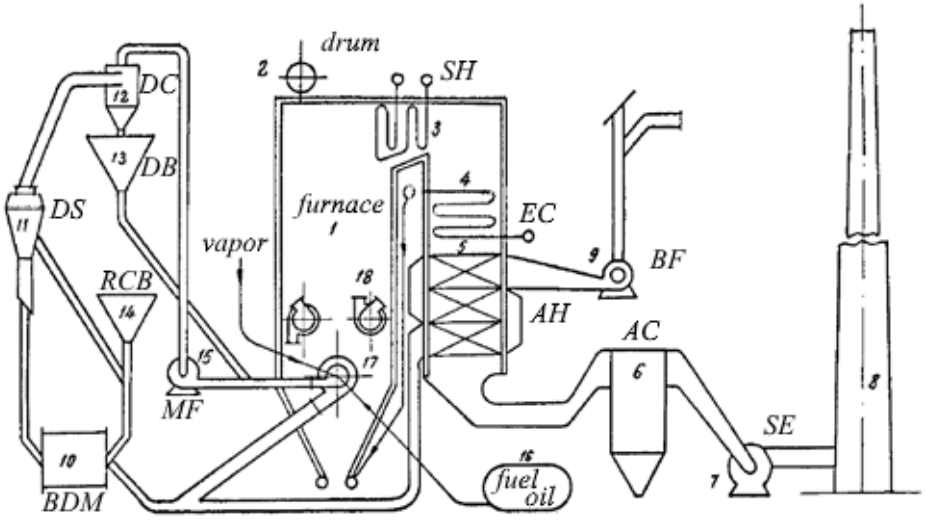
Figure 1.6 – Diagram of ignition of a pulverized coal torch from Babcock-Wilcox [72]

In relation to various thermal coals, the plasma ignition scheme proposed by F. Blackburn and other foreign scientists was studied at the Kazakh Research Institute of Energy named after academician Sh. Chokin. The plasma source was a single-chamber linear plasmatron (designed by the Siberian Branch of the USSR Academy of Sciences). A plasma jet torch operating at a power range of 17–22 kW and a coal feed rate of 400 kg per hour ensured stable ignition of the plasma jet. The torch’s power corresponds to approximately 0.75–1% of the total system power. Placing an electric arc directly into the pulverized coal stream can improve the energy efficiency of the plasma ignition process [73]. A series of experiments on the ignition and stabilization of combustion using plasma jets and an open electric arc were conducted by employees under the leadership of M.F. Zhukov [74, 75].

As opposed to direct ignition of coal dust at the base of the torch by plasma jets [76, 71] or at the exit from the burner into the combustion space by a long plasma torch [77]. It is most energy-efficient to use plasma technology for oil-free ignition, based on the separation and electrothermochemical preparation of fuel (ETCPF) for combustion using electric arc plasma [78, 79].

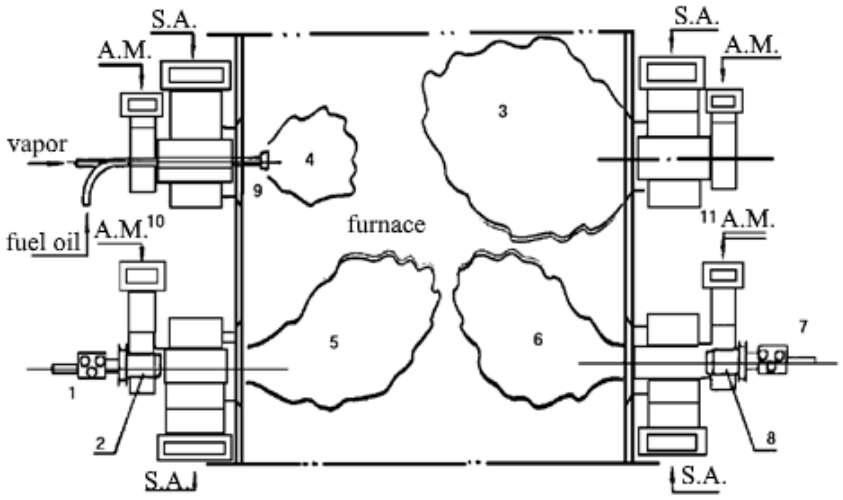
Figure 1.7 illustrates a plasma igniting coals using a boiler with 230 t/h steam capacity, burning low-reaction coal (anthracite). In Figure 1.8, a plasma torch is installed as a substitute for the fuel oil nozzles (labeled 9) using plasma technology.

The diagram depicts the operational principle of a coal-fired plasma system, which fundamentally relies on the plasma thermochemical treatment of the fuel before combustion. Using plasma thermochemical preparation, pulverized coal fuel torches 5 and 6, which were previously prepared for combustion in burners 10 and 11, ignite the main pulverized coal fuel torches.



1 – furnace, 2 – boiler drum, 3 – steam superheater, 4 – economizer, 5 – air heater, 6 – ash catcher, 7 – smoke exhauster, 8 – chimney, 9 – blower fan, 10 – ball drum mill, 11 – dust separator , 12 – dust cyclone, 13 – dust bunker, 14 – raw coal bunker, 15 – mill fan, 16 – fuel oil supply system, 17 – oil-steam nozzle, 18 – double-scroll heating pad

Figure 1.7 – Diagram of a boiler unit with a steam capacity of 230 t/h [78]



1, 7 – plasmatrons; 2, 8 – ETCPF chambers; 3 – oil-dust torch; 4 – fuel oil torch; 5, 6 – pulverized coal torch with plasma stabilization; 9 – fuel oil nozzle; 10, 11 – main pulverized coal burners; A.M. – air mixture; S.A. – secondary air

Figure 1.8 – Cross section of the combustion chamber of a boiler equipped with a coal plasma ignition system [79]

The Kazakh Scientific Research Institute of Energy (KazNRIE) conducted the first tests in 1989 using electric-arc coaxial DC plasmatrons with graphite cathodes to fire the boiler of Ust-Kamenogorsk TPP without oil. Additionally, heating oil was completely eliminated [78]. Combined with primary air, Kuznetsk coal was fed into a 65 kW plasma torch muffle burner. Pulverized coal torch ignited instantly and burned steadily. A thermocouple measured the temperature at the outlet of the ETCPF chamber at 1400 K. This resulted in a 0.5 – 0.7% energy consumption for the plasma torch during firing.

Erdenet Thermal Power Plant's boiler (Republic of Mongolia) is also equipped with plasma fuel-free kindling [80]. For fuel, Mongolian brown coal was used. The tests were designed to simulate boiler firing modes from hot and cold states using the plasma system of the main burner. The first step was to ignite the plasma torch on the muffle and feed dust from a nearby boiler's hopper. Upon entering the electrothermochemical preparation chamber, the dust ignited. The outlet temperature was measured with an optical pyrometer, and the torch temperature was 1390 – 1450 K. The plasmatron was turned off after 30 – 40 min. During the subsequent kindling, the burner's heating was sufficient to ignite the dust autothermally.

Tests of plasma stabilization of combustion of Donetsk AS were conducted on the boiler of Mironovskaya State District Power Plant [78]. A 400 kW coaxial plasma torch with ETCPF chambers was installed on two vortex burners, where 20% of the air mixture was supplied from the flow rate. At the outlet of both burners, the dust-coal mixture was 1200 – 1300 K. There was a 1.5 – 2% relative energy consumption per plasmatron. Fuel oil was saved by 55% for lighting.

At the Gusinoozerskaya State District Power Plant (Republic of Buryatia), plasma ignition tests were conducted on a boiler with a steam capacity of 640 t/h [81]. The pulverized coal-air mixture ignited simultaneously with the introduction of coal dust into the burner upon activation of the plasma torch. Combustion was sustained throughout all sections of the chamber, with temperatures ranging from 1300 to 1600 K. Initially, the plasmatrons operated at a power level of 60 kW. Tugnui coal dust can be reliably ignited by plasma in a cold industrial boiler, according to tests. After approximately 30 minutes of chamber warm-up, the plasma torch power was reduced to 35 kW. Notably, no significant decrease in flame brightness was observed when the plasma torch was turned off temporarily for periods between 15 and 25 minutes.

A plasma torch with a electrothermochemical preparation chamber was tested consistently when burning Korean anthracite in the boiler of the East Pyongyang Thermal Power Plant (Korea) from a cold state [82]. For oil-free kindling, plasmatrons with a power of 400 kW were installed in two vortex burners. At the outlet of the burners, intense combustion of fuel was observed at a temperature of 1500-1600 K. The plasma torch consumed 2% of the total energy consumed by the burners.

In the Baodi State District Power Plant (China), a plasmatron with a graphite cathode powered by 200 kW was used for fuel-free firing of a boiler using lean hard

coals [79, 83]. Using a high-voltage AC plasmatron with a power of 50 kW, industrial tests of plasma stabilization of coal combustion were conducted at the Bishkek Thermal Power Plant [74, 81]. Over 50 hours were spent on the tests. Pulverized coal flame temperature and fuel oil savings for lighting reached 1600 K and 35%, respectively.

The Almaty CHPP-3 conducted five industrial tests on oil-free kindlings from a cold state from May 30 to July 30, 1996 [84]. The Ekibastuz coal burned with the following characteristics: 12.2 MJ/kg calorific value, 25% volatile yield, 45% ash content, 5.4% moisture content, and 12 – 15% grinding fineness R_{90}. The lower and upper burners were equipped with plasmatrons (three in total) for oil-free kindling. Approximately the same conditions were used for all kindlings. Testing showed that two plasma torches were sufficient for kindling. A reduction in energy costs and an increase in economic efficiency were achieved by eliminating the third plasma torch from the oil-free kindling process. A kindling was also carried out with the partition removed in the electrothermochemical preparation chamber of the lower burner in accordance with the test and research program.

It took 2-3 seconds for the torches to ignite in the cold combustion space in the electrothermochemical preparation chamber. The pulverized coal torch entered the combustion space at an exit temperature of 1500 – 1600 K, and its length was 5 – 6 m. A bright yellow torch core was visible in the middle of the firebox. A cold firebox without a partition in the ETCPF chamber caused the torches to ignite slowly and unsteadily within 20 – 30 s. The pulverized coal torch's length and temperature decreased to 2 – 3 m and 1200 – 1300 K, respectively. After 3.5 h of lighting, the boiler reached its operating parameters. The two remaining pulverized coal burners have been started without plasmatrons, and the boiler unit has been connected to the main steam pipeline. Boiler heating has been completed. Having stabilized the combustion of the pulverized coal torch in the furnace, the plasmatrons were turned off one by one once the boiler was in a stable operating mode. The plasmatron units performed reliably during the tests. The tests confirmed that oil-free heating of boilers was technically feasible and energy efficient. The development and optimization of plasma technologies for oil-free coal ignition is currently underway in the CIS countries and abroad. From 1989 to 1997, industrial-scale experiments and pilot applications of technologies such as electrothermochemical fuel preparation, plasma-assisted ignition, coal gasification, and combustion were conducted across multiple countries, including Kazakhstan, China, Russia, South Korea, Mongolia, Ukraine, and Kyrgyzstan [84].

Advancement in thermochemical coal conversion technologies (encompassing electrothermochemical preparation, gasification, and integrated processing) primarily depends on information obtained through a combination of theoretical studies, computational simulations, and experimental verification. This comprehensive methodology enables the determination of optimal operating regimes as well as the specification of essential design characteristics for process equipment.

Theoretical and computational research methods are conventionally classified into three principal categories: heat and mass transfer modeling, thermodynamic analysis, and kinetic simulations of chemical reactions. Thermodynamic analysis makes it possible to determine fundamental parameters of the working medium (such as specific energy consumption, efficiency of target product formation, and the composition of by-products) under idealized equilibrium assumptions. In real systems, however, such equilibrium states are seldom achieved, since actual thermochemical processes typically diverge from ideal thermodynamic behavior. To adequately describe these deviations, kinetic modeling that explicitly accounts for heat and mass transfer phenomena within the system is applied.

In the development of technological processes (especially those of a novel nature) the initial stage typically involves a comprehensive evaluation of their thermodynamic characteristics [23, 84 – 90]. Such an analysis makes it possible to establish boundary values of key parameters and to exclude, at an early stage, solutions that are technically impracticable or conceptually inconsistent. This approach is justified under the assumption that the rates of chemical kinetics as well as heat and mass transfer are close to their maximum potential levels.

Various combinations of the fundamental laws of thermodynamics are used in thermodynamic analysis. A common method of calculating the equilibrium composition of ignition products and stabilizing solid fuel combustion in chemical thermodynamics [76 – 78] relies on the equations of chemical reactions of the processes under consideration for determining isobaric-isothermal Gibbs potential ($\Delta G_T^0 = \Delta H_T^0 - T \cdot \Delta S_T^0$):

$$\ln K_p = -\Delta G_T^0 / RT, \tag{1.10}$$

where ΔS_T^0 and ΔH_T^0 are changes in entropy and enthalpy of the system.

To determine the temperature dependence of concentrations, in the chemical reaction isotherm (1.1) is equal to the equilibrium constant expressed in terms of the equilibrium concentrations of the component (c_i) from the Guldberg and Waage law on mass action [87]:

$$K_p = \prod_i {c_i}^{n_i}, \tag{1.11}$$

where n_i are stoichiometric coefficients in the equations of chemical reactions.

The procedure for determining the equilibrium concentrations of components within a thermodynamic system involves several stages: (a) formulation of an independent set of chemical reactions that describe the pathways by which the system attains equilibrium; and (b) evaluation of the corresponding equilibrium constants using equations (1.10) and (1.11). In the case of coal–oxidizer systems, up to 25 chemical elements may be involved, giving rise to a highly complex reaction network that can encompass dozens of reactions and hundreds of equilibrium components [87].

According to the principle of maximum entropy, an isolated thermodynamic system reaches equilibrium when its entropy is maximized with respect to the available thermodynamic degrees of freedom. On this basis, a generalized approach can be employed for the analysis of heterogeneous multicomponent systems. Within this framework, the primary variables include the concentrations of individual constituents, along with key thermodynamic parameters such as temperature, specific volume, pressure, and enthalpy [87, 88].

In an isolated system, equilibrium arises through internal chemical reactions and phase transitions. By formulating the problem as an entropy maximization task subject to specific constraints (namely, the conservation of elemental mass, the requirement of overall charge neutrality, and the thermodynamic relationships among pressure, temperature, volume, and internal energy) the corresponding equilibrium parameters can be evaluated.

Consequently, there is no requirement to explicitly formulate chemical reaction equations or to calculate equilibrium constants through conventional approaches, such as those described in equations (1.10) and (1.11). It is therefore sufficient to include only two thermodynamic functions of individual substances when calculating equilibrium concentrations and other parameters: entropy (S_i^0) and total enthalpy ($J_i(T) = \Delta H_T^0(298) + \int_{298}^{T} C_{pi} dT$), which form a universal combination in all calculated expressions:

$$G_T^0 = \Phi_{\Pi i}^* = S_i^0 - \frac{J_i}{T}. \qquad (1.12)$$

Equation (1.12) defines the total isobaric–isothermal Gibbs free energy of the system. Applying the maximum entropy principle (formulated on the basis of the Nernst theorem (third law of thermodynamics) and combined with the conservation of mass and energy in an isolated system) enables the determination of the equilibrium composition of components in both gaseous and condensed phases. For this purpose, any thermodynamic function from the set T, p, S, J, U and V, together with the initial elemental composition of the medium, may be specified as input data. This methodology is particularly effective for investigating thermochemical transformations in the mineral and organic fractions of coal, with the mineral fraction consistently retained in the solid residue.

In [87, 88], the authors not only simplified the system of equilibrium equations and reduced the amount of data required for evaluating the thermodynamic properties of individual components, but also proposed a universal computational algorithm. This approach treats a thermodynamic system as a set of discrete substances, which allows the methodology to be applied beyond metallurgy to a wide range of scientific and engineering disciplines, including fuel utilization. As a result, the overall computational burden is significantly reduced, while the procedure becomes readily adaptable for computer-based implementation.

Equilibrium calculation methods based on the maximum entropy principle [87, 88] and those derived from the law of mass action [89, 90] exhibit a close

mathematical relationship. Under certain conditions, expressions for chemical equilibrium constants can be obtained directly from the interdependence between entropy and the concentrations of system components.

Taking advantage of these developments, the authors of [87, 88] introduced the ASTRA algorithm together with a universal software tool for thermodynamic calculations. This system was subsequently adapted and reimplemented as the TERRA software, optimized for the WINDOWS operating environment [91].

In the model developed by the authors [92], an attempt was made to take into account the role of an external heat source and the concept of modeling stages was introduced (dividing the burner into conditional design stages). The boundaries of the conventional stages at which portioned additional heat removal occurs are selected based on the achievement at the end of the stage of the maximum total concentration of combustible components in the gas phase ($CO + H_2 + CH_4 + C_6H_6$), formed as a result of ETCPF.

After performing the calculation of stage 1 with its initial conditions, they proceed to compiling the initial conditions for calculating stage 2, i.e., the final parameter values obtained at stage 1 serve as the initial conditions for stage 2, etc. The primary limitation of the stepwise heat supply method is the reaction mixture is the a priori choice of step lengths and the amount of pulverized coal mixture initially entering the reaction zone. For various coals, the specific energy consumption required for ETCPF has been practically determined.

The initial amount of the air mixture interacting with the plasma torch is selected based on the criterion of thermochemical transformations necessary to initiate. According to this calculation method, in principle, regardless of what power the plasmatron is used, it is possible to start the process of electrothermochemical preparation by only changing the length of the stages. At the same time, this technique is well suited for calculating specific burner devices.

While all the above models are one-dimensional (with the exception of [93]), in reality the processes of interaction between plasma and air mixture are three-dimensional, and the propagation of the reacting mixture along the axis of the reactor channel or burner device is two-dimensional for symmetry reasons (for cylindrical reactor geometries).

In the models considered, the interaction between the plasma torch and the air mixture was not explicitly simulated, although this process is critical for thermal preparation and combustion. Reference [94] presents a model that accounts for the plasma–air interaction along the reactor channel axis and the resulting distribution of the reaction mixture. Building on a mathematical model that incorporates the multiphase nature and polydispersity of the interaction between the pulverized coal–air mixture and the internal plasma source, a numerical method was established for studying plasma ignition processes and ETCPF for combustion.

Obviously from the above review, software packages capable of offering geometric and energy parameters of plasmatron-based burner devices with sufficient accuracy for engineering calculations have already been developed and are successfully used in PCB designs.

It is important to emphasize that the output characteristics of the PCB differ fundamentally from those of conventional pulverized coal burners. A torch of the reacting fuel mixture enters the furnace, which causes a change in the main parameters of the combustion process. In this regard, the optimization and study of the process of combustion of solid fuel in combustion devices, preliminary plasma ETCPF in the PCB for combustion and complex heat and mass transfer are of particular importance. The mechanics of multiphase media is one of the complex problems, and, despite the great interest and numerous studies of heterogeneous flows by researchers around the world, the current theory of multiphase turbulent flows is incomplete. This is due to two reasons. The first is that even the theory of single-phase turbulent flows of a continuous medium is currently far from complete. Secondly, the addition of a dispersed impurity in the form of particles to a turbulent flow significantly complicates the picture of a two-phase flow. First of all, this situation is associated with a large variety of particles and leads to the implementation of numerous flow regimes of a gas suspension.

A change in the concentration of particles, which is an important characteristic of heterogeneous flows, not only quantitatively changes the parameters of the initial movement and flow of particles, but also makes it possible to qualitatively change the configuration (for example, move from laminar to turbulent mode or vice versa, i.e. laminarize the flow). As a consequence, theoretical and experimental methods used in classical mechanics of single-phase continuums are usually not available for studying heterogeneous flows in principle. The available experimental data are often fragmentary and contradictory, and the developed physical concepts and mathematical models turn out to be unsatisfactory. The factors listed above limit the development of mechanics of heterogeneous media.

Flows of multicomponent mixtures differ significantly from homogeneous flows. In addition to the processes occurring in gaseous media (turbulence, compressibility, chemical reactions and others), there are additional mechanisms of intercomponent and especially interphase interactions (i.e. exchange of energy and momentum, phase transitions, rotation, collision and chaotic movement of particles) accompanying the movements of these media. The complexity of the problem is increased by the limited understanding of turbulent flow and the complex coupling between turbulent transport and chemical reactions, further complicated by the unique phase interactions occurring within reactive turbulent flows.

Turbulent flow of a heterogeneous (two-phase) medium has not been well studied either theoretically or experimentally. The first serious research in this direction was carried out by Laats M.K. [95]. In this work, the outflow of turbulent subsonic two-phase jets is experimentally simulated. The results showed that a two-phase jet expands much more slowly than a single-phase one. The main conclusion is that the mechanism of dissipation of inertial impurities differs significantly from the mechanism of dispersion of gaseous impurities. Subsequently, systematic experimental studies were carried out at the Institute of Thermophysics and Electrophysics of the Academy of Sciences of the Estonia under the leadership of M.K. Laats. In [96], comprehensive experimental investigations of two-phase jet

flows were conducted to examine how particle size (δ) and initial particle concentration (κ_0) affect the averaged properties of a turbulent jet. The use of an isokinetic sampling method enabled the simultaneous measurement of the mean longitudinal gas velocity $\overline{u}_g$ and the particle mass flux $G_p = \overline{\rho}_p \overline{u}_p$. The number of particles required for the axial velocity in a two-phase jet to decay more slowly than the axial velocity in a single-phase jet was determined. This is explained by the fact that in the absence of sliding in the initial section ($\overline{u}_g \approx \overline{u}_p$) in the main section of the jet, the particle speed does not have time to decrease as quickly as the additional acceleration of the carrier medium. This effect increases with increasing impurity concentration. In the main section, the gas jet expansion is only slightly affected by particle flow rate. In the initial section, higher particle concentrations slow the jet expansion, resulting in a longer and narrower two-phase jet, while the longitudinal gas velocity decreases more rapidly with increasing particle size.

When modeling two-phase flows, the problem of constructing an initial system of actual conservation equations arises. The system of equations for such flows was first and most clearly formulated by Rakhmatullin H.A. [97]. Its essence is that the state of each component of a heterogeneous mixture is described by partial densities, speed and energy.

A significant contribution to the construction of the original equations was made by Nigmatullin R.I. In his works [98], both a phenomenological approach and an approach based on averaging microequations were used to mathematically describe the movements of heterogeneous mixtures. In heterogeneous media, the laws describing the relative motion of phases are more complex. This is due to the fact that the movement is determined by the processes of interaction between phases as macroscopic systems, for example, the flow of a carrier liquid around particles of inclusions in a gas suspension. These processes are described by forces that provide a more consistent description of the phase inertia.

Based on this, the problem of multiphase motion within the framework of a multi-speed model is reduced to setting conditions for the joint determination of the quantities and motion of phases that describe interphase and intraphase interactions. In the general case, it is not possible to give an expression for the force for interphase interaction. This is due to the fact that the expression cannot be obtained even for the case of motion of a single sphere in a homogeneous flow of a viscous incompressible fluid with variable speed.

The patterns and nature of the averaged motion of particles are often influenced by aerodynamic drag, electrostatic and mass forces, the Magnus and Safman effects, turbo and thermophoresis. A more detailed discussion of the work on determining one of these forces - the drag coefficient - is presented in [99], which presents a review of work on determining the drag and heat transfer coefficients of particles when moving in a two-phase medium, where the influence of the thermal interaction of particles with gas on the two-phase flow is much less.

The majority of theoretical and experimental studies focused on determining the drag coefficient of a sphere pertain to the scenario of a solitary solid sphere moving through a viscous, incompressible fluid.

As is known, with a uniform flow around a single smooth non-deformable spherical particle in an unlimited flow of an incompressible isothermal medium, the drag coefficient C_D depends only on the Reynolds number $Re_p = 2r|\vec{u}_r|\rho/\mu$, where $\vec{u}_r = \vec{u}_g - \vec{u}_p$.

The dependence $C_D(Re_p)$ for these conditions (standard resistance curve) has been well studied, and many formulas of various types are given to approximate it. Let's look at some of them.

Stokes studied in 1851 the flow field created by a solid sphere in a uniform flow of a viscous incompressible fluid at very low relative velocities [100, 101]. One of the cases of integrating the Navier-Stokes equations: the inertial terms are used and the condition of adhesion of the liquid on the surface of a solid sphere is neglected. The resulting resistance force in this case is equal to $P = 6\pi\mu ru$. The value of P is determined two-thirds by frictional drag and one-third by pressure forces, which is undefined and is often referred to as Stokes' law for spherical drag. In this case, the resistance coefficient is equal to $C_D = \frac{P}{\rho u^2 \pi r^2/2} = \frac{24}{Re}$.

This is one of the drag coefficients of a sphere at low Reynolds numbers. When the Reynolds number exceeds unity, the analytical analysis of the flow field becomes considerably more complex due to the onset of boundary layer separation, resulting in the formation of a vortex region and wake. This occurs alongside an increase in inertial forces and a corresponding rise in Reynolds number in the rear portion of the sphere.

In the range of Reynolds numbers $1 < Re < 1000$, the possibilities for analytical studies of flows are sharply narrowed due to the influence of viscosity and inertial forces in the flow field, and data on the nature of the flow around a sphere and the drag coefficient of spheres can be obtained mainly experimentally. The resistance forces of spheres at medium and high Reynolds numbers have been determined experimentally by many researchers [99, 102]. Due to the complexity of standard resistance curves, it is impossible to express the $C_d = f(Re)$ relationship in a single equation that provides acceptable accuracy over the entire range of Reynolds number variations. In this regard, many authors [103] replace the standard resistance curve with a broken curve described by the following equation $C_{D_i} = \frac{A_i}{Re^{n_i}}$, $i = 1,2,\dots,l.$. Such dependencies are widespread and simple, convenient for integrating the equations of particle motion.

In the usual case, the Stokes ($A_1 = 24$, $n = 1$) and Newton ($A_2 = 0.44$, $n = 0$) dependences can be considered as a very rough description of the standard resistance curve. Most often, for better approximation, the standard resistance curve is divided into three or four segments. It has been established that the resistance force consists of two components - frictional resistance and shape.

Therefore, two-term formulas can be proposed for the resistance coefficient.

The formula proposed by L.S. Klyachko, convenient for integrating equations of motion, is widely known, giving good accuracy for $Re < 1000$ [103]:

$$C_D = \frac{24}{Re} + \frac{4}{Re^{\frac{1}{3}}} = \frac{24}{Re}(1 + 0.167Re^{0.67}). \quad (1.13)$$

It is well established that the drag force exerted on a spherical liquid particle moving relative to the surrounding medium is determined by considering the velocity profiles of both interacting phases.

A review of works on numerical modeling of two-phase flows [104] shows that full consideration of phase interactions even in the simple case of gas motion with suspended solid particles is currently a difficult task. All calculation schemes used to close the system of equations require certain assumptions. Let us dwell on the basic assumptions used in most of these studies:

1 The medium is a two-fluid medium. The actual gas flow carrying particles is modeled as the interpenetrating motion of the gas phase and a continuous medium representing the dispersed phase, which serves as an approximation for the behavior of discrete particles.

2 Absence of mass transfer: The flow involves no introduction of gas or particles, and no phase transitions occur within the system.

3 Heat exchange with the external environment is neglected; only convective heat transfer between the gas and particles is considered.

4 Viscous forces between the channel walls and the gas, as well as internal gas friction, are neglected; only viscous interactions between the gas and particles (interfacial effects) are considered.

5 The flow is assumed to be steady (time-invariant).

6 All particles are assumed to be uniform in size and do not interact with each other.

7 The parameters of particles and gas are constant in each cross section of the flow.

8 The influence of particles on creating environmental pressure is negligible.

9 Particles are spheres completely filled with particle «material».

10 Particle rotation is not taken into account.

11 The temperature gradient inside the particles is negligible, since the particle sizes are small and the thermal conductivity of their material is quite high.

12 When considering flows with a relatively low particle content in the gas, the particle volume can be neglected.

13 Gravitational and electrostatic forces are not taken into account. An important contribution to overcoming the problems associated with the closedness of the system of equations describing the outflow of a subsonic two-phase turbulent jet was made by works [105 – 107].

It has been demonstrated that the system of equations governing two-phase turbulent flows is inherently unclosed, as it involves fluctuations in the carrier phase velocities as well as correlations between the velocity and concentration fluctuations of the dispersed phase.

By employing different modeling approaches, a closed system of equations can be derived to describe the averaged motion of a gas containing particles. Among the most commonly used are the algebraic one-parameter (k) model, which is based on the transport equation for turbulent kinetic energy, and the two-parameter k-ε model, which incorporates transport equations for both the turbulent kinetic energy and its dissipation rate.

Algebraic models generally employ a semi-empirical formulation derived from Prandtl's turbulence theory. This category of models was further advanced in [106]. Among them, the widely utilized one-parameter (k) model is founded on the turbulent kinetic energy equation. The first attempt to use this model was made in 1977. A number of works [105] attempted to estimate the magnitude of the terms responsible for the dissipation of turbulence energy due to pulsating interphase sliding for different types of flows with particles.

In investigations of single-phase turbulent flows, the two-parameter k-ε turbulence model is the most commonly employed, utilizing the dissipation rate equation as the complementary governing equation. Development of a two-parameter k-ε model for turbulent two-phase flows began in the 1980s. Subsequently, a number of works were published [107] aimed at clarifying, generalizing and improving the two-parameter turbulence model for various conditions, and the authors in [105] developed a two-parameter model for an isothermal jet and a non-isothermal two-phase jet. This takes into account the radial and longitudinal slip of the phases, the Magnus force, the nonlinearity of the aerodynamic drag, and the rotation of particles. For volumetric concentrations of dispersed impurities $\alpha_p \sim 10^3$, it was found that additional dissipative terms ε_p, Φ_p significantly affect the pulsation characteristics of a two-phase jet. For a two-parameter model of a gas-droplet polydisperse jet, taking into account the processes of droplet fragmentation and coagulation, it was proposed in [108]. The only definition of the dynamic interaction of phases is the resistance force. This work [108] examines the dynamics of the distribution of parameters of the gas and dispersed phases throughout the entire area of particle motion. The calculations also encompass the stabilized flow region, where the impurity moves with a constant lag relative to the gas phase, influenced by physical parameters such as particle size, material density, and Reynolds number. We can mention work [109], which simulates a two-dimensional turbulent flow of a gas suspension in an inclined and horizontal channel based on a two-parameter k-ε turbulence model. For important dispersed phase and carrier equations, they are described by the Eulerian approach and their discretization is implemented using a semi-implicit numerical algorithm. The influence of particle diameter on the characteristics of turbulent flow is studied. Numerical calculations are compared with experimental data and satisfactory agreement is found.

In addition to the listed works using the "classical version" of the two-parameter model, the combined Eulerian-Lagrange approach has gained significant popularity. In this case, the parameters of the gas field are determined based on the k-ε model, and the characteristics of particle motion are determined by constructing

Lagrangian trajectories. This approach determines the characteristics of a dispersed medium quite well and tracks the trajectory of particles. In this area, the work [110, 111] attracts attention.

Saffar-Avval M.S. et al. [111] carried out one of the latest studies in which the two-dimensional turbulent flow of a gas suspension moving upward in a vertical pipe using the k-ε turbulence model is simulated based on the Euler-Lagrange approach. In this study, numerical calculations were carried out for different particle flow ratios and gas.

The results indicate that particle collisions significantly impact the flow structure within the developing region, with upward flow amplifying this effect, particularly influencing the intensity of gas turbulence and particle concentration levels. In addition, it is presented that the particle velocity and concentration profiles became uniform due to collisions between particles. This effect became more pronounced as expenditure ratios increased. In the region close to the wall, a strong increase in the particle vibration profiles in the direction of the flow is observed. It was found that the intensity of gas turbulence decreases due to collisions between particles, and this effect becomes more significant with increasing flow ratio.

In [112] and [113], extensive coverage is provided of the homogeneous flow of reacting gas mixtures and numerical modeling of turbulent plumes. Based on boundary layer equations [113] and parabolized Navier-Stokes equations [112], these works model turbulent combustion problems of unmixed gases in two dimensions.

In combustion processes involving gas mixtures within devices featuring complex geometries and confined spaces, the Navier-Stokes equations must be supplemented with one or more turbulence models to achieve closure. Based on the averaged Navier-Stokes equations, the three-dimensional turbulent flow of gas mixtures reacting in a combustion device is modeled in [114].

A number of numerical studies have been carried out in [115] relating to the calculations of the aerodynamics of some technological devices, including the combustion process inside combustion devices, in the context of comparisons of mathematical models of solid fuel ignition processes. In a pulverized coal torch, particle combustion is calculated using two interconnected components: first, the aerodynamics of the flow field is calculated, second, a system of ordinary differential equations is calculated that describes how the solid phase moves, and how an individual particle ignites in an annular combustion chamber. A particle motion equation only takes into account aerodynamic drag force in this case. The work emphasizes the use of semi-empirical theories of turbulence for closure in order to calculate turbulent flows based on averaged Reynolds equations in a cylindrical coordinate system. To solve the complex nonlinear partial differential equations in this study, the grid method is employed. Once the velocity field in the combustion chamber is determined from the gas-dynamics solution, the motion, combustion, and heat-transfer equations for a single coal particle can be integrated numerically. By substituting the values of the gas flow components into the system of equations for particles, the Runge-Kutta method is used to integrate the system of equations for

particles, taking into account the known initial conditions that correspond to the conditions in which the particles are introduced into the furnace.

In order to simulate real combustion devices, works devoted to the study of turbulent reacting flows of two-phase media are of particular interest. Here are some of them. According to works [116, 117], the authors propose a kinetic model of coal combustion based on the assumption that coal transformation is divided into three phases: pyrolysis of raw coal, combustion volatiles, and coke burnout. The coal combustion process is founded on the premise that raw coal undergoes pyrolysis, resulting in the release of combustible volatiles and the subsequent burnout of coke. This two-stage process involves the initial pyrolysis phase, where coal decomposes into volatiles and coke residue, followed by a secondary pyrolysis stage that further breaks down the remaining material.

2 THERMODYNAMIC MODELING OF PLASMA IGNITION OF THERMAL COALS

2.1 Description of the universal thermodynamic calculation software TERRA

The investigation of multicomponent heterogeneous isolated systems (coal + air) was performed using the TERRA software package [91]. This program was specifically designed to evaluate the thermodynamic characteristics of nearly 3,000 substances incorporated into a proprietary high-temperature process thermodynamics database. The dataset encompasses a wide range of organic and inorganic compounds typically found in hydrocarbon fuels. To conduct thermodynamic assessments of complex heterogeneous systems over an extended temperature interval (300–6000 K) under atmospheric pressure, the TERRA code in combination with its ETCPF database was applied [118].

Unlike conventional approaches in chemical thermodynamics, which are based on Gibbs free energy, equilibrium constants, and the classical law of mass action introduced by Guldberg and Waage, the present methodology is founded on the maximum entropy principle applied to isolated systems. Within this framework, all thermodynamic calculations are carried out strictly in accordance with the fundamental conservation laws of mass, energy, and electric charge [87, 119].

This approach enables the development of a comprehensive mathematical model that describes the equilibrium conditions of systems comprising both gaseous and condensed phases, including neutral and ionized species. According to the second law of thermodynamics, the equilibrium state in these systems is defined by the maximization of entropy over the thermodynamic variables (specifically temperature, pressure, and component concentrations). Upon reaching complete thermodynamic equilibrium, the chemical and phase compositions become directly linked to other state parameters such as pressure (P), temperature (T), density (ρ), and internal energy (U) [88, 120].

The thermodynamic calculation model outlined below has been implemented in a versatile computational tool known as TERRA [91]. The main (working) window of the TERRA software interface is shown in Figure 2.1.

The *Initial System Composition* panel is designed for entering and displaying information on the substances that determine the elemental composition of the system, including its starting chemical makeup.

In the *Equilibrium Parameters* panel, users can define two thermodynamic state variables that serve as the basis for equilibrium calculations, assign their numerical values, and specify permissible variation ranges.

The *Special Conditions* panel provides functionality for refining the set of substances included in the computation and for applying additional constraints to customize the modeling process.

The TERRA software is intended to evaluate the final equilibrium state of complex multicomponent systems. Since the adopted computational procedure does

not account for the kinetic pathway leading to equilibrium, it is sufficient to specify only the elemental mass fractions to describe the system's initial composition.

As an illustration, in evaluating the equilibrium parameters of a model reaction such as CO + H_2O, the system composition may be specified in the following manner:

1 mol C+2 mol O+2 mol H or 12.011 g C+32 g O+2.016 g H

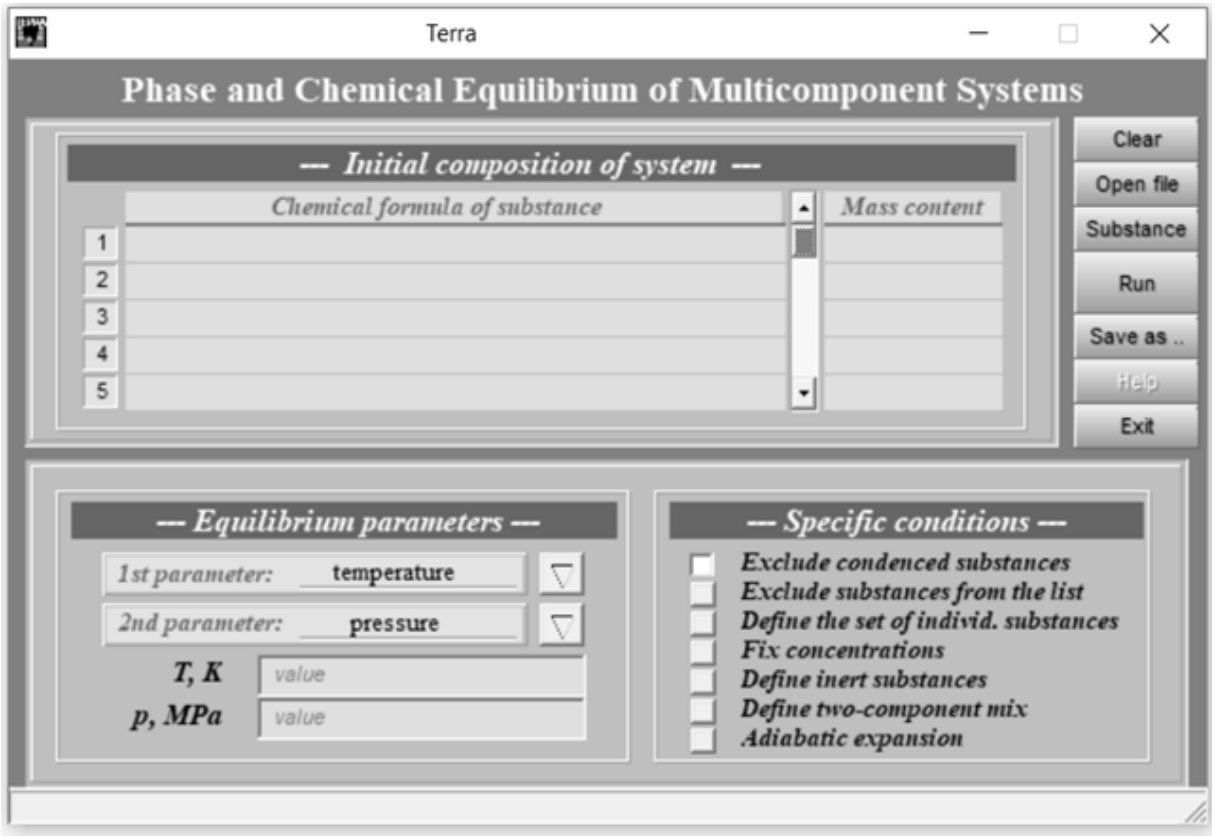


Figure 2.1 – The central working window of the TERRA thermodynamic modeling software [2]

Two state variables define the equilibrium condition of a closed, isolated thermodynamic system. In practical applications, it is generally sufficient to specify any two thermodynamic properties from the following set:

- pressure (MPa);
- temperature (K);
- specific volume (m^3/kg);
- specific entropy (kJ/kg);
- specific enthalpy (kJ/kg);
- specific internal energy (kJ/kg).

Table 2.1 presents the variable designations corresponding to the thermophysical and thermodynamic characteristics of the working medium obtained from equilibrium calculations. As shown in the table, constants may be expressed in any convenient system of units.

Table 2.1 – Designations and Units of the Derived Output Quantities

Designation	Parameters	SI	Technical system
T	Temperature	K	degree C
P	Pressure	MPa	kgf/cm^2
V	Specific volume	m^3/kg	m^3/kg
S_i	Specific entropy	kJ/kg	kcal/kg
U_i	Specific internal energy	kJ/kg	kcal/kg
I_i	Specific enthalpy	kJ/kg	kcal/kg
M	Total number of moles of components	mol/kg	mol/kg
C_p	Isobaric specific heat capacity (frozen)	J/(kg·K)	kcal/(kg·K)
K	C_p / C_V	1	1
C_p’	Isobaric specific heat capacity, including the effects of chemical reactions	kJ/(kg·K)	kcal/(kg·K)
K’	C_p' / C_V'	1	1
A	The equilibrium velocity of sound	m/s	m/s
MM	Average molar mass	g/mol	g/mol
C_p *G*	Specific heat of the gas phase at P=const (frozen)	kJ/(kg·K)	kcal/(kg·K)
K G	$C_P(\Gamma) / C_V(\Gamma)$	1	1
MMG	The average molar mass of the gas phase	g/mol	g/mol
R G	Gas constant	kJ/(kg·K)	kgf M/(kg·K)
Z	Mass fraction of all condensed components	1	1
MU	Physical viscosity	N s/m^2	dyne s/sm^2
LT	Thermal conductivity of the gas phase	W/(m·K)	kcal/(m·s·K)
LT’	Gas-phase thermal conductivity including the effects of chemical reactions	W/(m·K)	kcal/(m·s·K)

The preparation of input data for determining compositional and equilibrium parameters consists of two main components:

- procedural instructions that specify the conditions for activating a selected calculation mode and govern its execution;

- initial information describing the elements that define the elemental composition of the thermodynamic system, together with the parameters that characterize its equilibrium state, such as temperature (*T*) and pressure (*P*).

The iterative procedure for equilibrium calculations, along with the evaluation of thermodynamic functions, requires supplementary data, parameters, and constants, which are either derived from interrelated variables or directly specified within the software. The program is capable of modeling thermodynamic systems (such as coal-oxidizer mixtures) containing up to 20 chemical elements. All computations are performed automatically using an integrated thermodynamic database specifically created for this purpose. This database includes information on more than 3,000 compounds representing 65 elements, with properties defined over a broad temperature range of 300–6000 K. The dataset is primarily based on thermochemical compilations prepared by the Institute of High Temperatures of the Russian Academy of Sciences and the U.S. National Bureau of Standards [121].

2.2 Methods for determining the initial composition of the thermodynamic system, specific energy consumption for the plasma ignition process, and the degree of gasification of thermal coals

In this study, the thermodynamic systems are defined as material domains enclosed by impermeable boundaries, which preclude any exchange of heat or work with the external environment. These are typically identified as isolated or closed systems. It is assumed that such systems are already in a state of thermodynamic equilibrium, implying that their entropy remains constant, as no internal heat transfer or dissipative phenomena can lead to its increase. Commonly, these systems exhibit heterogeneity, comprising multiple phases demarcated by distinct interfaces. The gas phase encompasses all volatile components, while the condensed phase may include a variety of substances.

According to the entropy increase principle, an equilibrium system is defined as one that reaches a state of maximum entropy with respect to its thermodynamic variables, including equilibrium composition, temperature, and pressure. The attainment of thermodynamic equilibrium requires consistency between the system’s phases and chemical constituents and its state parameters, such as temperature, pressure, density, and total energy [118]. Determining the concentrations of combustion gases and slag in boiler furnaces operating at elevated temperatures, as well as evaluating their thermodynamic and transport properties, presents significant challenges in modeling heat and mass transfer, physicochemical processes, and thermogasdynamic behavior. In coal combustion, these parameters are strongly influenced by the composition of the working medium, which typically consists of complex mixtures of dissociating gases and condensed phases. At the early stages of model development, accurately representing the combined effects of reaction kinetics and heat transfer is particularly difficult. Highly detailed

computational schemes often result in excessive mathematical complexity and require input data that may be unavailable, while oversimplified models risk excessive generalization and loss of physical accuracy. In this context, thermodynamic methods have proven to be highly effective, as they assume that the working medium achieves both phase and chemical equilibrium within a conditionally isolated thermodynamic system. Under this assumption, the system's state can be described solely by its elemental composition, temperature, and pressure. For a closed multicomponent system in equilibrium, the second law of thermodynamics and the principle of energy conservation can be directly applied to analyze phase and chemical transformations occurring at high temperatures [122]. The attainment of chemical and phase equilibrium represents an inherently irreversible process, accompanied by an increase in entropy *S*, in accordance with the second law of thermodynamics:

$$dS \geq \frac{\delta Q}{T}, \tag{2.1}$$

where δQ represents the variation in thermal energy within the system.

As a system undergoes a reversible transformation, it may include an internal heat-generating mechanism responsible for entropy production. This internal source diminishes progressively as the system advances toward equilibrium, eventually halting once equilibrium is fully established. At this final state, the entropy of the system attains its maximum feasible value.

Drawing upon the entropy maximization principle, one can derive an equation that characterizes the behavior of a system in thermal and mechanical equilibrium as it progresses toward chemical equilibrium:

$$S = \sum_{i=1}^{R} \left(S_i^0 - R_0 ln \frac{R_0 T M_i}{V} \right) M_i + \sum_{l=1}^{K} S_l^0 \, M_l \Rightarrow S_{max}, \tag{2.2}$$

where K denotes the number of condensed components, each constituting a separate phase, whereas R represents the number of components present in the gaseous state. The quantities M_i and M_l refer to the number of gram-moles of the i-th and l-th substances within the system, respectively. R_0 stands for the universal gas constant, and V is the system's specific volume.

The condition $M_j = \text{const}$, where j indexes chemical elements, implies that no nuclear transformations occur within the system. Equation (2.2) is formulated under standard assumptions: the gaseous components obey the ideal gas law, and the volume contribution of the condensed phases is considered negligible compared to that of the gaseous phase. As a result, the total pressure of the system is attributed entirely to the gas phase.

$$S = S_{max} \text{ at } M_j = const, \; U_n = const,$$

$$U_n = Q_{chem} + \int_0^T C_V dT, \tag{2.3}$$

where C_V denotes the heat capacity at constant volume, and Q_{chem} represents the chemical energy of the substance.

Utilizing the Mendeleev–Clapeyron equation together with principles of chemical thermodynamics, it is possible to express both the specific volume and the total internal energy of the system as functions dependent on the concentrations of the individual components, as well as on the system's pressure and temperature:

$$U_n - \sum_{i=1}^{R} U_{ni} M_i - \sum_{l=1}^{K} U_{nl} M_l = 0 ; \quad (2.4)$$

$$V - \frac{R_0 T}{P} \sum_{i=1}^{R} M_i = 0 ; \quad (2.5)$$

where U_{nl}, and U_{ni} correspond to the formation enthalpies of the solid and gaseous components, respectively.

$$U_{ni} = \int_{T_0}^{T} C_{V_i} dT + \left(\Delta H_{T_0}^0\right)_i;$$

$$U_{nl} = \int_{T_0}^{T} C_{V_l} dT + \left(\Delta H_{T_0}^0\right)_l;$$

where $\left(\Delta H_{T_0}^0\right)_{i,l}$ denotes the standard enthalpy of formation at the reference temperature $T = T_0$ for the gaseous and condensed components, respectively.

A fundamental prerequisite for the validity of equations (2.4) and (2.5) is that the system reaches internal equilibrium, which is defined by the maximization of entropy or by constraints restricting the permissible variations in the mole numbers M_i and M_l.

Additionally, the conservation laws governing the chemical elements and the condition of electrical neutrality introduce further restrictions on the thermodynamic degrees of freedom within the system:

$$-\left[EL_j\right] + \sum_{i=1}^{R} n_{ji} M_i + \sum_{l=1}^{K} n_{jl} M_l = 0 \quad (j = 1, 2, \dots, m); \quad (2.6)$$

$$\sum_{i=1}^{R} n_{ei} M_i = 0, \quad (2.7)$$

where n_{ji} and n_{jl} are the numbers of atoms of the *j*–th chemical element in the *i*–th and *l*–th components; $\left[EL_j\right]$ is the content of the chemical element EL_j, mol/kg; in a chemical system, *m* represents the total number of chemical elements, while n_{ei} denotes the ionization multiplicity of the i-th component, taking negative values for negatively charged species.

In the process of approaching equilibrium, it is necessary, in addition to the previously stated constraints, to guarantee that the mole numbers of all components remain non-negative. This condition can be formally imposed by defining M_i as a function that is strictly positive over its entire domain. For example,

$$M_i = \exp X_i \qquad \text{or} \qquad X_i = \ln M_i \tag{2.8}$$

The determination of equilibrium parameters is achieved by solving the entropy extremum problem (2.1), while simultaneously accounting for the constraints and relationships defined by equations (2.4) – (2.8).

TERRA represents an automated system for thermodynamic analysis, specifically designed for this purpose and based on the Lagrange variational approach. Within this framework, the Lagrangian function is formulated using equations (2.1) and (2.4) – (2.8), subject to the condition that its partial derivatives with respect to all unknowns, including the undetermined Lagrange multipliers, vanish. The resulting multipliers define the interdependencies among the state variables through a corresponding system of algebraic equations [123].

The determination of Lagrange multipliers is accompanied by the formulation of a system of algebraic equations consisting of (R + K + m + 7) relations. These equations describe the interdependencies among (R + K + m + 9) equilibrium parameters of a general thermodynamic system, under the assumption that both volume and pressure are nonzero. As a result, two thermodynamic variables, pressure (P) and temperature (T), must be specified externally, while the remaining unknown parameters are determined from the ensuing set of algebraic equations:

$$PV - R_0 \sum_{i=1}^{R} \exp X_i = 0, \tag{2.9}$$

$$-I + \sum_{i=1}^{R} I_i \exp X_i + \sum_{l=1}^{K} I_l \exp X_l = 0, \tag{2.10}$$

$$S_i^0 - \frac{I_i}{T} - R_0 X_i \ln \frac{R_0 T}{V} + \sum_{j=1}^{m} n_{ji}\lambda_j + n_{ei}\lambda_l = 0, \quad (i = 1,2,\dots k), \tag{2.11}$$

$$S_l^0 - \frac{I_l}{T} + \sum_{j=1}^{m} n_{jl}\lambda_j = 0, \quad (l = 1,2,\dots k), \tag{2.12}$$

$$\sum_{j=1}^{m} n_{ei} \exp X_i = 0; \tag{2.13}$$

$$-S + \sum_{i=1}^{R} \left(S_i^0 - M_i R_0 \ln \frac{R_0 T}{V} \right) \exp X_i + \sum_{l=1}^{k} S_l^0 \exp X_i = 0, \tag{2.14}$$

where S and I are the entropy and total enthalpy of the system, $I = \Delta H^0(T_f) + \int_{T_f}^{T} C_p dT$, T_f is the standard temperature.

The system of equations (2.9) – (2.14) becomes fully defined only when the values of temperature and pressure are specified, as these parameters establish the equilibrium state between the working medium and its surroundings. Due to the transcendental nature of these equations, an analytical solution is not attainable. Therefore, the system is solved numerically using Newton's iterative method, which relies on linearizing the algebraic equations at each iteration step. Starting from an

initial guess, the nonlinear terms are expanded using a first-order Taylor series approximation:

$$f(X_1, X_2, \dots, X_n) \cong f(X_1^0, X_2^0, \dots, X_n^0) + \sum_{i=1}^{n}(X_i - X_i^0)\frac{\partial}{\partial X_i}(f(X_1^0, X_2^0, \dots, X_n^0)), \quad (2.15)$$

where X_i are the initial approximations of the unknowns.

Because the system of equations (2.2) – (2.14) becomes linear after applying operation (2.15), it can be solved iteratively. This linearization allows the system to be efficiently employed in numerical analysis and computational simulations:

1 Equation governing the concentration of individual gaseous species:

$$X_i = \frac{I_i(T)}{R_0(T_0)^2}T + Y + \sum_{i=1}^{m}\frac{n_{ji}}{R_0}\lambda_j + \frac{n_{li}}{R_0}\lambda_l + \left(\frac{S_l^0(T_0)}{R_0} - \frac{2I_i(T_0)}{R_0T_0}\right), \quad (2.16)$$

where $Y = \ln\frac{R_0T}{V}$. The index «0» in S and T indicates that the values of entropy and temperature are iterative and the linearization of the equation is valid near these values.

2 The equation of concentration of individual condensed components:

$$X_l = \frac{AI_l(T_0)}{(T_0)^2}T + \sum_{j=1}^{m}An_{jl}\lambda_j + \left(AS_l^0(T_0) - \frac{2AI_i(T_0)}{T_0}\right), \quad l = 1,2,\dots,k. \quad (2.17)$$

For $A \to \infty$, equation (2.17) is equivalent to the expression

$$\left(S_l^0(T) - \frac{I_i(T)}{T} + \sum_{j=1}^{m}An_{jl}\lambda_j\right)\exp X_l, \quad l = 1,2,\dots,k. \quad (2.18)$$

It should be noted that, even at $A = 10^3$, the errors in calculating X_l due to the transition from equation (2.18) to (2.17) remain within a few tenths of a percent.

3 The ideal gas law governing the system's equation of state:

$$[-\exp(-Y^0)]p + 2Y\sum_{i=1}^{R}\exp X_i + \sum_{i=1}^{K}\exp X_i = 2Y^0\sum_{i=1}^{R}\exp X_i. \quad (2.19)$$

4 The equation of the general electroneutrality of a thermodynamic system:

$$\sum_{i=1}^{R}n_{ei}\exp X_i = 0. \quad (2.20)$$

5 The equation of conservation of mass of chemical elements:

$$\sum_{l=1}^{R}n_{jl}\exp X_i + \sum_{l=1}^{K}\left(n_{jl}\exp X_l^0\right)X_l = \left[EL_j\right] + \sum_{l=1}^{K}n_{jl}(X_l^0 - 1)\exp X_l^0, \quad j = 1,2,\dots,m \quad (2.21)$$

6 The entropy equation of a thermodynamic system:

$$\begin{aligned}
&-S + \sum_{l=1}^{R} S_l^0(T_0) - R_0(1 + X_l^0 + Y_l^0)\exp X_l + \\
&\quad + \sum_{l=1}^{R} \left(\frac{C_p^0(T_0)}{R_0}\exp X_l^0\right) \mathrm{T} + \sum_{l=1}^{R}(R_0 \exp X_l)\mathrm{Y} + \\
&\quad\quad + \sum_{k=1}^{K} \left(\frac{C_{Pk}(T_0)}{T_0}\exp X_k^0\right) T + \sum_{k=1}^{K}(S_k^0(T_0)\exp X_k^0)X_k = \\
&\quad\quad\quad = \sum_{l=1}^{R}(C_{Pl}(T_0) + R_0(Y^0 - 1))\exp X_l + \\
&\quad\quad\quad\quad + \sum_{k=1}^{K}(C_{Pk}(T_0) + S_k^0(T_0)(X_k - 1))\exp X_k^0. \qquad (2.22)
\end{aligned}$$

7 The equation for determining the enthalpy of the system:

$$\begin{aligned}
&-I + \sum_{l=1}^{R} I_i(T_0)\exp X_i + \sum_{i=1}^{R}(C_{Pl}(T_0)\exp X_l^0)\, T + \\
&\quad + \sum_{k=1}^{K}(I_k(T_0)\exp X_k^0)X_k + \sum_{i=1}^{K}(C_{Pk}(T_0)\exp X_k^0)T = \\
&\quad\quad = \sum_{i=1}^{R} C_{Pi}(T_0)\exp X_i^0 + \sum_{k=1}^{K}(H_k(T_0)(X_k^0 - 1) + \\
&\quad\quad\quad + C_{Pk}(T_0)T_0)\exp X_k^0. \qquad (2.23)
\end{aligned}$$

Analysis of the system of equations (2.16)–(2.23) shows that the ETCPF may involve as many as 300 variables, which necessitates a large number of iterations to achieve convergence. In the TERRA software, the solution procedure is limited to a maximum of 150 iterations. A computation is considered converged when the maximum relative error falls below 0.0001%.

The specific energy consumption (Q_{sp}) associated with the plasma chemical treatment of coal is a critical parameter for assessing energy efficiency. In plasma burners and reactors, electrical power is essential to generate and sustain the plasma.

In the context of high-temperature gasification and plasma-chemical processing of low-rank coal, various methods for determining the initial composition of the coal-oxidizer mixtures have been evaluated [77, 124, 125]. Bench-scale and pilot-industrial experiments [126, 127] demonstrated a close correlation between the calculated and experimentally measured specific energy consumption required for plasma stabilization during the combustion and gasification of low-grade coals.

The Q_{sp} of the process of ETCPF consists of energy costs for heating coal and oxidizer to a certain temperature and implementing thermochemical transformations which lead to thermodynamic equilibrium in the system. The formula for Q_{sp} (kW·h/kg) is as follows [119]:

$$Q_{sp} = I_{eq} - I_{st}, \qquad (2.24)$$

where I_{st} and I_{eq} are the total enthalpy per kg of working body (coal + oxidizer) in the initial and equilibrium states (after all transformations).

A thermodynamic analysis method based on the calculation of phase and chemical compositions of the thermal transformation of coal and oxidizer is used to

calculate the total enthalpy I_{eq} of the working body, both in the initial and equilibrium states, since it is not possible to experimentally measure the total enthalpy of the working body, both at the initial and equilibrium states.

TERRA software is used to calculate the value of I_{eq} in multicomponent heterogeneous mixtures for specific thermodynamic systems.

The enthalpy of the initial mixture can be written as [124]:

$$I_{st} = \Delta H_f^0(T_0) + \int_{T_{st}}^{T_0} C_p(T)dT, \quad (2.25)$$

where $\Delta H_f^0(T_0)$ is the standard heat of formation of the working body; $T_0 = 298.15\,K$ is the standard temperature; T_{in} is the initial temperature of the process at which the reagents enter the reaction zone.

If $T_{st} = T_0$ are equal, i.e. if the reagent is heated from $T_{st} = 298.15\,K$, then equation (2.25) has the form:

$$I_{st} = \Delta H_f^0(298)_{st}. \quad (2.26)$$

During the electrothermochemical preparation of coal in an oxidizer, the formula (2.26) is disclosed as follows:

$$\Delta H_f^0(298)_{st} = Z_{sf} H_f^0(298)_{sf} + Z_{ox} H_f^0(298)_{ox}, \quad (2.27)$$

where Z_{sf}, Z_{ox} are the mass fractions of coal and oxidizer in the thermodynamic system. $\Delta H_f^0(298)_{sf}$ and $\Delta H_f^0(298)_{ox}$ are the standard heats of formation of fuel and oxidizer.

When air used as an oxidizer without taking into account impurities (Ar, CO_2, H_2), $\Delta H_f^0(298)_{ox}$can be obtained with an accuracy equal to zero, which is sufficient for engineering calculations. If the oxidizer is water vapor H_2O, then $\Delta H_f^0(298)_{ox} = -13422.7$ kJ/kg.

Based on Hess's law [128], the colorimetric method of determining the heat of combustion of coal in air can be used to determine the standard heat of solid fuel formation (ΔH_f^0 kW·h/kg):

$$\Delta H_f^0(298)_{ox} = Q_h^d + I_{pc}, \quad \text{kW·h/kg}, \quad (2.28)$$

where Q_h^d is the highest heat of combustion of coal per dry mass, measured at $T_0 = 298.15\,K$; $I_{pc}$is the standard enthalpy of combustion products of solid fuels.

A solid fuel combustion product's enthalpy value can be determined based on the remaining “cold” ($T_0 = 298.15\,K$) combustion products. The value of I_{pc} can also be determined through chemical thermodynamic calculations using the TERRA software, under the assumption that the gaseous “cold” combustion products are in

thermodynamic equilibrium with the solid residues. Based on equations (2.24), (2.26-2.28), the specific energy consumption can be expressed as follows:

$$Q_{sp} = I_{eq} - Z_{sf}\left(Q_h^d + I_{pc}\right) - Z_{ox}\Delta H_f^0(298)_{ox}. \quad (2.29)$$

At $Q_{sp} > 0$, the process of heat treatment of coal is carried out by heat absorption (endothermically), and at $Q_{sp} < 0$ - by heat release (exothermically).

It is therefore necessary to calculate the equilibrium enthalpy of the products of electrothermochemical preparation of coal in the oxidizer (at a given process temperature) and the standard enthalpy of coal combustion at $T = 298.15\ K$ with stoichiometric oxygen to determine specific energy consumption or heat release.

Using the specific energy consumption, the following formula can be used to calculate the minimum power of the plasma generator needed for chemical-thermal treatment of coal:

$$P_e = Q_{sp}(G_{coal} + G_{ox}),\ \text{kW}, \quad (2.30)$$

where G_{coal} and G_{ox} are the consumption of coal and oxidizer (kg/h), respectively.

The PICS processes are characterized by several key factors, among which is the relationship between the combustion temperature and the extent of carbon gasification in coal. This relationship can be quantified using the following equation:

$$X_C = \frac{C_{in} - C_{fin}}{C_{in}} \cdot 100\%, \quad (2.31)$$

where C_{in} represents the initial carbon concentration in the fuel (expressed as %), whereas C_{fin} indicates the final carbon concentration in the condensed products of ETCPF (%).

2.3 Results of calculations of plasma ignition of thermal coals

For the production of high-reactive dual-component fuel, plasma ignition and combustion stabilization were calculated for an optimal coal dust concentration and air mixture of 0.7 kg/kg (1000 kg of coal + 1429 kg of air) [129]. In this study, Ekibastuz coal with a 40% ash content was used at a temperature of 300-2000 K and a pressure of 0.101 MPa, as shown in Table 2.2. In order to achieve stable ignition as a result of plasma ignition and stabilization of combustion of high-reactive dual-component fuel, combustible gases ($CO+H_2+CH_4$) must be present at a concentration exceeding 15% and at a temperature high enough to ensure the self-ignition of dual-component fuel (>1073 K). The calculation results are shown in Figures 2.2-2.4.

Table 2.2 – Technical Characteristics and Composition of Ekibastuz Coal, wt.%

Technical characteristics											
W^w		V^{daf}		Fixed carbon		A^d		Total		HHV, kJ/kg	
5.8		24.0		30.2		40.0		100.0		16,740.0	
Chemical composition											
H	C	S	N	O	SiO_2	Al_2O_3	Fe_2O_3	CaO	MgO	K_2O	Na_2O
3.05	48.86	0.73	0.8	6.56	23.09	13.8	2.15	0.34	0.31	0.16	0.15

Designations: W^w – moisture content per working mass, V^{daf} – volatile yield per combustible mass, A^d – ash content per dry mass, HHV – high heat value per dry mass

As illustrated in Figure 2.2, the total concentration of combustible components rises with increasing process temperature, starting at approximately 1200 K. These flammable gases exhibit a high calorific value of 9,268 kJ/kg. From an environmental standpoint, it is essential that nitrogen in the initial mixture predominantly exists in molecular form (N_2), maintaining a nearly constant concentration of about 49.4% over the temperature range of 1000–1600 K. Furthermore, nitrogen oxide (NO_x) emissions remain low, ranging between 1 and 5 mg/nm^3, which is roughly half the typical concentration observed in flue gases. Sulfur present in the fuel primarily exists as hydrogen sulfide (H_2S), which volatilizes into the gas phase at around 1200 K with a concentration of 0.14%, while sulfur oxide (SO_x) levels remain minimal, below 1 mg/nm^3. The study also demonstrates that as temperature increases, the concentration of synthesis gas (composed primarily of carbon monoxide and hydrogen) rises significantly. The maximum combined concentration of these components reaches 57.6% at a temperature of 1880 K and a pressure of 0.1 MPa. This temperature regime promotes more complete thermal decomposition of the feedstock and enhances the reactions leading to the formation of the target gaseous products. Due to these conditions were identified as optimal for the efficient progression of the PICS processes.

As shown in Figure 2.3, the carbon concentration in the coke residue gradually decreases between 600 and 1500 K. This reduction is attributed to the conversion of carbon into the gas phase through the reactions $C + H_2O \rightarrow CO + H_2$ and $C + CO_2 \rightarrow 2CO$. When the temperature is increased, the carbon concentration in the mineral mass of coal drops to zero after an increase in temperature. This is because of the reduction in carbon oxides within the mineral mass. As a result of the reaction represented by the general equation $Me_xO_y + yC \rightarrow xMe + yCO$, where Me denotes a metal or metalloid and *x* and *y* are stoichiometric coefficients, carbon oxides within the coal's mineral matrix undergo reduction. This reaction pathway includes not only the reduction of mineral oxides but also leads to the formation of compounds such as aluminum nitride (AlN) and silicon carbide (SiC). In the temperature range of 300–1700 K, the predominant components of the condensed phase are silica (SiO_2) and alumina (Al_2O_3), with concentrations reaching approximately 9% and 6% at 1400 K, respectively. Minor phases include compounds of iron (e.g., FeS, FeS_2,

Fe_3C, Fe_3O_4), magnesium (e.g., $MgAl_2O_4$, $MgSiO_3$), and calcium (e.g., $CaSiO_3$, CaS), each present at concentrations below 1%. Above 1700 K, silicon carbide (SiC) emerges as a distinct component of the condensed phase.

As illustrated in Figure 2.4, methane (CH_4) concentrations decrease with rising temperature, while the concentrations of carbon monoxide (CO) and hydrogen (H_2) increase correspondingly. At a T = 900 K, the high-reactivity thermochemical fuel (HRDF) primarily consists of synthesis gas (CO + H_2) and elemental carbon (C), with mass fractions of 30.1% and 7.6%, respectively. Additionally, the combustion heat of the HRDF produced by this process reaches 14,020 kJ/kg. When the physical enthalpy of the HRDF is taken into account, the total energy content rises to 16,490 kJ/kg, highlighting the material's significant flammability upon introduction into the combustion chamber.

During the ETCPF process, the initially low-reactivity coal undergoes a transformation into a fuel with significantly enhanced reactivity, enabling it to reach its ignition temperature more readily. Upon mixing with secondary air within the furnace chamber, the fuel ignites vigorously and sustains combustion independently, eliminating the need for auxiliary oil-based ignition. There is a strong correlation between the composition of the original technological mixture and the composition of the final ETCPF products (gas and condensed phases) in determining the degree of carbon gasification as well as the specific energy costs. The energy efficiency of this process is demonstrated by these data.

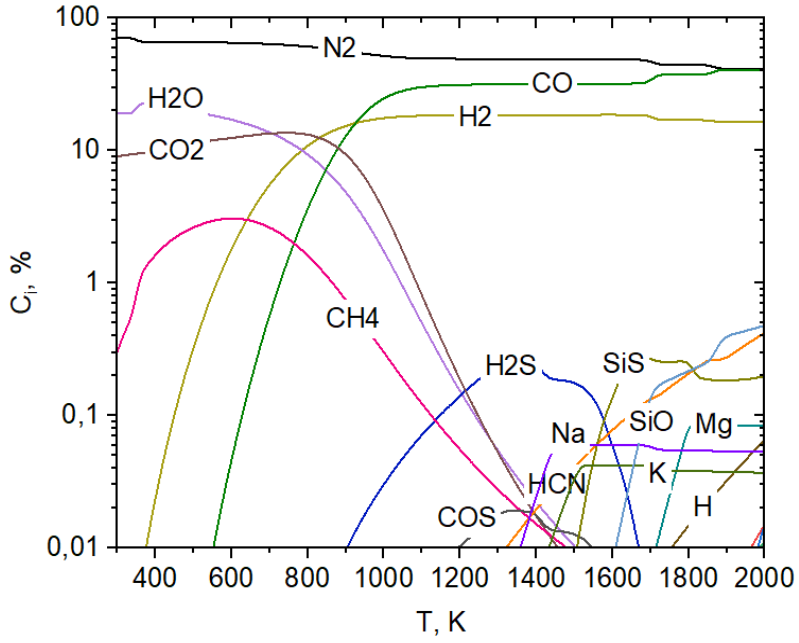


Figure 2.2 – Temperature-dependent variation in gas-phase component concentrations during the PICS processes [29]

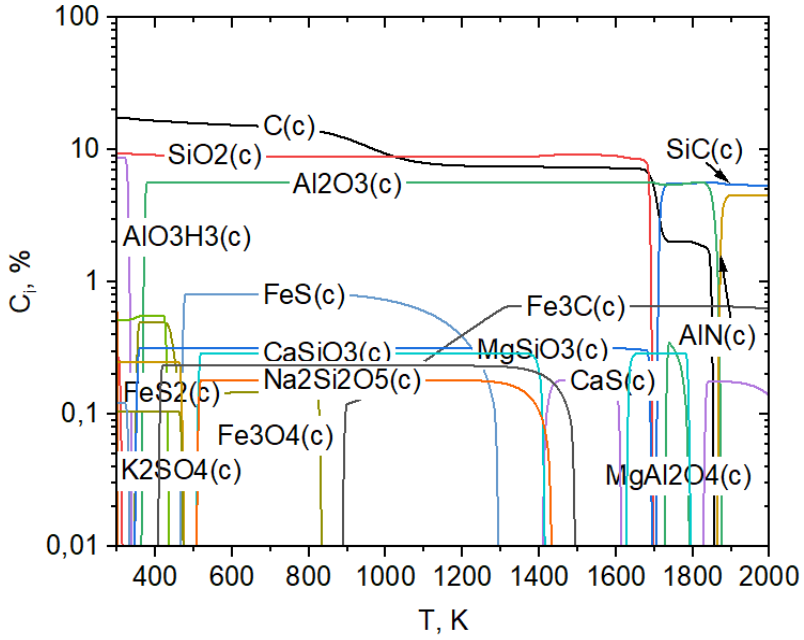


Figure 2.3 – Temperature-dependent variation in condensed-phase component concentrations during the PICS processes [29]

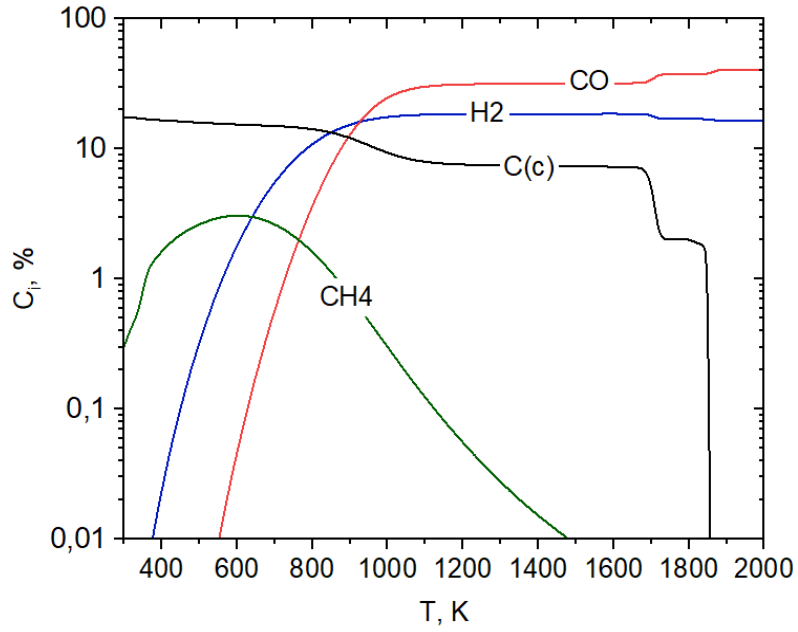


Figure 2.4 – Temperature-dependent variation in mass concentration of combustible components of HRDF from coal during the PICS processes [29]

The carbon content in the solid residue determines the extent of carbon gasification, denoted as X_C (Equation 2.3), which is a key indicator of PICS processes.

As illustrated in Figure 2.5, carbon gasification increases with temperature, reaching approximately 56.5% at 1200 K (sufficient for initiating plasma ignition

and maintaining stable combustion). Between 1200 K and 1700 K, the gasification degree remains relatively unchanged due to the absence of oxidizing agents in the gas phase. However, a marked increase in gasification, ranging from 60% to 90%, is observed upon reaching 1700 K. This implies that the conversion of condensed-phase carbon into gaseous products is enhanced, most likely as a result of intensified carbon monoxide formation or chemical reactions between carbon and oxygen-containing oxides. These processes promote the formation of metallic and metalloid compounds, as illustrated in Table 2.2, which details the mineral composition of the coal.

Figure 2.6 illustrates the specific energy costs associated with 1 kg of coal, depending on the temperature. A noticeable correlation can be observed between the trend of specific energy consumption and the extent of carbon gasification, as illustrated in Figure 2.5. Specifically, a gradual rise in specific energy consumption is observed at 1000 K, increasing from 0.6 to 0.9 kW·h/kg. A more pronounced surge occurs at 1700 K, where the energy consumption escalates from 0.9 to 1.2 kW·h/kg. At high temperatures, the intensification of carbon gasification processes and the development of endothermic processes explain all these increases with temperature. An optimal temperature (T = 1880 K) for achieving maximum syngas yield, that shown in Figure 2.2, leading to a specific energy consumption of 1.18 kW·h/kg.

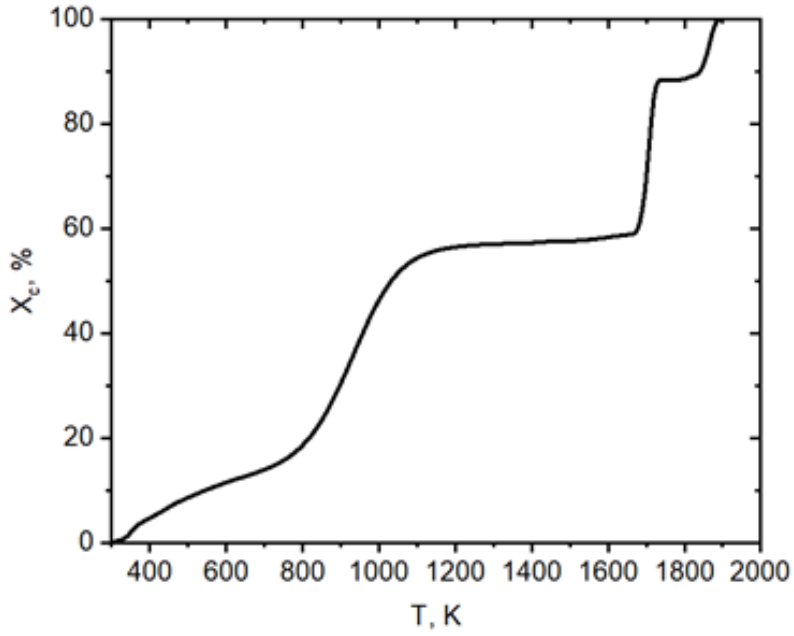


Figure 2.5 – Temperature-dependent variation in the extent of carbon gasification during the PICS processes [29]

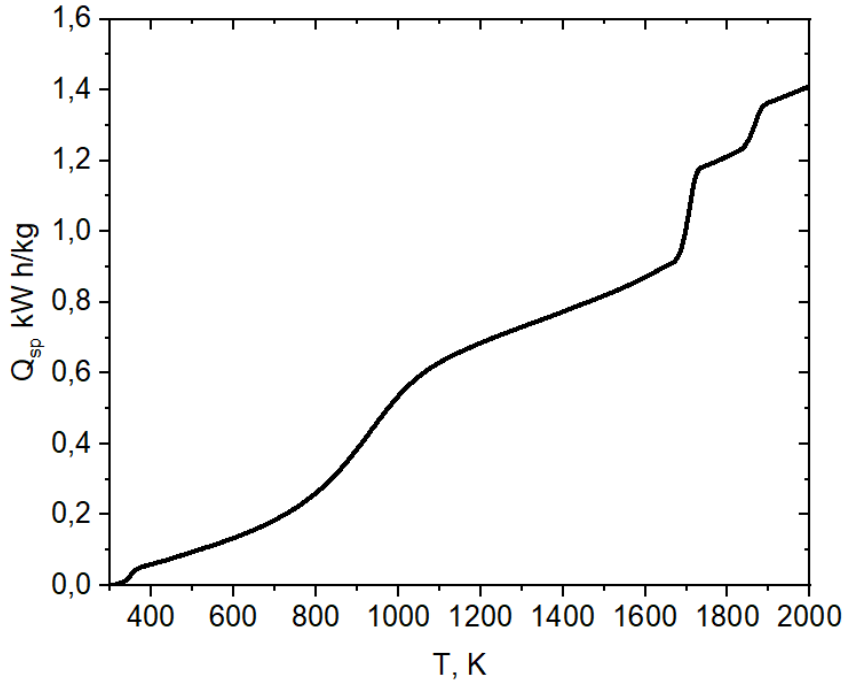


Figure 2.6 – Temperature-dependent variation in specific energy consumption during the PICS processes, kW·h/kg [29]

As an initial data source for the kinetic modeling of the PISC process within the PCB, a thermodynamic model of the PISC process was used.

Appendix A shows an example of a listing of thermodynamic calculations of plasma ignition of power coal using the TERRA software.

3 KINETIC MODELING OF THE PROCESSES OF HEATING AND IGNITION OF THERMAL COALS IN A PLASMA-COAL BURNER

3.1 Description of the mathematical model and the PlasmaKinTherm software for kinetic calculations of heating and ignition of thermal coals in a plasma-coal burner

The mathematical model of PICS processes in coal dust considers a two-phase flow of coal particles and an oxidizing gas, which chemically interact within a burner containing an internal thermal energy source, such as an electric arc. Both the coal particles and the gas are assumed to enter the burner at the same initial temperature [130].

The model includes heat and mass transfer between coal particles, the oxidizing gas, and the electric arc, as well as thermal and momentum interactions with the burner's internal surfaces. Key chemical transformations are incorporated, including the formation of primary volatile compounds, their release into the gas phase, and the production of coke residues [131].

The mathematical model of the coal dust PICS processes was developed based on the following assumptions, as outlined in references [132]:

- the process is considered to be quasi-steady and one-dimensional;
- the gas is assumed to behave as an ideal gas;
- the gas–particle mixture entering the burner is treated as homogeneous;
- heat transfer between the gas and solid phases occurs through convection and thermal conduction;
- coal particles are considered isothermal, maintaining a uniform temperature throughout their volume;
- heat released from heterogeneous reactions is assumed to influence only the temperature of solid particles, while heat generated by gas-phase reactions affects solely the gas temperature;
- owing to the small particle size, particle–wall friction and interparticle interactions are neglected;
- viscous effects are taken into account only in the interaction between the gas and solid phases;
- ash is regarded as an inert component with no participation in chemical or thermal processes.

The majority of computational and theoretical investigations of plasma processes assume one-dimensional, steady-state conditions, an approach that generally aligns well with experimental observations [133, 134]. As is customary, coal heat treatment processes are performed at atmospheric pressure and temperatures ranging from 1500 to 3000 K. As a result of the highly turbulent gas flow, temperature and velocity distributions along the radius of the burner are almost uniform. In the study of the plasma torch process, it is important to note that the electric arc generates disturbances in the flow, promoting turbulence and enhanced mixing due to its momentum transfer capabilities [135].

A method for estimating the validity of the assumption about the isothermicity of coal particles was developed by B.V. Kantorovich [136]. If for such particles the Biot B_i and Fourier F_0 criteria are satisfied, the thermal resistance of a coal particle can be ignored in comparison to the resistance to heat exchange on its surface:

$$B_i = \frac{Nu\lambda_\partial}{2\lambda_s} \ll 0.5, F_0 = \frac{\alpha_s \tau}{\sigma^2} > 5,$$

where Nu is the Nusselt number, α_s and λ_s are the thermal conductivity and coefficient of the material of the solid surface, σ is the characteristic length, and τ is the time

For a particle with a size of 100-150 microns at 1000-2000 K, these values were estimated to be $B_i = 0.2 - 0.4$, and $F_0 = 10 - 20$. For the heat treatment of coal particles in water vapor plasma, $B_i = 0.15 - 0.2$, and $F_0 = 8 - 10$. Thus, the values of B_i and F_0 make it possible to abandon the consideration of heat exchange inside industrially ground coal particles with an average size of less than 150 microns and consider them isothermal. These estimates are confirmed by data from V.I. Babiya [137], where it is reported that the error in calculating the temperature of coal particles (more than 200 μm in size) from changes in their surface temperature is no more than 10%, for Biot numbers it is less than 1 and the Fourier criterion is more than 5.

A study by [138] found that the movement of particles and the exchange of heat with a gas phase are significantly influenced by interactions between solid particles when the true mass concentration of particles in a gas does not exceed 30 kg/m.

The true mass concentration of particles in a two-phase plasma flow with coal dust concentrations of μ = 0.5 – 5 kg/kg does not exceed 1 – 5 kg/m^3, which is significantly less than the maximum permissible concentration of particles. Additionally, particles occupy only 10^{-3} – 10^{-4} m^3/m^3, which corresponds to a distance between particles of l/δ = 15 – 25. In other words, the distance between particles in a pulverized coal flow is more than 15 times the size of the particles, and particle collisions have little effect on drag coefficients and heat exchange coefficients. As a result, the relative behavior of particles can be used to model the processes under investigation. At the inlet of the combined plasma torch, homogeneity of the gas–particle mixture is practically achieved through the forced mixing of coal dust with an oxidizing agent using specialized spray nozzles [78]. Under the adopted assumptions, heat transfer and hydrodynamic behavior can be described using ordinary differential equations, which streamlines the computational methodology and enables the integration of chemical transformation processes into the model. To develop a comprehensive mathematical framework for PICS with polydisperse coal particles, the governing equations account for variations in component concentrations via chemical kinetics, as well as the dynamics of velocities and temperatures for both the gas and particles. The electric arc is represented by an energy conservation equation, while the plasma is modeled as an internal heat source with an empirically determined axial heat distribution.

Finally, without loss of generality, the elements of the system of equations are indexed as follows:

$i = 1, \dots, n$ – gaseous components,
$i = n+1, \dots, N$ – solid-phase components,
$j = 1, \dots, m$ – heterogeneous reactions,
$j = m+1, \dots, M$ – gas-phase reactions,
$l = 1, \dots, L$ – fractions of solid particles.

Accordingly, the system of equations is formulated as follows:

- The governing equation for the concentrations of gaseous species

$$\frac{dC_i}{dx} = \frac{f_i}{v_g} - C_i\left(\frac{1}{v_g}\frac{dv_g}{dx} + \frac{1}{S}\frac{dS}{dx}\right) \qquad i = 1, \dots, n \tag{3.1}$$

- The governing equation for the concentrations of solid-phase species

$$\frac{dC_{il}}{dx} = \frac{f_{il}}{v_g} - C_i\left(\frac{1}{v_{sl}}\frac{dv_{sl}}{dx} + \frac{1}{S}\frac{dS}{dx}\right) \qquad t = 1, \dots, N; \quad l = 1, \dots, L \tag{3.2}$$

- The governing equation for the conservation of particle number

$$\frac{d}{dx}(N_l v_{sl} S) = 0 \tag{3.3}$$

where N_l denotes the volumetric concentration of particles.

$$N_l(x) = N_l^0 \frac{v_{sl}^0 S^0}{v_{sl}(x) S(x)}$$

where the superscript ^{0} denotes initial volumes.

- The governing equation for momentum conservation

$$\frac{d}{dx}\left(\left[\rho_g v_g^2 + \sum_{l=1}^{L} \rho_{sl} v_{sl}^2\right] \cdot S\right) = -S\frac{dP}{dx} - S \cdot F_w \tag{3.4}$$

- The governing equation for energy conservation

$$\begin{aligned}\frac{d}{dx}\left(\left[\rho_g v_g \frac{v_g^2}{2} + \sum_{l=1}^{L} \rho_{sl} v_{sl} \frac{v_{sl}^2}{2}\right] \cdot S\right) + S C_{Pg} v_g \frac{dT_g}{dx} = S\Big\{\sum_{j=m+1}^{M} W_f Q_f - \\ - \sum_{l=1}^{L} \pi d_l^2 N_l \left[a_l\left(T_g - T_{sl}\right) + \varepsilon\sigma\left(T_g^4 - T_{sl}^4\right)\right]\Big\} + \\ + \pi D(\Theta - 1) q_w\end{aligned} \tag{3.5}$$

where q_w denotes the energy loss from the system caused by convective and radiative heat transfer through the burner's lateral surface area $\pi D dx$. This equation

also incorporates the energy input from the electric arc, taking into account heat losses through the burner walls. The thermal power supplied by the arc is expressed as the difference between the arc's electrical power, P_{arc}, and the heat dissipated to the burner walls, P_2:

$$\frac{(P_{arc}-P_2)}{\mathcal{V}} = \xi q_{arc},$$

where q_{arc} represents the energy input into the cylindrical volume $\mathcal{V} = Sdx$, and $\xi = (1 - \frac{P_2}{P_{arc}})$ denotes the thermal efficiency of the plasma burner.

The total heat flux into the burner wall is given by:

$$P_2 = \pi D \int_0^{L_B} q_w(x)dx.$$

where q_w represents the specific heat flux into the plasma burner wall, and L_B is the length of the plasma burner.

The dimensional proportionality coefficient between $q_{arc}(x)$ and $q_w(x)$, defined as $\psi = q_{arc}(x)/q_w(x)$, is expressed as:

$$\xi = \frac{\psi P_{arc}-P_2}{\psi P_{arc}}.$$

For the calculation of energy input, it is more practical to utilize the dimensionless coefficient defined as: $\Theta = \frac{D(x)}{4} \cdot \frac{q_{arc}(x)}{q_w(x)} = \frac{D(x)}{4} \cdot \psi$. Accordingly, the expression for the burner efficiency can be formulated as:

$$\xi = \frac{\Theta P_2 - P_2}{\Theta P_2} = 1 - \frac{1}{\Theta}$$

or

$$\Theta = \frac{1}{1-\xi}.$$

- The governing equation for particle motion

$$\frac{dv_{sl}}{dx} = \frac{1}{M_{sl}v_{sl}} C_{Dl} \frac{\pi d_1^2 \rho_g (v_g - v_{sl})|v_g - v_{sl}|}{8} + \frac{g}{v_{sl}} \qquad l = 1, \dots, L \qquad (3.6)$$

here, the subscript l denotes the particle size fraction number. The parameter M is defined as $M = \frac{\mu_{sl}\rho_{sl}}{C_{n+1}\mu_{n+1}}$.

The drag coefficient, which dictates particle motion under Stokes' drag force, is defined by equation (1.6). Here, $Re_{sl} = \frac{d_{sl}|v_g - v_{sl}|\rho_g}{\eta}$ denotes the Reynolds number for the particle [137].

- The governing equation for particle temperature

$$\frac{dT_{sl}}{dx} = \frac{1}{C_{Pl}\rho_{sl}\vartheta_{sl}}\left\{\sum_{j=1}^{L} W_j Q_j - \sum_{l=1}^{L} \pi d_l^2 N_I \left(\alpha_I\left(T_g - T_{sl}\right) + \varepsilon\sigma(T_w^4 - T_{sl}^4)\right)\right\}, \quad (3.7)$$

where the heat capacity of the particles at constant pressure, C_{Pl}, is determined by the expression $C_{Pl} = \sum_{i=n+1}^{N}\sum_{l=1}^{L} C_{il}C_{Pl}$, and the heat transfer coefficient of the particles is given by the formula:

$$\alpha_l = \frac{\lambda}{d_l} Nu_l,$$

where Nu_l is the Nusselt number for the particle.

The heat transfer rate between the particles and the gas phase is determined using the correlation provided in references [21, 139]:

$$Nu_l = \frac{\alpha_l d_l}{\lambda} = 2 + 0.654 Re_{sl}^{1/2} Pr^{1/3}$$

The Prandtl number $Pr = \frac{\eta}{\rho\alpha}$, is assumed constant within the temperature range of 1000 K to 3500 K. The thermal conductivity of the gas is then calculated using the Prandtl number according to the following expression:

$$Pr = \frac{\eta \sum_{l=1}^{n} C_l C_{Pl}}{\lambda \rho_g}$$

alternatively, considering that $\sum_{l=1}^{n} C_l C_{Pl} = C_{P_g}$, the thermal conductivity of the gas can be expressed as: $\lambda = \frac{\eta C_{P_g}}{Pr\rho_g}$.

During carbon oxidation, heat is released from the surfaces of coal particles of varying sizes, as represented by the first term in equation (3.7). The specific heat capacities of individual components are estimated using polynomial approximations, with coefficient values sourced from the TERRA database. For complex hydrocarbons, the heat capacities and heats of formation were calculated based on data from the literature [140], while the heat capacity of ash was determined using information from sources [141, 142]. The thermal effects of chemical reactions (excluding those associated with the primary decomposition of coal) are computed using the heats of formation of the participating compounds. Additionally, the thermal effects associated with the release of volatile substances are obtained by calculating the difference between the coal's effective and measured heat capacities.

To close the system of equations, the following conditions were imposed:

- The ideal gas law is formulated as:

$$P = RT_g \sum_{l=1}^{n} C_l. \tag{3.8}$$

- The gas residence time is defined by the following expression:

$$\frac{d\tau_g}{dx} = \frac{1}{\vartheta_g}. \tag{3.9}$$

- The residence time of solid particles is given by the following expression:

$$\frac{d\tau_{sl}}{dx} = \frac{1}{\vartheta_{sl}}. \tag{3.10}$$

From equations (3.4) and (3.5), one can find obvious expressions for $\frac{dv_g}{dx}$ and $\frac{dT_g}{dx}$:

$$\frac{dv_g}{dx} = \frac{b_1 a_{22} - b_2 a_{12}}{a_{11} a_{22} - a_{12} a_{21}},$$

$$\frac{dT_g}{dx} = \frac{b_2 a_{11} - b_1 a_{21}}{a_{11} a_{22} - a_{12} a_{21}},$$

where $a_{11} = \rho_g v_g - \frac{P}{v_g}$; $a_{12} = \frac{P}{T_g}$; $a_{21} = \rho_g v_g^2$; $a_{22} = v_g C_{Pg}$;

$$b_1 = -\frac{RT_g}{v_g} \sum_{i=1}^{n} f_i - v_g \sum_{i=1}^{n} \mu_i f_i - \sum_{l=1}^{L} \left(v_{sl} \sum_{i=1}^{n} \mu_i f_{il} + \rho_{sl} v_{sl} \frac{dv_{sl}}{dx} \right) - SF_w + \frac{P}{S} \frac{dS}{dx};$$

$$\begin{aligned} b_2 = -\frac{v_g^2}{2} \sum_{i=1}^{n} \mu_i f_i + \sum_{j=m+1}^{M} W_j Q_j \\ - \sum_{l=1}^{L} \left[\frac{v_{sl}^2}{2} \sum_{i=1}^{n} \mu_i f_{il} + \rho_{sl} v_{sl}^2 \frac{dv_{sl}}{dx} + \pi d_I^2 N_I \left(\alpha_I \left(T_g - T_{sl} \right) \right) \right. \\ \left. - \varepsilon\sigma (T_{sl}^4 - T_w^4) \right] + \frac{4}{D} (\Theta - 1) q_w. \end{aligned}$$

The model provides a detailed representation of chemical reaction kinetics, including both the decomposition of primary products and their subsequent transformations. Reaction rates are determined by temperature-dependent rate constants described using the Arrhenius equation (1.9).

Infrared spectroscopy was used to study different types of coals and revealed that they differed primarily in their functional groups concentrations. Using the same method, functional groups can be released and decomposed, and their concentrations (CH_4, H_2O, CO, H_2, CO_2, etc.) can be determined, and the rate constants for the release and decomposition of functional groups, as well as for the formation of final reaction products, can be determined. It has been shown, with an acceptable degree of accuracy, that the rate constants for the release of these functional groups are largely independent of coal type. The concentrations of various functional groups are not known for many coals. In such circumstances, it may be possible to estimate the composition and amount of the released primary products of coal decomposition.

In this model, the composition of volatiles is represented by a single set of functional groups with varying concentrations. Coal is represented in the model as a composite of organic and mineral components. The organic portion encompasses functional groups including H_2, H_2O, CO, CO_2, CH_4, resin, and carbon, whereas the mineral fraction is composed of ash, defined by its distinct thermophysical characteristics. Table 3.1 summarizes the kinetic parameters for reactions involving water, hydrogen, carbon monoxide, carbon dioxide, ethylene, methane, and resin formation. These parameters are applied to describe the kinetics of volatile release during coal decomposition.

Table 3.1 – The kinetic parameters of reactions

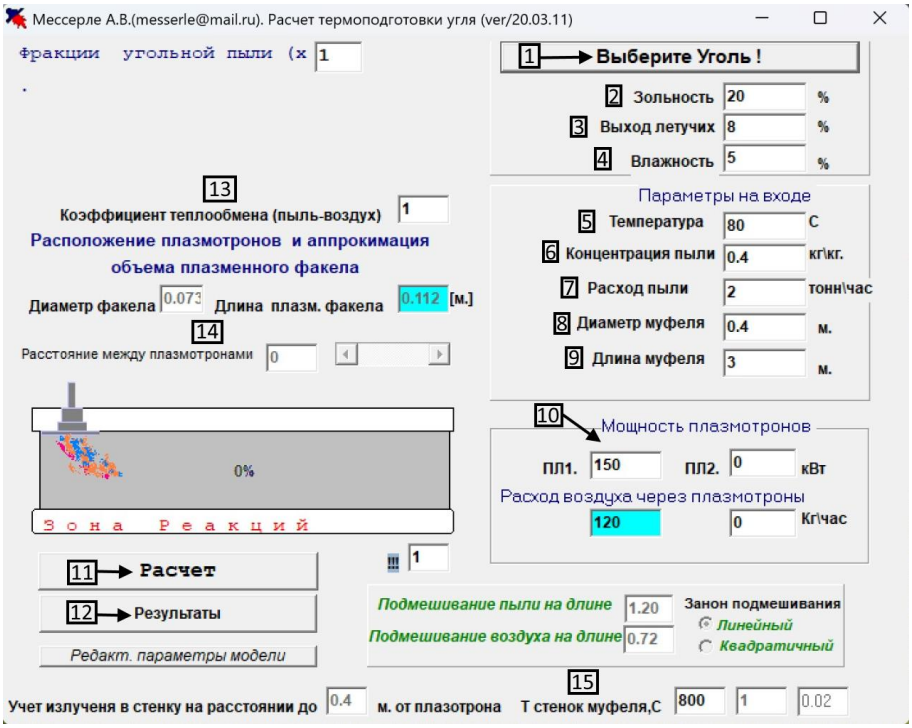
No.	Reaction	lg$A$	E_a
1	$H_{2T} = H_2$	18.2	88.8
2	$H_2O_T = H_2O$	13.9	51.4
3	$CO_T = CO$	12.3	44.4
4	$CO_{2T} = CO_2$	11.3	32.6
5	$CH_{4T} = CH_4$	14.2	51.6
6	$C_6H_{6T} = C_6H_6$	11.9	37.4
7	$C+H_2O = CO+ H_2$	11.3	60.8
8	$C+CO_2 = CO + CO$	13.2	83.6
9	$C+O_2 = CO_2$	9.4	38.0
10	$C + C + O_2 = CO + CO$	9.7	41.8

When establishing the initial conditions for equations (3.1) – (3.10), it is essential to specify the initial velocities and temperatures of both the gas and particle phases, the inlet pressure of the burner, the temperature of the burner walls, the initial composition of the coal, the gas-to-solid ratio, and the mass flow rate of the solid phase. Several ordinary differential equations within this system can only be solved numerically. To determine the velocities, temperatures, and residence times of the gas and particle phases, the Gear method [143] was employed. In addition, computations were carried out using a modified version of the K-81 program, as detailed in [144].

Based on this model, it is possible to study how a plasma torch operates under various conditions based on factors such as coal quality (i.e., the chemical composition), plasma source design and power, fineness of coal grinding, and coal dust concentration.

To achieve a HRDF possessing the desired characteristics (such as chemical composition, temperature, and density of the mixed air flow) at the burner outlet, analysis of the computational results is conducted to identify the optimal design parameters and operating conditions of the PCB.

PlasmaKinTherm is a software that implements the above-described mathematical model for kinetic calculations. The main window of the program, which provides input of initial data, is shown in Figure 3.1. It is important to note that the software operates in the Russian language.



1 – coal selection, 2 – ash content, 3 - volatile matter yield, 4 – moisture content, 5 – temperature (input parameter), 6 – coal dust concentration, 7 – coal dust consumption, 8 – muffle diameter, 9 – muffle length, 10 – plasmatron power, 11 – calculation, 12 – results, 13 – heat transfer coefficient, 14 – plasma torch flame diameter and length, 15 - muffle wall temperature.

Figure 3.1 – The central window interface of the software [2]

3.2 Results of kinetic calculations of plasma heating and ignition of thermal coals in a plasma-coal burner according to the PlasmaKinTherm software

Based on the temperature of the PICS process, thermodynamic models can be used to estimate HRDF composition and carbon gasification. Consequently, it does not provide a complete understanding of the thermal and dynamic processes that

occur when a two-phase reacting flow interacts with a plasma source on the PCB because it does not consider important factors such as process time and the time it takes for the reagents to move through the PCB. It is not possible to implement PICS without knowing the dimensions and configuration of the PCB. For this purpose, a kinetic model of the PICS process was generated using PlasmaKinTherm.

This simulation aims to determine the conditions for plasma ignition of low-grade coal. Two essential criteria must be satisfied for stable ignition and combustion of the fuel mixture at the PCB outlet: the concentration of combustible gases (CO and H_2) must exceed 15%, and the gas temperature must reach the self-ignition threshold of over 1073 K [145]. To determine oxidation of coke residue carbon and volatile release kinetics, PlasmaKinTherm, developed with the help of TERRA and Plasma-Coal software packages, uses a thermodynamic approach combined with electrothermochemical calculations of primary coal degradation products in gas phase. In a two-phase reaction channel, coal and air particles are simulated using a plasma source. Upon entering the PCB, the particles and gas become thoroughly mixed. In the plasma combustion system, the gas is heated by plasma-generated flames, which subsequently transfer thermal energy to the coal particles. During the heating stage, volatile compounds are released into the gas phase according to kinetic reaction mechanisms. The model assumes a one-dimensional flow under quasi-steady-state conditions, treating coal particles as isothermal and considering the mineral matter (ash) to be chemically inert. Interactions between particles are neglected in this approach.

Pulverized coal is heated through interaction with the high-temperature gas stream generated by the plasma. In the model, the coal composition is represented as a combination of organic and mineral components. The organic fraction comprises carbon and volatile species, including methane (CH_4), benzene (C_6H_6), carbon monoxide (CO), hydrogen (H_2), water vapor (H_2O), and carbon dioxide (CO_2), all of which actively participate in combustion reactions. As the coal particles absorb heat, volatiles are released according to their kinetic properties and subsequently react with the surrounding high-temperature gas.

Gas-phase reactions are simulated using the TERRA software, which applies local thermodynamic equilibrium models. The computational analysis includes evaluation of high-temperature electrothermochemical transformations of the primary coal degradation products in the gas phase, accounting for both oxidation of coal residues and the kinetics of volatile release.

A straight-flow cylindrical PCB with Ekibastuz coal was numerically simulated in the PICS processes. The specific heat of combustion of Ekibastuz hard coal is 4000 kcal/kg, due to its 40% ash content, 24% volatile yield, and 5.8% moisture content. The chemical composition of coal is shown in Table 2.2. The following model composition was determined using the data in Table 2.2, wt. %: ash content – 40, C – 46.18, H_2 – 2.63, H_2O – 1.84, CO – 3.95, CO_2 – 1.4, CH_4 – 0.55, C_6H_6 – 3.45.

There was a consumption of coal dust of 1000 kilograms per hour, whereas the consumption of air was 1429 kilograms per hour, which implies that the dust

concentration in the air mixture was 0.7 kilograms per kilogram. The study [145] demonstrated that the dust concentration in the air mixture required to sustain a HRDF flame for Ekibastuz coal was achieved. The PCB features an inner wall length of 3 meters and a diameter of 0.15 meters. The air mixture entering the system is preheated to 300 K. To estimate the PICS of coal, simulations were conducted using plasmatron power levels of 40, 60, and 80 kW. The coal dust fractional composition, based on sieve analysis results, is summarized in Table 3.2. On average, the coal particles measured approximately 60 microns in diameter, roughly equivalent to the thickness of a human hair.

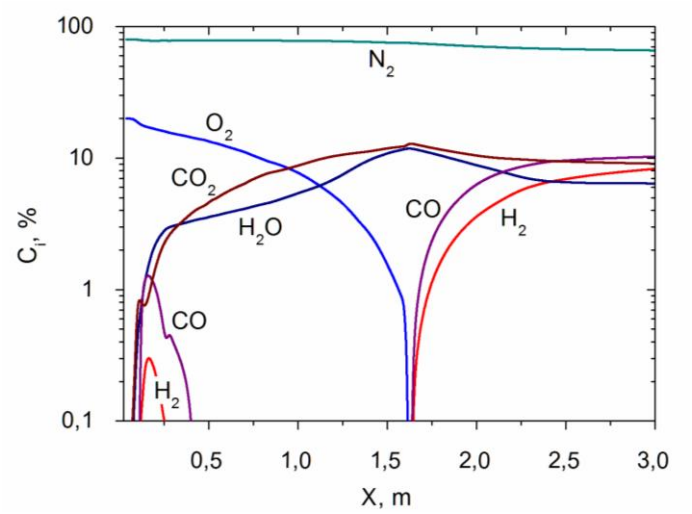
Table 3.2 – Ekibastuz coal fractional composition

Fraction	Particle diameter, microns	Fraction share, mass. %
1	10	10
2	30	20
3	60	40
4	100	20
5	120	10

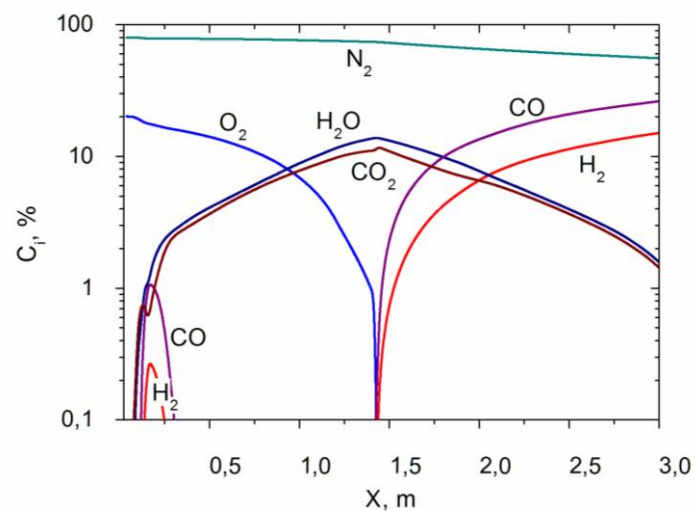
Figures 3.2–3.6 illustrate the results of the kinetic calculations.

A comparison of the gas phase compositions of 40, 60, and 80 kW plasmatron powers is shown in Figure 3.2. As shown in Figure 3.2 (a) – (c), ignition occurs in all plasmatron powers. There is almost no difference between the curves of the products of ETCPF for combustion for all plasmatron powers, although the contents are slightly different. Among the most important indicators is the concentration of flammable components ($CO + H_2$). At the beginning of the channel (0.1-0.4 m), small-scale extremes of the concentration curves of flammable gas ($CO + H_2$) have been observed: 1.4%, 1.4%, and 1.6% for 40, 60, and 80 kW, respectively. It has been shown that the concentration of flammable components increases with increasing plasmatron power, reaching a level of 18.6, 41.7, and 29.4%, respectively, when the PCB exits the plasmatron at power levels of 40, 60, and 80 kW. At the PCB outlet, the concentration values of flammable components are significantly higher than the concentration values required for a stable ignition of the air mixture at the PCB outlet (> 15%) due to the presence of these components. In terms of the environment, harmful gases are important. There is a peak in the CO_2 gas content at the half-length of the PCB at the power levels of 40, 60, and 80 kW as shown in Figure 3.2. As compared to traditional burners, these results are much more environmentally friendly when compared to traditional burners.

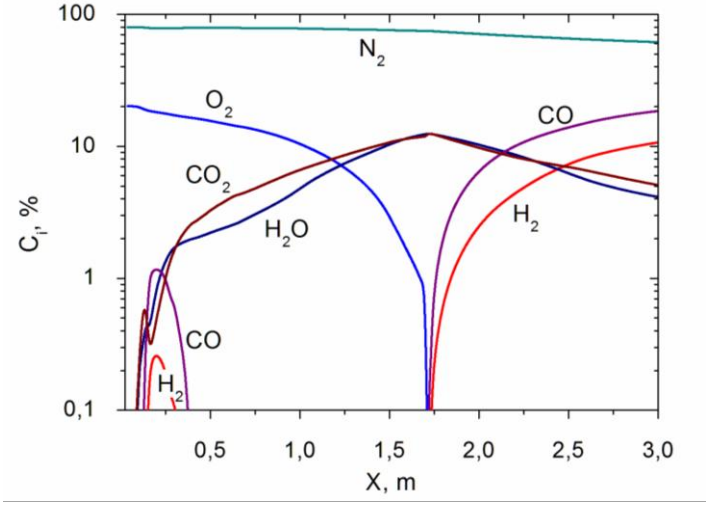
A comparison of power levels at 40, 60, and 80 kW showed that for a power of 60 kW, the maximum syngas ($CO + H_2$) concentration at the burner outlet in a setup 3 m long and 0.15 m in diameter was 41.7%, while the minimum CO_2 concentration was 1.43%. Therefore, under these geometric conditions, a burner power of 60 kW is considered optimal [146].



(a)



(b)



(c)

Figure 3.2 – Change in the composition of the gas phase at a plasmatron power of 40 kW (a), 60 kW (b) and 80 kW (c) along the length of the PCB [145]

As illustrated in Figure 3.3, the gas temperature in all simulated cases is adequate to initiate coal particle ignition. At the inlet of the PCB channel (X = 0 m), the gas temperature increases in proximity to the plasma source as the power of the plasma torch is raised. The maximum temperature values for 40 kW are 1716 K at 1.68 m, for 60 kW — 1849 K at 1.38 m, and for 80 kW — 1409 K at 1.58 m.

Figures 3.4 (a) – (c) illustrate the qualitative similarity between the temperature curves in each of them. Along the entire length of the PCB, temperatures of both the gas and coal particles progressively rise. For example, as shown in Figure 3.4 (b), the gas temperature attains a maximum of 1849 K at 1.38 m from the inlet under a power input of 60 kW. In contrast, the coal particles do not reach their peak temperature within the full 3-meter length of the flow section. Notably, a fine particle fraction with a size of ten microns reaches its highest temperature of 1415 K at 2.06 m along the PCB. In the PCB, except for fractions 1 and 2, the gas temperature is higher than the coal temperature. According to Table 3.2, as the coal fraction size increases, the temperature difference between the gas and particle exit temperatures increases. Because larger coal particles heat up more slowly than smaller ones, the carbon oxidation reaction in these larger particles produces less heat. Observations indicate that, due to carbon oxidation occurring on the coal surface, particle fractions 1 and 2 exiting the PCB exhibited temperatures exceeding that of the gas by 11°C and 13°C, respectively. Furthermore, at a distance of 3 meters from the PCB outlet, the temperatures of the gas and particles appear to converge, suggesting that thermal equilibrium between them is being approached.

Figure 3.4 demonstrates that plasmatron power levels of 40, 60, or 80 kW are adequate to ignite the particles, as the gas temperature at the PCB outlet exceeds the ignition threshold of 1073 K.

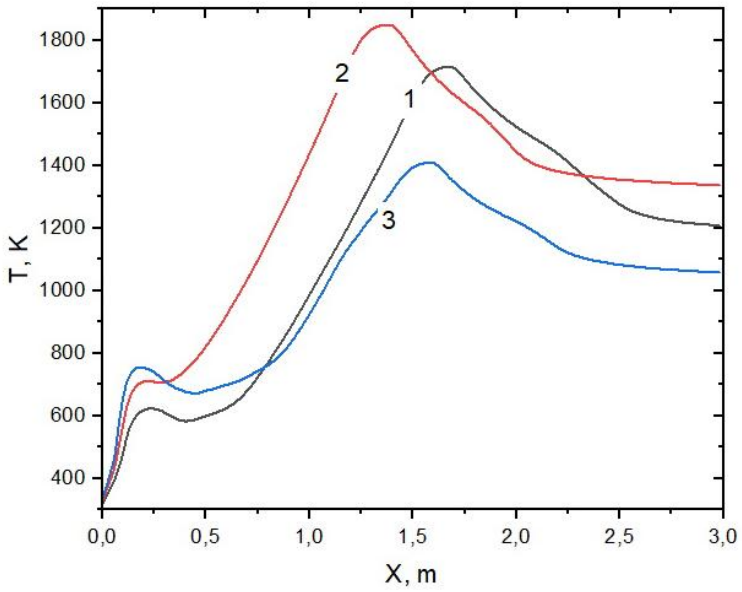
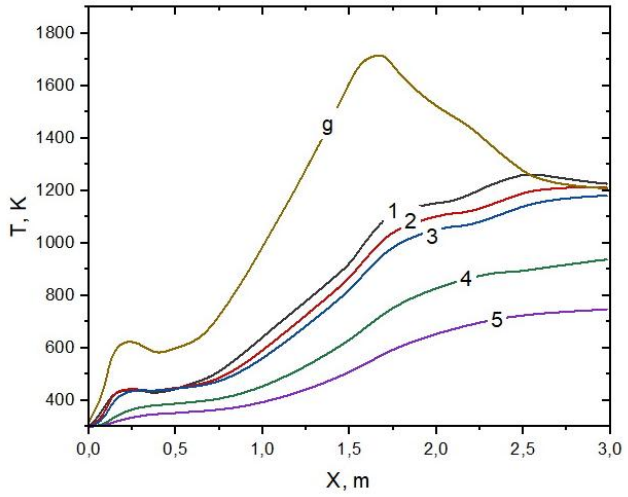
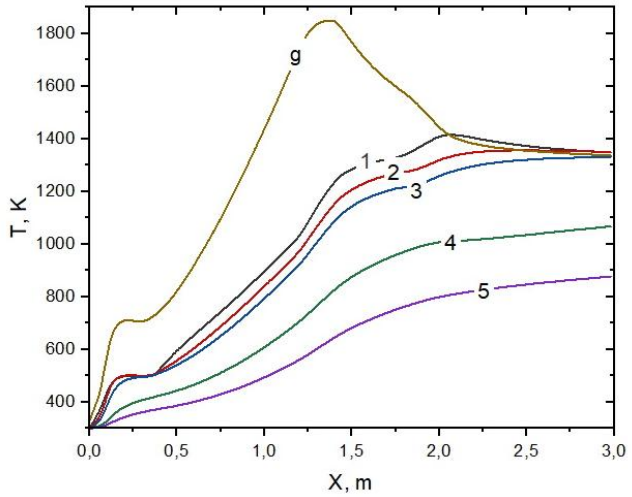


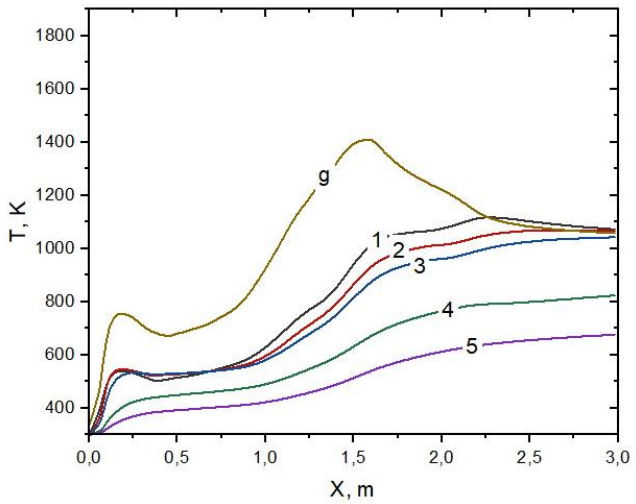
Figure 3.3 – Change in gas phase temperature at a plasmatron power of 40 kW (1), 60 kW (2) and 80 kW (3) along the length of the PCB [145]



(a)



(b)



(c)

Figure 3.4 – Change in the temperature of coal fractions at a plasmatron power of 40 (a), 60 (b) and 80 kW (c) along the length of the PCB: 1–5 – size fractions of coal particles according to Table 3.2 [145]

There is a qualitative similarity between the velocity curves in Figures 3.5 (a–c). The speeds of both coal particles and the gas phase rise progressively along the length of the PCB. Specifically, as they travel through the PCB, the gas and coal particles accelerate from an initial velocity of 13 m/s up to their peak speed. Throughout the entire length of the device, the coal particles categorized as fractions 2 (30 microns) and 3 (60 microns) maintain equivalent velocities.

As illustrated in Figure 3.5 (a), the gas velocity attains its maximum value at 64.9 m/s at a length of 1.64 m. The velocity peaks for the coal fractions (1–5) were as follows: 58.8 m/s at 1.90 m, 57.3 m/s at 2.0 m, 57.3 m/s at 2.0 m, 51.8 m/s at 2.32 m, and 48.0 m/s at 3.0 m (at the burner outlet), respectively. There were minor peaks in the velocities of both gas and coal fraction 1 in the initial section (0.0–0.5 m). Gas velocity peaked at 32.8 m/s at 0.3 m, and coal velocity peaked at 31.8 m/s at 0.38 m for fraction 1.

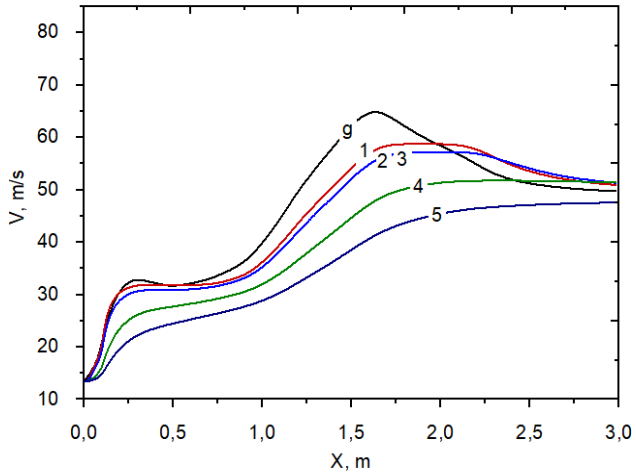
As shown in Figure 3.5 (b), at a length of 1.72 m, the maximum gas velocity is 77.3 m/s. The velocity peaks for coal fractions (1–5) were: 69.2 m/s at 2.04 m, 67.2 m/s at 2.14 m, 67.2 m/s at 2.14 m, 60.2 m/s at 2.42 m, and 54.2 m/s at 3.0 m. In the initial section, a velocity peak was observed only for gas (27.0 m/s at 0.34 m), while the behavior of the coal fractions tended toward their respective maxima.

According to Figure 3.5 (c) at the exit of the PCB, the gas velocity decreases to 62.1 m/s, which is consistent with a maximum velocity of 84.3 m/s over a channel length of 1.44 m. There is no extremum to the velocity curves of coal particles accelerated by gas. There is a 75 m/s coal particle velocity in fraction 1 at a length of 1.7 m for a PCB. There are maximum velocity values of 72.7, 72.7, 64.6, and 58.9 m/s for coal particles of other fractions at the PCB output (curves 2–5). At the PCB outlet, gas and coal particles exhibit substantially higher velocities compared to air mixtures exiting conventional coal burners, which typically flow at speeds of approximately 20–30 m/s. The observed convergence of gas and particle velocity profiles at the 3-meter mark downstream of the PCB suggests an approach towards dynamic equilibrium between the two phases.

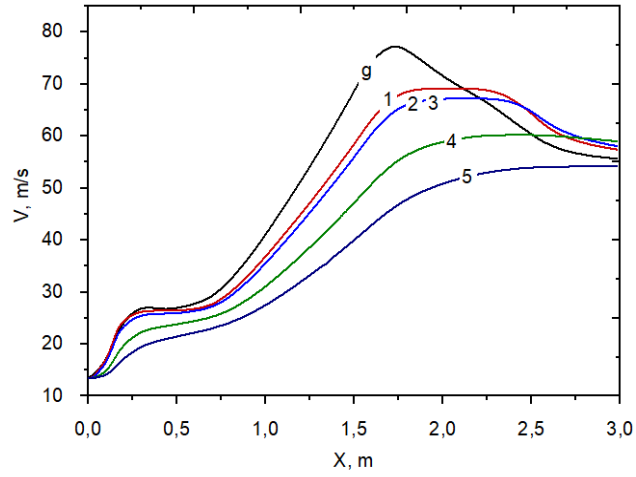
There is an extremum in the gas velocity curves at plasmatron powers of 40 to 80 kW (curves 1–3), as shown in Figure 3.6. When a plasmatron power is increased, the gas velocity shifts toward the plasma source in response to an increase in its maximum velocity as a result of the increased plasmatron power. It is important to note that the maximum gas velocity varies from 64.9 to 84.28 m/s. As a result of plasmatron power levels of 40, 60, and 80 kW, maximum gas velocity was recorded at lengths of 1.72, 1.64, and 1.44 m, respectively. At the burner exit, the velocity of the gas followed the same sequence as the temperature.

After leaving the PCB, coal particle fractions attain velocities greater than 50 m/s, which notably surpasses the flow speeds observed in conventional solid fuel combustion air-fuel mixtures. Within the PCB itself, all particle fractions sustain velocities exceeding 15 m/s, ensuring effective transport without segregation through the horizontal dust conduit.

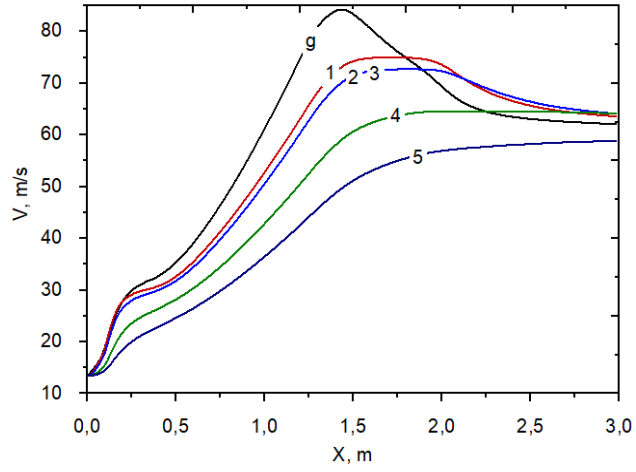
These kinetic modeling outcomes served as the foundation for planning and executing the experimental procedures.



(a)



(b)



(c)

Figure 3.5 – Change in the velocity of coal fractions at a plasmatron power of 40 (a), 60 (b) and 80 kW (c) along the length of the PCB: 1–5 – size fractions of coal particles according to Table 3.2 [145]

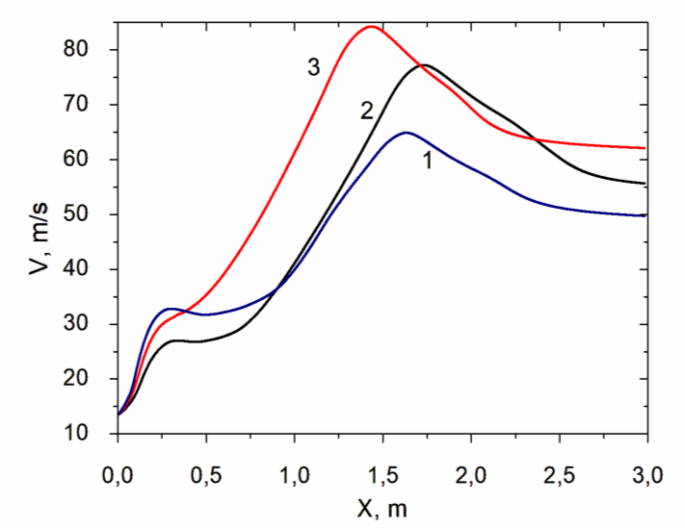


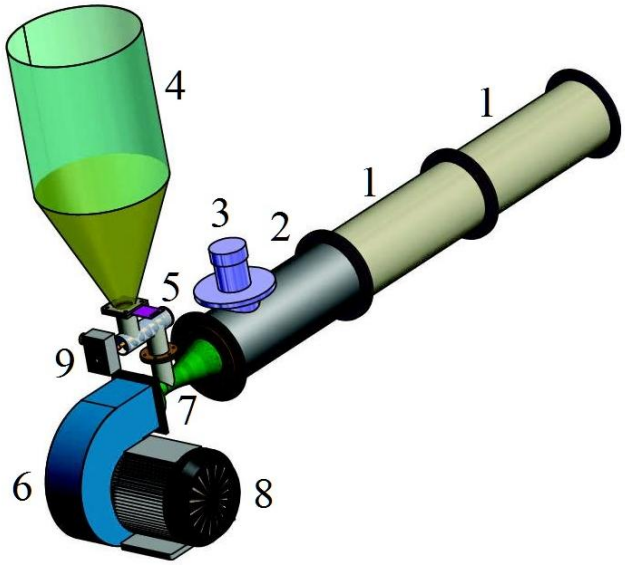
Figure 3.6 – Change in gas phase velocity at a plasmatron power of 40 kW (1), 60 kW (2) and 80 kW (3) along the length of the PCB [145]

Appendix B provides an example of kinetic calculations for the heating and plasma ignition of thermal coal performed using the PlasmaKinTherm software.

3.3 Results of experimental studies of plasma ignition of thermal coal in a plasma-coal burner

Within the PICS experiments, the parameters ensuring stable ignition and combustion of the HRDF flame at the PCB outlet were examined and confirmed, with the calculated outcomes being evaluated against the experimental measurements. Figure 3.7 shows a diagram of the experimental setup. On the PCB, plasmatron (3) is located at the beginning (the cylinder-lined section 2). An air mixture is created by mixing coal dust from hopper (4) with air from centrifugal fan (6). Air mixture in the PCB is initially moving at 15 m/s due to the fan's air flow of 1430 kg/h. Plasmatron (3) creates the flame that interacts with the air mixture in the PCB. In order to create plasma flames, air is blown between electrodes and heated until it becomes plasma. Flames produced by plasmatrons reach temperatures greater than 5270 K [147-152]. The experiments were conducted on a PCB with a diameter of 0.15 m and a length of 3 m. A plasmatron with a power of 70 kW was used in the experiments. The plasmatron operated at an efficiency of 85%, which corresponds to a power output of 60 kW. According to Table 2.2, Ekibastuz coal was used in the experiments. The fractional composition of coal dust is shown in Table 3.2 based on sieve analysis. Using 300 K for the air mixture resulted in 1000 kilograms of coal and 1430 kilograms of air consumed per hour. A PICS experiment was conducted after the system was commissioned. Experimental objectives included igniting the air mixture with plasma and obtaining a stable HRDF flame at the PCB outlet, as well as determining the composition, temperature, and degree of carbon gasification of the HRDF flame. During the experiments, an air mixture with a dust concentration

of 0.7 kg/kg was established and maintained. These conditions resulted in an HRDF flame that self-ignited and burned steadily at the PCB outlet, as can be seen in Figure 3.8. There is a greater risk of igniting and burning a HRDF flame in the open air than in a boiler with an organized secondary air supply. Open-air combustion of HRDF flame is more challenging. The HRDF flame measured 4–5 m in length. The torch's temperature ranged between 870 and 3270 K as measured by the digital pyrometer Ircon Ultrimax Plus UX10P. When determining the measurement error, it is important to consider the temperature range in which the measurement is taken. The error in measuring temperatures below 1770 K can be as much as 0.5%, higher temperatures may be as much as 1%, and temperatures over 2300 K may be as much as 2%. Temperature resolution is at least one degree. During the ignition of high-ash Ekibastuz coal, the temperature of the HRDF flame fluctuated between 1420 and 1450 K, ensuring stable combustion when combined with oxygen from the air. Gas sample analysis was conducted using a specialized heat-resistant probe. The procedure for sampling is illustrated in Figure 3.9. The following steps were followed to collect gas samples. Upon activation of the centrifugal fan (2), coal dust is supplied from the hopper (3) and an air mixture is formed, which is ignited by the plasma flame. In the volume of the HRDF flame, a stainless steel probe with a diameter of 5 mm was attached to a PCB. The required amount of gas was collected using a gas extraction syringe (6), a high-temperature filter (4), and a three-way valve (5). Replaceable superfine basalt fibers make up the filter. As part of the analysis of the composition of the sample, the Chromatek-Gazochrom-2000 gas chromatograph was connected to the syringe containing the sample so that its composition could be determined.



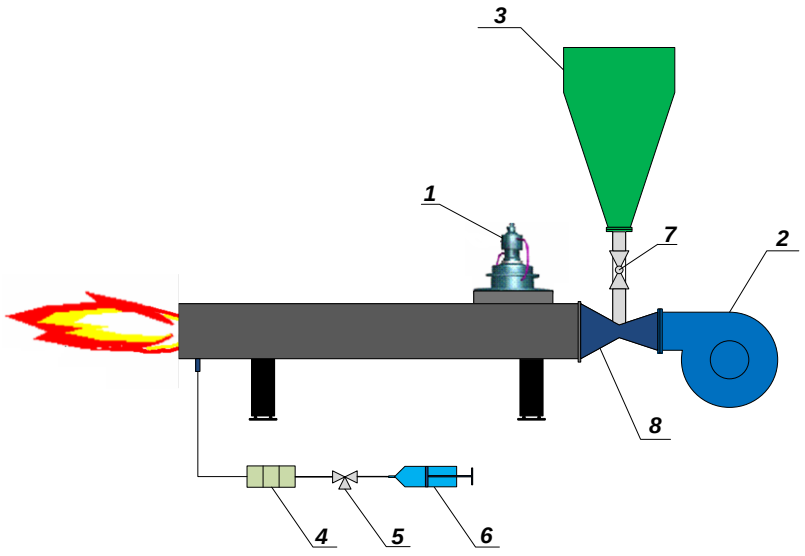
1 – muffelized section of the PCB, 2 – plasmatron installation nozzle in muffelized section, 3 – plasmatron, 4 – coal dust hopper, 5 – dispenser for dust, 6 – PCB air supply centrifugal fan, 7 – nozzle confuser-diffuser; 8 – fan drive motor, 9 – the screw mechanism is driven by a motor.

Figure 3.7 – Diagram of experimental PCB [148]



Figure 3.8 – HRDF flame at PCB outlet during bench testing [149]

The main advantage of this technology is that there is no slag on the inner surfaces of the plasma-coal burners. To prevent the combustion of solid fuel within the PCB, the temperature of the PICS processes is regulated to stay below the ash softening point of the coal by maintaining the concentration of coal dust in the air-fuel mixture at 0.7 kg per kg of air. For Ekibastuz coal, the ash softening temperature is T_3 = 1520 K. After the completion of the process, the resulting solid residue is passed through a high-temperature filtration unit equipped with a replaceable filler (4) to assess the remaining carbon content, as depicted in Figure 3.9. The carbon content of condensed PICS products was determined using an absorption gravimetric method.



1 – plasmatron; 2 – centrifugal fan; 3 – dust hopper; 4 – filter made of superfine basalt fiber with replaceable filler for high temperatures; 5 – three–way valve; 6 – syringe for gas extraction; 7 – shut-off valves; 8 – diffuser

Figure 3.9 – Diagram of exhaust gases extraction from PCB [149]

The cylindrical channel of the plasma-coal burner is made of steel grade 3, which prevents it from melting at temperatures up to 1690 K. A circular pattern of bricks (mortal) is arranged inside this channel in Figure 3.10. The bricks are made of three aluminum oxides. These bricks provide effective thermal insulation (up to 2140 K) for the metal cylinder.



Figure 3.10 – Bricks inside a metal cylindrical burner

The experimental setups in Figure 3.11 were operated under strict safety measures, including the use of protective clothing as part of the operating procedures. In addition, sound insulation was provided, along with other necessary measures to ensure safety and comfort.



Figure 3.11 – Experimental studies

Coal and heavy fuel oil co-combustion presents a range of environmental, economic, and technical challenges. Among these are the complications of fuel oil storage and handling during winter conditions, relatively low gross efficiency (typically around 4–5%), elevated levels of unburned carbon in coal combustion residues (approximately 10–15%), and significantly increased emissions of nitrogen oxides (by 40–50%), along with heightened releases of sulfur compounds and vanadium pentoxide.

Considering all of the above, plasma technologies are more environmentally friendly than fuel oil when it comes to fuel combustion [149 – 152]. Plasma-based technologies have demonstrated the potential to lower nitrogen oxide emissions by approximately 1.5 to 2 times and to reduce the content of unburned carbon in coal combustion products by a factor of 2 to 3. Moreover, the removal of fuel oil from the combustion process results in a 90–95% reduction in vanadium pentoxide emissions.

It has been officially established by the law of Kazakhstan that specific emission standards will apply to pollutants such as NO_x and SO_2 that are set at 0.002 and 0.006 kilograms per kWh, respectively [153].

Analyses conducted by the environmental protection laboratory of the UK TPP revealed that all samples contained less than 30 mg/Nm^3 of NO_x. The NO_x samples were collected using a ceramic probe at the ETCPF chamber outlet. NO_x concentrations in the products of ETCPF at 1000-1500 K have been demonstrated previously to be no more than 10-20 mg/Nm^3. According to the results of experimental studies, it has been found that the plasma ignition technology for solid fuel reduces NO_x emissions and the amount of unburned carbon of coal by a factor of 2 compared to traditional combustion of thermal coal [78].

3.4 Comparison of the results of calculations using TERRA and PlasmaKinTherm software packages with the results of an experimental study of plasma ignition of thermal coals

There is a comparison between the experimental results and the calculations of PICS presented in Table 3.3. On the basis of identical initial data (composition of Ekibastuz coal, coal and air consumption, PCB geometric parameters, plasmatron power), experimental and numerical studies are compared. Based on Table 3.3, the HRDF temperature varies within a narrow range of 1443 – 1453 K and does not differ more than 8% from the calculated temperature (1340 K). Only 1% of the calculated value was different from the actual degree of carbon gasification, which varied from 53.8% to 60.5%. Therefore, it is safe to say that there is not more than 23% discrepancy between experimental and numerical values of key parameters in PICS. Given the intrinsic complexity of two-phase plasma PICS processes, some divergence between experimental observations and computational predictions is expected in multicomponent heterogeneous plasma environments. For systems operating at high temperatures, a discrepancy of less than 25% is considered

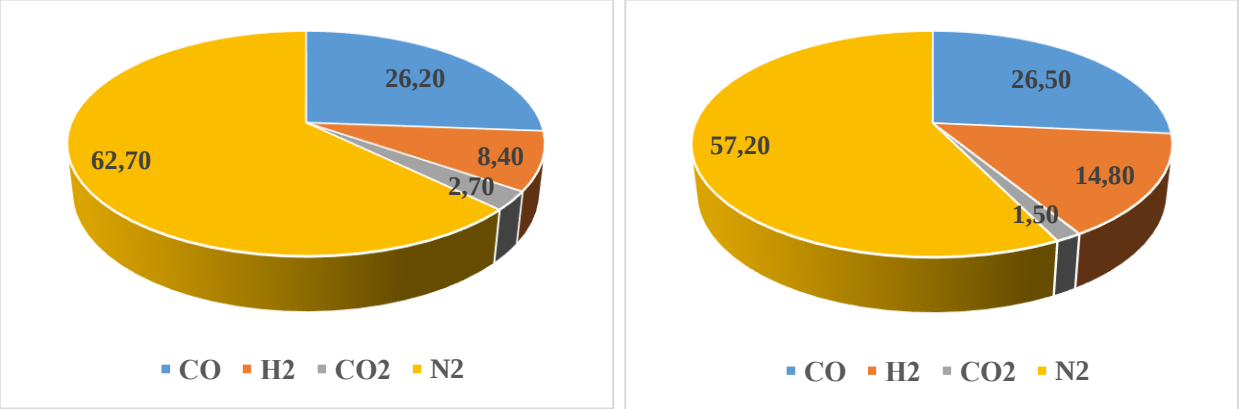
excellent. Furthermore, PlasmaKinTherm can be used for engineering calculations for plasma-coal burners because it accurately reflects the basic laws of PICS.

Table 3.3 – PCB parameter comparison between experimental and numerical values

Method	T_{HRDF}, K	C_i, %				X_C, %
		CO	H_2	CO_2	N_2	
1st experiment	1443	24.6	7.5	3.2	64.7	53.8
2nd experiment	1453	27.8	9.3	2.2	60.7	60.5
Numerical simulation	1340	26.5	14.8	1.5	57.2	57.6

Below is a comparison of experimental and calculated results as illustrated in Figure 3.12. The concentration of carbon monoxide (CO) represents almost 1/4 of the total concentration in Figure 3.12 (a), ranging between 24.6% and 27.8%, with an average concentration of 26.2%. The concentration of hydrogen, which is highly flammable, has a range of 7.5-9.3%, with an average value of 8.4%. During the experiments, the combustible elements (CO + H_2) accounted for 34.6% of the syngas (with a variation between 32.1% and 37.1%). In the PCB volume, N_2 represents more than half of the concentration (varying between 64.7% and 60.5%). CO_2 concentration provides an indication of the ecological efficiency of the PCB. It was determined that the concentration of this gas was less than 4% (2.7%), which is considered sufficient to ensure the safety of the environment.

Based on the calculation results shown in Figure 3.12 (b), the concentrations of the gases are quite similar. It should be noted that the differences in the gases are primarily due to the reaction with secondary air in the experiments, as the calculations use an isolated system at the PCB outlet that does not interact with other gases.



(a) (b)

(a) – experiments; (b) – numerical simulation.

Figure 3.12 – Concentrations of gases

Appendix C presents the results of numerical modeling and experimental investigations of PICS processes in a pulverized coal torch. These findings were utilized to inform technical decisions in the development of a PCB for the TPE-215 boiler at the Gusinoozersk State District Power Plant (Gusinoozersk, Republic of Buryatia, Russian Federation).

CONCLUSION

Several technologies have been considered for plasma ignition and combustion stabilization of solid fuels, but the PCB technology has proven to be the most promising.

An analysis of the thermodynamics of the PICS process of the low-grade Ekibastuz coal was conducted using the TERRA software package in the temperature range of 300 to 2000 K. An optimal temperature of 1880 K was determined for the PICS process, resulting in a specific energy consumption of 1.18 kW·h/kg.

The PlasmaKinTherm software was used to perform kinetic calculations for the low-grade coal PICS process. This enabled the determination of the distributions of temperature, velocity, and concentrations of the HRDF components along the length of the PCB. According to the study, the main product of the PICS process is a HRDF, consisting of combustible gas and coke residue. With the optimal parameters found in numerical calculations (plasma torch power of 60 kW at atmospheric pressure, PCB length and diameter of 3 m and 0.15 m, respectively), the HRDF flame reaches a temperature of 1340 K, with a synthesis gas concentration (CO – 26.5%, H_2 – 15.2%) of 41.7% at the PCB outlet, which meets the criteria for a stable ignition process.

Experimental studies were conducted using the optimal parameters from the numerical research for PICS process in a bench-scale PCB. The experiments showed that a high-calorific value HRDF could be obtained from low-grade, high-ash Ekibastuz coal. In all experiments on plasma ignition of low-grade Ekibastuz coal, a bright HRDF flame with a core temperature of up to 1453 K was observed at the PCB outlet. In addition to measuring the HRDF flame temperature, it was found that the degree of coal gasification as a result of the PICS process reached 60.5%.

By comparing the results of calculations using the TERRA and PlasmaKinTherm software packages, it was possible to achieve good agreement between the experimental and numerical results.

Assessment of the comprehensive solution to the stated objectives

The dissertation fully addresses all the stated goals and objectives. During the course of the research, the validity of the obtained results was demonstrated. The results were discussed and analyzed by both domestic and international scientific advisors, as well as by the staff of the Department of Thermal Physics and Technical Physics.

Recommendations for the application of the results obtained in the course of the dissertation research

The results of the dissertation can be applied at pulverized coal-fired thermal power plants and boiler installations to optimize plasma-coal burners.

Assessment of the scientific level of the dissertation

The computational modeling and experimental investigations presented in this dissertation were performed at the Department of Thermophysics and Technical Physics, Faculty of Physics and Technology, al-Farabi Kazakh National University, and at the Scientific and Technical Production Center 'Zhalyn', respectively. The reliability of the obtained results is confirmed by published scientific data derived from the research work. The results of the study were published in high-impact international and domestic scientific journals, discussed at international conferences, and an implementation certificate was obtained.

REFERENCES

1 Messerle V.E., Ustimenko A.B. Thermodynamic and kinetic modeling and experiment on plasma ignition of pulverized high-ash coal // Applications in Energy and Combustion Science. – 2024. – Vol. 17. - 100248.

2 Messerle V.E., Ustimenko A.B. Plasma ignition and solid fuel combustion (Scientific and technical bases) [Plazmennoe vosplamenenie i gorenie tverdogo topliva]. - Saarbrucken, Germany: Palmarium Academic Publishing, 2012. – 404 p. (in Russian)

3 Coal facts // Internet newspaper "Language selection - Natural Resources Canada". - 2024. https://natural-resources.canada.ca/our-naturalresources/minerals-mining/mining-data-statistics-and-analysis/minerals-metalsfacts/coal-facts/200711

4 Coal energy industry worldwide // Internet newspaper "Statista". - 2024. https://www.statista.com/topics/3255/coal-energy-industry-worldwide/#statisticChapter

5 China's energy-security push drives up fossil-fuel approvals, Greenpeace research shows // Internet newspaper "Reuters". - 2023. - 3 August. https://www.reuters.com/business/energy/chinas-energy-security-push-drives-up-fossilfuel-approvals-research-2023-08-03/

6 What's the Role of Coal Consumption in Energy Production? // Internet newspaper "Just Energy". - 2023. - 24 January. https://justenergy.com/blog/coal-consumption-in-energy/

7 'Clean Coal' Technologies, Carbon Capture and Sequestration // Internet newspaper "World Nuclear Association". - 2021. - 16 November. https://world-nuclear.org/informationlibrary/energy-and-the-environment/clean-coal-technologies

8 Coal // Internet newspaper "IEA". - 2023. https://www.iea.org/energy-system/fossil-fuels/coal

9 Fu C., Anantharaman R., Jordal K., Gundersen T. Thermal efficiency of coal-fired power plants: From theoretical to practical assessments // Applications in Energy Conversion and Management. – 2015. – Vol. 105. - P. 530-544.

10 High-efficiency, low-emissions coal plants: come HELE or high water // Internet newspaper "GE Vernova". - 2021. https://www.gevernova.com/gas-power/resources/articles/2018/come-hele-or-high-water

11 Energy Security and Coal, ECoal // Internet newspaper "World Coal Institute". - 2001. - December. http://www.wci-coal.com

12 Coal Power for Progress // Internet newspaper "World Coal Institute". - 2000. http://www.wci-coal.com.

13 Karpenko E.I., Messerle V.E., Zhuravel N.M., Churashev V.N. Ecological and economic efficiency of plasma technologies for processing solid fuels [Ekologo-ekonomicheskaya effektivnost' plazmennykh tekhnologiy pererabotki tverdykh topliv]. - Novosibirsk: Science. - 2000. – 159 p. (in Russian)

14 Messerle V.E., Ustimenko A.B. Solid Fuel Plasma Gasification // Applications in Advanced Combustion and Aerothermal Technologies. - 2007. - P. 141-156.

15 Messerle V.E., Ustimenko A.B. Plasma-Supported Coal Combustion. Modelling and Full-Scale Trials // Applications in Advanced Combustion and Aerothermal Technologies. - 2007. - P. 115-129.

16 Energy fuel of the USSR: Handbook [Energeticheskoye toplivo SSSR: Spravochnik] // Energy, 1986. – 676 p. (in Russian)

17 Hoffman E. Energy-technological use of coal [Energotekhnologicheskoye ispol'zovaniye uglya] // Energoatomizdat, 1983. – 328 p. (in Russian)

18 Lipovich V.L. Chemistry and processing of coal [Khimiya i pererabotka uglya] // Chemistry. - 1988. – 336 p. (in Russian)

19 Singer S. Pulverized Coal Combustion. (Recent Developments). - Noyes Publications: New Jersey, USA, 1984. – 184 p.

20 Zhukov M.F., Kalinenko R.A., Levitsky A.A., Polak L.S. Plasma-chemical processing of coal [Plazmokhimicheskaya pererabotka uglya] // Science, 1990. – 200 p. (in Russian)

21 Smoot L.D., Smith P.J. Coal Combustion and Gasification. Plenum Press: New York, 1985. – 443 p.

22 Smoot L.D. Role of Combustion Research in the Fossil Energy Industry, Energy and Fuels // An American Chemical Society Journal, 1993. - Vol. 7. - No. 6. – P. 689.

23 Williams A., Pourkashanian M., Jones J.M., Skorupska T. Combustion and Gasification of Coal. – Taylor and Francis: New York, USA, 2000.

24 Abbas T., Costen P.G. and Lockwood F.C. Solid Fuel Utilisation: From Coal to Biomass, in Twenty-Sixth Symposium (International) on Combustion. – The Combustion Institute, Pittsburgh, 1996. - 3041 p.

25 Keay M. The View from Europe – and elsewhere. World Coal Institute: London, 2003. - 243 p.

26 Cletcins K. World power policy. Using a technology of a three-stage combustion for NO_x suppression on solid fuel boilers in Europe and CIS // Opening Rep. Europ. Commission for Power Engineering and Transport. – 2000. – P. 4-17.

27 Coal facts, natural-resources.canada.ca // Internet newspaper “Government of Canada”. - 2017. https://natural-resources.canada.ca/our-natural-resources/minerals-mining/mining-data-statistics-and-analysis/minerals-metals-facts/coal-facts/20071

28 Coal energy industry worldwide // Internet newspaper “Statista”. - 2024. https://www.statista.com/topics/3255/coal-energy-industry-worldwide/#statisticChapter

29 Messerle V., Orynbasar M., Ustimenko A. Efficiency of plasma technology for preparing solid fuels for combustion [Effektivnost' plazmennoy tekhnologii podgotovki tverdykh topliv k szhiganiyu] // Combustion and Plasma Chemistry, 2024. - Vol. 22. - No. 3. - P. 169–178. (in Russian)

30 Coal's importance to the world // Internet newspaper "Society for mining, Metallurgy and Exploration". - 2021. https://www.smenet.org/What-We-Do/Technical-Briefings/Coal-s-Importance-in-the-US-and-Global-Energy-Supp

31 Karpenko E., Messerle V. The Current Status and Prospects of Using Plasma-Energy Technologies in Heat Power Industry // Proceeding of the Sixth International Conference on Technologies and Combustion for a Clean Environment "Clean Air". Vol. II. Porto, Portugal, 2001. - P. 791-794.

32 Kalinenko R.A., Levitsky A.A., Messerle V.E., Polak L.S., Sakipov Z.B., Ustimenko A.B. Electrothermochemical processing of coals [Elektrotermokhimicheskaya pererabotka ugley. Matematicheskaya model' i eksperiment]. Mathematical model and experiment // High Energy Chemistry. - 1990. - Vol. 24. - No. 2. - P. 176-182. (in Russian)

33 Aliyarov B.K. Development of combustion of Ekibastuz coal at thermal power plants [Osvoyeniye szhiganiya Ekibastuzskogo uglya na teplovykh elektrostantsiyakh]. Almaty: "Gylym", 1996. – 272 p. (in Russian)

34 Suleimenov K.A., Kaspiev A.G., Ismailov A.D. Experimental installation laboratories «clean coal technologies» [Eksperimental`nye ustanovki laboratorii "chistye ugol`nye tehnologii"] // NU Research and Innovation System of Nazarbayev University. - Astana, 2020. - P. 139-145. (in Russian).

35 Rao Z., Zhao Y., Huang C., Duan C. Recent developments in drying and dewatering for low rank coals // Applications in Progress in Energy and Combustion Science. - 2015. - Vol. 46. - P. 1–11.

36 Coal Facts // Internet newspaper "Future Coal". - 2020. https://www.futurecoal.org/coal-facts/

37 Bolegenova S., Askarova A., Ospanova Sh., Zhumagaliyeva S., Makanova A., Aldiyarova A., Nurmukhanova A., Idrissova G. Technology of reducing greenhouse gas emissions for decarbonization and decreasing anthropogenic pressure on the environment // Physical Sciences and Technology. - 2024. - Vol. 11. - No. 1-2. - P. 64-75.

38 Bolegenova S., Askarova A., Slavinskaya N., Ospanova Sh., Maxutkhanova A., Aldiyarova A., Yerbosynov D. Statistical modeling of spray formation, combustion, and evaporation of liquid fuel droplets // Physical Sciences and Technology. - 2022. - Vol. 9. - No. 3-4. - P. 69-82.

39 Bolegenova S., Askarova A., Ospanova Sh., Pilipenko N., Shortanbayeva Z., Aldiyarova A. Simulation of atomization and ignition of high-pressure jet stream // Recent Contributions to Physics. - 2023. - Vol. 86. - No. 3. - P. 67–76.

40 Ibragimov M.Kh., Marchenko E.M., Tuvalbaev B.G. Analysis of methods for stabilizing a coal-dust flare [Analiz sposobov stabilizatsii pyleugol'nogo fakela] // Power Engineering and Electrification. - 1990. - No. 1. - P. 8-10. (in Russian)

41 Knapp R. Coal: Fuel with a Future // Conference Energy Resources. – London, 2000. – 31 p.

42 Ibragimov M.Kh., Marchenko E.L., Tuvalbaev B.G. Coal gasification for obtaining power gas [Gazifikatsiya uglya dlya polucheniya energeticheskogo gaza] // Collection of works / VZPI. Series: Thermal power plants (Energy-technological use of fuels). - 1983. – P. 16-29. (in Russian)

43 Chernenkov I.I., Shafir G.S. State and Prospects of Coal Gasification [Sostoyaniye i perspektivy gazifikatsii ugley] // Review. - 1982. – 46 p. (in Russian)

44 Falbe Yu. Chemical substances from coal [Khimicheskiye veshchestva iz uglya] // Chemistry. - 1980. – P. 19. (in Russian)

45 Kelsall G.J., Soothill C.D. Power Generation for a Cleaner Environment – a Perspective // 28th Florida Conference Clean Air. - 2003. - Vol. 4. - P. 203-221.

46 Xiang X., Yunhan X., Chunzhen Q. Conceptual Design and Performance Analysis of Coal Based Direct Hydrogen Production System with CO2 Capture // The Proceedings of the 31-th International Technical Conference on Coal Utilization and Fuel systems. – Clearwater; Florida, USA. - 2006. - P. 668-679.

47 Arun C.B. Co-Production of Hydrogen and Electricity Using Circulating Fluidized Bed Technologies // The Proceedings of the 31-th International Technical Conference on Coal Utilization and Fuel systems. - Clearwater; Florida, USA. - 2006. - P. 903-913.

48 Sathe N., Botte G.G. Assessment of Coal and Graphite Electrolysis for the Production of Hydrogen // The Proceedings of the 31-th International Technical Conference on Coal Utilization and Fuel systems. – Clearwater; Florida, USA. - 2006. – 925 p.

49 Parkinson W.J., Ziock H.J. Heat Removal from High Temperature Tubular Solid Oxide Fuel Cells Utilizing Product Gas from Coal Gasifiers // The Proceedings of the 28-th International Technical Conference on Coal Utilization and Fuel systems. - Clearwater, Florida, USA. – 2003. – P. 35.

50 Kayukawa N. Open-cycle magnetohydrodynamic electrical power generation: a review and future perspectives // Progress in Energy and Combustion Science. - 2004. - Vol. 30 (1). - P. 33–60.

51 Bilger R.W. The Future for Energy from Combustion of Fossil Fuels // Proceedings of the 5th International Conference on Technologies and Combustion for a Clean Environment, ‘Clean Air’. - Lisbon, Portugal, 1999. – P. 617.

52 Messerle V., Orynbasar M., Umbetkaliev K., Ustimenko A. Gasification of carbon–containing waste in a plasma–chemical reactor [Gazifikatsiya uglerodsoderzhashchikh otkhodov v plazmokhimicheskom reaktore] // Combustion and Plasma Chemistry. - 2023. - Vol. 21. - No. 3. - P. 191-200. (in Russian)

53 Messerle V.E., Lavrichshev O.A., Ustimenko A.B., Orynbasar M.N. Plasma-chemical waste processing: numerical analysis and experiment. Part 3. Rubber of used tires // Thermophysics and Aeromechanics. - 2023. - Vol. 30. - P. 595–599.

54 Lavrichshev O.A., Messerle V.E., Mosse A. L., Paskalov G., Orynbasar M.N., Ustimenko A.B. Plasma-Chemical Processing of Agricultural Waste:

Numerical Analysis and Experiment // Proceedings SARDINIA. 19th International Symposium on Waste Management and Landfilling. - 2023. – P. 4.

55 Knapp R. The Vision for the Future: Moving to the CO_2 – Free Coal Plant // Perspectives of Modern Coal Technologies Conference. – Berlin, 2001. – P. 13.

56 Hu Y., Naito S., Kobayashi N., Hasatani M. CO_2, NO_x and SO_2 emissions from the combustion of coal with high oxygen concentration gases // Applications in Fuel. - 2000. - Vol. 97. - P. 1925-1932.

57 Chmel V.N., Dunaevskaya N.I., Ogiy V.N., Barbyshev B.N. Increasing the efficiency of combustion of low-grade fuels by thermochemical treatment [Povysheniye effektivnosti szhiganiya nizkosortnykh topliv metodom termokhimicheskoy obrabotki] // News of Higher Education Institutions. Power Engineering. - 1985. - No. 3. - P. 96-100. (in Russian)

58 Seulin N.A., Osokin L.G., Ivannikov V.M. On oil-free kindling and illumination of steam generators burning Kansk-Achinsk coals [O bezmazutnoy rastopke i podsvetke parogeneratorov, szhigayushchikh kansko-achinskiye ugli] // Electric stations. - 1986. - No. 10. - P. 21-22. (in Russian)

59 Dyachkov B.G., Blinova V.A., Nefedova M.G. Efficiency of fuel-electric processes [Effektivnost' toplivno - elektricheskikh protsessov]. - M.: Energoatomizdat, 1989. - 136 p. (in Russian)

60 Shen T., Song M., Huang Y., Zhu R., Li Z., Yu Q., Lu P., Wang M. The effectiveness of a novel coal-igniting-fuel technology and application in a direct current burner // Advances in Fuel. - 2021. - Vol. 306. - 121503.

61 Orynbasar M.N. The clean combustion of solid fuel using a plasma-coal burner // Combustion and Plasma Chemistry. - 2022. – Vol. 20. - No. 1. - P. 83-91.

62 Orynbasar M.N., Messerle V.E. The utilization of plasma technology in thermal power plants for technical modernization and environmental safety // XIV Konferencja “Młodzi w energetyce”. - Wroclaw, 2022. – P. 48.

63 Oil-free technologies at thermal power plants save billions [Bezmazutnyye tekhnologii na TES ekonomyat milliardy] // Internet newspaper “Kommersant”. - 2024. https://www.kommersant.ru/doc/6559928. (in Russian)

64 Askarova A.S., Bolegenova S.A., Bolegenova S.A., Maksimov V.Yu., Beketaeva M.T. 3D modeling of the aerodynamics and heat transfer in the combustion chamber of the BKZ-75 boiler of the Shakhtinsk cogeneration plant // Thermophysics and Aeromechanics. - 2019. - Vol. 26. - P. 295-311.

65 Askarova A., Bolegenova S., Bolegenova S., Beketayeva M., Maximov V., Nugymanova A., Šafařík P. Simulation of low-grade coal combustion in real chambers of energy objects // Acta Polytechnica. - 2019. - Vol. 59 (2). - P. 98−108.

66 Askarova A.S., Bolegenova S.A., Georgiev A., Bolegenova S.A., Maximov V.Yu., Manatbayev R.K., Yergaliyeva A.B., Nugymanova A.O., Baizhuma Zh.T. The use of a new “clean” technology for burning low-grade coal in on boilers of Kazakhstan TPPs // Bulgarian Chemical Communications. – 2018. – Vol. 50. - P. 53−60.

67 Howarth RW. The greenhouse gas footprint of liquefied natural gas (LNG) exported from the United States // Energy Science and Engineering. - 2024. Vol. 12. - P. 4843-4859.

68 Goyal A., Gidaspow D. Modelling of entrained of flow coal hydrolysis reactors. 1. Mathematical formulation and expiremental verification. 2. reactor // Ind. Eng. Chem. Process Des. Dev. - 1982. - Vol. 21. - P. 611-632.

69 Levitsky A.A. Mathematical modeling of plasma-chemical processes [Matematicheskoye modelirovaniye plazmokhimicheskikh protsessov] // Plasma chemistry-89. - M.: Institute of Petrochemical Synthesis of the USSR Academy of Sciences, 1989. - Part II. - P. 180-226. (in Russian)

70 Messerle V.E., Ustimenko A.B. and Tastanbekov A.K. Plasma ignition of solid fuels at thermal power plants. part 1. mathematical modeling of plasma-fuel system // Thermophysics and Aeromechanics. - 2022. - Vol. 29. - No. 2. - P. 295–310.

71 Blackburn P.R. Pulverized coal heated igniter system// Pat. №1585943 (B). - 1982. - No. 3.

72 Ryabinin V.P., Sakipov Z.B., Toboyakov B.O. Experimental study of plasma ignition of a pulverized coal torch on a fire stand [Eksperimental'noye issledovaniye plazmennogo vosplameneniya pyleugol'nogo fakela na ognevom stende] // Thermal engineering studies of boilers on low-grade coals. - 1985. - P. 32-45. (in Russian)

73 Electric arc plasma torches (advertising brochure) [Elektrodugovyye plazmotrony (reklamnyy prospekt)] / Edited by Corresponding Member of the USSR Academy of Sciences M.F. Zhukov. – Novosibirsk, 1980. - 82 p. (in Russian)

74 Zhukov M.F., M.F., Karpenko E.I., Peregudov V.S., Buyantuev S.L., Messerle V.E. Plasma-oil-free starting of boilers and stabilization of combustion of a pulverized coal torch [Plazmennaya bezmazutnaya rastopka kotlov i stabilizatsiya goreniya pyleugol'nogo fakela] // Novosibirsk: Siberian Presidium of the Russian Academy of Sciences «Science». - 1995. – 304 p. (in Russian)

75 Peregudov V.S., Pozdnyak B.A., Volobuev A.N. Heat treatment of coal dust by plasma jet in industrial boiler conditions [Termoobrabotka ugol'noy pyli plazmennoy struyey v usloviyakh promyshlennogo kotla] // High-temperature dusty jets in powder materials processing processes: Abstract of the report of the International Conference. – Novosibirsk, 1988. - P. 167-173. (in Russian)

76 Blackburn P.R. Ignition of pulverized coal with Arc Heated Air// Energy. - 1980. - Vol. 4. - No. 3. - P. 98-99.

77 Drouet M.G. La technologie des plasmas. Potentiel d'application au Canada // Revue generale d'electricite. – 1986. - No. 1. – P. 51–56.

78 Sakipov Z.B., Messerle V.E., Ibraev Sh.Sh. Electrothermochemical preparation of coals for combustion [Elektrotermokhimicheskaya podgotovka ugley k szhiganiyu]. - Almaty: Gylym (Science), 1993. - 259 p. (in Russian)

79 Karpenko E.I., Messerle V.E. Introduction to plasma-energy technologies for the use of solid fuels [Vvedeniye v plazmenno-energeticheskiye

tekhnologii ispol'zovaniya tverdykh topliv] // Novosibirsk: Nauka, Siberian Branch of the Russian Academy of Sciences, 1997. – 118 p. (in Russian)

80 Peregudov V.S., Buyantuev S.L., Karpenko E.I. Plasma-coal kindling of the BKZ-75 boiler [Plazmennougol'naya rastopka kotla BKZ-75] // Report of the International Seminar «New Technologies and Equipment in Thermal Power Engineering». – Novosibirsk: Gusinoozersk, 1995. – Part 1. - P. 21-24. (in Russian)

81 Karpenko E.I., Peregudov V.S., Buyantuev S.L. On testing the plasma ignition system of coals on the TPE-215 boiler [Ob ispytaniyakh sistemy plazmennogo vosplameneniya ugley na kotle TPE-215] // Energetik. - 1994. - No. 12. - P. 24-25. (in Russian)

82 Zhukov M.F., Messerle V.E., Peregudov V.S., Engelsht V.S. New materials and technologies. Extreme technological processes [Novyye materialy i tekhnologii. Ekstremal'nyye tekhnologicheskiye protsessy] // Novosibirsk: Science, Siberian Branch, 1992. - 178 p. (in Russian)

83 Williams A., Pourkashanian M., Jones J.M., Skorupska T. Combustion and Gasification of Coal. – Taylor and Francis: New York, USA, 2000. – 336 p.

84 Karpenko E.I., Buyantuev S.L. Ibraev Sh.Sh., Messerle V.E. Plasma-energy processes and devices in solving environmental problems [Plazmo-energeticheskiye protsessy i apparaty v reshenii prirodookhrannykh zadach]. - Ulan-Ude: BNC SB RAS, 1992. - 114 p.

85 Stanmore B.R., Visona S.P. The Contribution to Char Burnout from Gasification by H_2O and CO_2 During Pulverized-Coal Flame Combustion // Combustion and Flame. - 1998. - No. 113. – P. 274.

86 Yang L., Liang J., Yu L. Clean Coal Technology – Study on the Pilot Project Experiment of Underground Coal Gasification // Energy. - 2003. - Vol. 28, – No. 14. – P. 1445-1460.

87 Sinyarev G.B. Complete thermodynamic functions and their use in calculating equilibrium states of complex thermodynamic systems [Polnyye termodinamicheskiye funktsii i ispol'zovaniye ikh pri raschete ravnovesnykh sostoyaniy slozhnykh termodinamicheskikh sistem] // News of Higher Education Institutions/Transport and Power Engineering. - 1966. - No. 2. - P. 99-110. (in Russian)

88 Sinyarev G.B., Slynko L.E., Trusov B.G. Principles and method for determining the parameters of the equilibrium state [Printsipy i metod opredeleniya parametrov ravnovesnogo sostoyaniya] // Proceedings of the Moscow Higher Technical University. - 1978. - No. 268. - P. 4-21. (in Russian)

89 Rozhdestvensky I.B., Olevinsky K.K., Shevelev V.P. Composition and thermodynamic functions of a heterogeneous reacting system [Sostav i termodinamicheskiye funktsii geterogennoy reagiruyushchey sistemy] // Studies in thermodynamics. - 1973. - P. 49-55. (in Russian)

90 Alemasov V.E., Dregalin A.F., Tishin A.P., Khudyakov V.A. Thermodynamic and thermophysical properties of combustion products [Termodinamicheskiye i teplofizicheskiye svoystva produktov cgoraniya] // VINITI AN USSR. - 1978. - Vol. 1. - No. 4. – 454p. (in Russian)

91 Trusov B.G. Software system TERRA for modeling phase and chemical equilibria at high temperatures [Programmnaya sistema TERRA dlya modelirovaniya fazovykh i khimicheskikh ravnovesiy pri vysokikh temperaturakh] // III Int. Symposium «Combustion and Plasma Chemistry». - 2005. – P. 52-58. (in Russian)

92 Karpenko E.I., Messerle V.E., Ustimenko A.B. Mathematical model of the processes of ignition, combustion and gasification of pulverized coal fuel in devices with an electric arc [Matematicheskaya model' protsessov vosplameneniya, goreniya i gazifikatsii pyleugol'nogo topliva v ustroystvakh s elektricheskoy dugoy] // Thermal physics and aeromechanics. - 1995. - No. 2. - P. 173-187. (in Russian)

93 Lesinski J., Baronnet J.M., Meillot E. Modelling of plasma entrained-bed coal gasifiers // International Symposium on plasma Chemistry. – Eindchoven, 1985. - P. 261-266.

94 Messerle A.V. Mathematical modeling of processes of thermochemical preparation of pulverized coal fuels for combustion in burner devices with a plasma source [Matematicheskoye modelirovaniye protsessov termokhimicheskoy podgotovki pyleugol'nykh topliv k szhiganiyuv gorelochnykh ustroystvakh s plazmennym istochnikom] // High Energy Chemistry. – 2003. - No. 1. – P. 35. (in Russian)

95 Laats M.K. Experimental study of the dynamics of a dust-air jet [Eksperimental'noye issledovaniye dinamiki pylevozdushnoy strui] // Engineering Physics Journal. – 1966. – Vol. 10. - No. 1. – P. 11-15. (in Russian)

96 Laats M.K. Treatise on the motion of particles and the discrete phase of fine-dispersed tube flow (FDF): ideas of experimenters [Traktat o dvizhenii chastits i diskretnoy fazy melkodispersnogo trubnogo techeniya (MDTT): predstavleniya eksperimentatorov] // In the collection: Turbulent two-phase flows. – Tallinn, 1979. – P. 60-71. (in Russian)

97 Rakhmatullin H.A. Fundamentals of gas dynamics of interpenetrating motions of continuous media [Osnovy gazovoy dinamiki vzaimopronikayushchikh dvizheniy sploshnykh sred] // Applied Mathematics and Mechanics. – 1956. – Vol. 20. - No. 2. – P. 184-195. (in Russian)

98 Nigmatullin R.I. Fundamentals of mechanics of heterogeneous media [Osnovy mekhaniki geterogennykh sred]. - M.: Nauka, 1978. – 336 p. (in Russian)

99 Sternin L.E., Maslov B.N., Shreiber A.A., Podvysotsky A.M. Two-phase mono- and polydisperse gas flows with particles [Dvukhfaznyye mono- i polidispersnyye techeniya gaza s chastitsami]. – M.: Mashinostronie, 1980. – 172 p. (in Russian)

100 Sow S. Hydrodynamics of multiphase systems [Gidrodinamika mnogofaznykh sistem]. – M.: Mir, 1971. – 536 p. (in Russian)

101 Varaksin A.Yu. Turbulent flows of gas with solid particles [Turbulentnyye techeniya gaza s tverdymi chastitsami]. – M.: Fizmatlit, 2003. – 192 p. (in Russian)

102 Shraiber A.A., Gavin L.B., Naumov V.A., Yatsenko V.P. Turbulent flows of gas suspension [Turbulentnyye techeniya gazovzvesi]. – Kyiv: Nauk. Dumka, 1987. – 240 p. (in Russian)

103 Gavin L.B., Shraiber A.A. Turbulent gas flows with particles. Results of science and technology [Turbulentnyye techeniya gaza s chastitsami] // Series Mechanics of liquids and gases. - 1991. - Vol. 25. - P. 90-187. (in Russian)

104 Sternin L.E., Shraiber A.A. Multiphase gas flows with particles [Mnogofaznyye techeniya gaza s chastitsami]. – M.: Mashinostroenie, 1994. – 320 p. (in Russian)

105 Gavin L.B., Mulgi A.S., Shor V.V. Numerical and experimental study of a non-isothermal turbulent jet with a heavy impurity [Chislennoye i eksperimental'noye issledovaniye neizotermicheskoy turbulentnoy strui s tyazheloy primes'yu] // Engineering and Physics Journal. – 1986. – Vol. 50. - No. 5. – P. 735-743. (in Russian)

106 Zuev Yu.V., Lepeshinsky I.A. Calculation of pulsation parameters of phases of dispersed two-phase dynamically nonequilibrium flow [Raschet pul'satsionnykh parametrov faz dispersnogo dvukhfaznogo dinamicheski neravnovesnogo potoka] // Turbulent two-phase flows. - Tallinn, 1982. - Part 1. - P. 16-20 (in Russian)

107 Gavin L.B., Naumov V.A., Shor V.V. The k-ε model for a two-phase turbulent jet and its numerical study [Model' k-e dlya dvukhfaznoy turbulentnoy strui i yeye chislennoye issledovaniye] // In the collection: Physical and chemical processes in power plants. – Minsk, 1983. – P. 11-15. (in Russian)

108 Medvedev S.V. Application of a two-parameter model for calculating a turbulent gas-droplet jet taking into account coagulation and fragmentation [Primeneniye dvukhparametricheskoy modeli dlya rascheta turbulentnoy gazokapel'noy strui s uchetom koagulyatsii i drobleniya] // In the collection: Turbulent two-phase flows and experimental technique. – Tallinn, 1985. – P. 71-75. (in Russian)

109 Cao J., Ahmadi G. Gas-particle two-phase turbulent flow in horizontal and inclined ducts // International Journal of Engineering Science. – 2000. – Vol. 38. – P. 1961-1981.

110 Zhou H., Flamant G., Gauthier D., Lu J. Lagrangian approach for simulating the gas-particle flow structure in a circulating fluidized bed riser // International journal of multiphase flow. – 2002. – Vol. 28. – P. 1801-1821.

111 Saffar-Avval M., Basrat Tabrizi H., Mansoori Z., Ramezani P. Gas–solid turbulent flow and heat transfer with collision effect in a vertical pipe // International Journal of Thermal Sciences. – 2007. – Vol. 46. – P. 67-75.

112 Khodjiev S. Mathematical modeling of heat and mass transfer processes of internal and external spatial turbulent jets of reacting gases [Matematicheskoye modelirovaniye protsessov teplo- i massoobmena vnutrennikh i vneshnikh prostranstvennykh turbulentnykh struy reagiruyushchikh gazov]: dis. of Doctor of Physical and Mathematical Sciences: 01.02.05. – Tashkent, 1994. – 295 p. (in Russian)

113 Vulis L.A., Ershin Sh.A., Yarin L.P. Fundamentals of gas torch theory. – L.: Energy, 1968. – 203 p. (in Russian)

114 Stankov P., Toporov D. Modeling of Turbulence-chemical Reactions Interaction in Industrial Furnace Using an Advanced Model // Sixth international conference on “Technologies and Combustion for a clean environment”. – Portugal, 2001. – P. 489-494.

115 Ustimenko B.P., Dzhakupov K.B., Krol V.O. Numerical modeling of aerodynamics and combustion in furnace and technological devices [Chislennoye modelirovaniye aerodinamiki i goreniya v topochnykh i tekhnologicheskikh ustroystvakh]. – Alma-Ata: Nauka, 1986. – P. 224. (in Russian)

116 Antifora A., Mainini G. and Vigevano L. On the Prediction of Large-Scale Furnace Coal Combustion in Oxygen-Lean Conditions // Sixth International Conference on “Technologies and Combustion for a Clean Environment”. – Portugal, 2001. – P. 131-139.

117 Ruckert F.U., Strohle J., Sabel T., Fortsch D., Schnell U., Hein K. Advantages of Combining Different Grid-Types for 3D-Furnace Modelling // Sixth International Conference on “Technologies and Combustion for a Clean Environment”. – Portugal, 2001. – P. 99-105.

118 Gorokhovski M., Karpenko E.I., Lockwood F.C., Messerle V.E., Trusov B.G., Ustimenko A.B. Plasma Technologies for Solid Fuels: Experiment and Theory. // Journal of the Energy Institute, 2005. - Vol. 78. - No. 4. - P. 157-171.

119 Sinyarev G.B., Vatolin N.A., Trusov B.G., Moiseev G.K. Application of computers for thermodynamic calculations of metallurgical processes [Primeneniye EVM dlya termodinamicheskikh raschetov metallurgicheskikh protsessov]. - M.: Nauka, 1982. – 263 p. (in Russian)

120 Gibbs J.W. Thermodynamics. Statistical mechanics. – M.: Science, 1982.

121 JANAF Thermochemical Tables (Third Edition) // Internet newspaper “J. Phys. Chem. Ref.”. – 1985. - Vol. 14 (NIST Chemistry WebBook: http://webbook.nist.gov).

122 Karpenko E., Messerle V., Trusov B. A comparative analysis of plasma and fire technologies of pulverized coal ignition, combustion and gasification using a mathematical model of chemically nonequilibrium system // Thermophysics and Aeromechanics. – 1995, Vol. 2. - No. 3. - P. 245-250.

123 Krasnov M.L., Makarenko G.I., Kiselev A.I. Calculus of variations [Variatsionnoye ischisleniye]. – M.: Nauka, 1977. – 127 p. (in Russian)

124 Messerle V.E., Sakipov Z.B., Trusov B.G. Specific energy consumption during high-temperature gasification of low-grade coals [Udel'nyye energozatraty pri vysokotemperaturnoy gazifikatsii nizkosortnykh ugley] // NEWS SB ANSSSR. Ser. tech.sc. - 1988. – No. 18. – Ed. 5. - P. 95-98. (in Russian)

125 Messerle V.E. Method for determining specific energy consumption during plasma-chemical preparation of low-reactivity coals and assessment of the economic efficiency of its use for ignition and stabilization of combustion of pulverized coal flares at thermal power plants [Metod opredeleniya udel'nykh

energozatrat pri plazmokhimicheskoy podgotovke nizkoreaktsionnykh ugley i otsenka ekonomicheskoy effektivnosti yeye ispol'zovaniya dlya vosplameneniya i stabilizatsii goreniya pyleugol'nykh fakelov na TES] // Technical and economic assessments of plasma-chemical processes for processing coals and hydrocarbons. Irkutsk, 1989. - P. 4-10. (in Russian)

126 Sakipov Z.B., Messerle V.E., Imankulov E.R. Method of plasma stabilization of combustion of low-grade coals [Sposob plazmennoy stabilizatsii goreniya nizkosortnykh ugley] // Power Engineering and Electrification. – 1990. – No. 1. – P. 5-7. (in Russian)

127 Nenakhova V.N., Ibraev Sh.Sh., Messerle V.E., Ustimenko A.B., Frolova I.B., Frolov V.A. Study of magnetite reduction by coal plasma gasification products [Issledovaniye vosstanovleniya magnetita produktami plazmennoy gazifikatsii ugley] // Physics and Chemistry of Materials Processing. – 1989. – No. 5. – P. 57-61. (in Russian)

128 Messerle V.E., Sakipov Z.B., Trusov B.G. Determination of standard heat of formation, equilibrium composition of products and specific energy consumption during thermal processing of fuels [Opredeleniye standartnoy teploty obrazovaniya, ravnovesnogo sostava produktov i udel'nykh energozatrat pri termicheskoy pererabotke topliv] // Chemistry of solid fuels. - 1989. – No. 6. - P. 72-76. (in Russian)

129 Messerle V.E., Ustimenko A.B. Modeling of Coal Ignition in Plasma-Fuel Systems with an Electric Arc Torch // IEEE Transactions on Plasma Science. – 2020. – Vol. 48 (2). – P. 343-349.

130 Kalinenko R.A., Levitski A.A., Messerle V.E., Polak L.S., Sakipov Z.B., Ustimenko A.B. Pulverized Coal Plasma Gasification // Plasma Chemistry and Plasma Processing. - 1993. - Vol. 13. - No. 1. - P. 141-167.

131 Ustimenko A., Messerle V., Karpenko E., Jankoski Z., Lockwood F.C., Gorokhovski M. Mathematical Modelling of the Pulverised Coal Preparation for Combustion Using Plasma // 31st EPS Conference on Plasma Phys. London, 2004. - Vol. 28. – P. 1027.

132 Dresvin S.V., Donskoy A.V., Goldfarb V.M., Klubnikin V.S. Physics and technology of low-temperature plasma [Fizika i tekhnika nizkotemperaturnoy plazmy]. – M.: Atomizdat, 1972. – 352 p. (in Russian)

133 Gonopolsky A.M. On the applicability of a one-dimensional model for calculating the characteristics of plasma torches [O primenimosti odnomernoy modeli raschetu kharakteristik plazmotronov] // Mechanics of liquids and gases. - 1977. – No. 4. - P. 122-126. (in Russian)

134 Pustovoitenko A.I. Mathematical modeling of heating and heating and evaporation of polydisperse powder in a plasma gas jet [Matematicheskoye modelirovaniye nagreva i nagreva i ispareniya polidispersnogo poroshka v plazmennoy struye gaza] // Physics and Chemistry of Materials Processing. - 1977. - No. 2. - P. 15-20. (in Russian)

135 Sergeev P.V., Ibraev Sh.Sh., Loksha B.K., Shepel G.A. On the bearing capacity of an arc burning in a coaxial heater [O nesushchey sposobnosti dugi,

goryashchey v koaksial'nom nagrevatele] // Problems of thermal power engineering. Issue 10. - Alma-Ata: Science, 1975. - P. 157-163. (in Russian)

136 Kantorovich B.V. Fundamentals of the theory of combustion and gasification of solid fuel [Osnovy teorii goreniya i gazifikatsii tverdogo topliva]. - M.:Nauka, 1958. – 598 p. (in Russian)

137 Babiy V.I., Kuvaev Yu.F. Combustion of coal dust and calculation of a coal dust torch [Goreniye ugol'noy pyli i raschet pyleugol'nogo fakela]. - M.: Energoatomizdat, 1986. – 208 p. (in Russian)

138 Babukha G.L., Rabinovich M.I. Mechanics and heat transfer of flows of polydisperse gas mixture [Mekhanika i teploobmen potokov polidispersnoy gazovoy smesi]. – Kyiv, 1969. – 218 p. (in Russian)

139 Smoot L.D., Pratt P.J. Pulverised-Coal Combustion and Gasification: theory and applications for continuous flow processes. – Plenum Press: New York, 1979. – 333 p.

140 Benson S.W. Thermochemical kinetic. – John Willey: New York, London, 1976. – P. 34.

141 Agroskin A.A., Gleibman V.B., Goncharov E.I. Heat capacity of mineral impurity and coal ash // Coke and chemistry. – 1974. – No. 2. – P. 3-4.

142 Agroskin A.A., Goncharov E.I., Lovetski L.V. Thermal characteristics of some East coals // Coke and chemistry. – 1968. - No. 11. – P. 1-6.

143 Gear G.W. The automatic Integration of Ordinary Differential Equations // Comm. Of the ACM. - 1971. - Vol. 14. - No. 3. - P. 176-179.

144 Polak L.S., Goldenberg M.D., Levitsky A.A. Calculation methods of chemical dynamics [Raschetnyye metody khimicheskoy dinamiki]. - M.: Nauka, 1984. – 280 p. (in Russian)

145 Messerle V.E., Orynbasar M.N., Ustimenko A.B. Simulation and experiment of plasma ignition of low-grade coal // Combustion and Plasma Chemistry. - 2024. - Vol. 22. - No. 1. - P. 27–36.

146 Messerle V.E., Mossé A.L., Orynbasar M.N., Ustimenko A.B. Plasma ignition of solid fuel: Mathematical simulation and experiment // Journal of Engineering Physics and Thermophysics. - 2024. - Vol. 97. - No. 3. - P. 116–125.

147 Messerle V.E, Orynbasar M.N., Pawlak-Kruczek H., Ustimenko A.B. Plasma ignition of coal: numerical simulation and experiment // XV Konferencja “Młodzi w energetyce”. - Wroclaw, 2023. – P. 105.

148 Orynbasar M., Messerle V., Ustimenko A. Modeling and experiments on plasma ignition of Ekibastuz coal in the form of dust // Combustion and Plasma Chemistry. - 2024. - Vol. 22. - No. 3. - P. 179–186.

149 Messerle V., Orynbasar M. Ecological efficiency of utilization solid fuel plasma technology // Combustion and Plasma Chemistry. - 2021. - Vol. 19. - No. 4. - P. 289-298.

150 Messerle V.E., Orynbasar M.N. Ecological efficiency of plasma-coal burners // XII International Symposium “Combustion and Plasmochemistry. Physics and Chemistry of Material Science” dedicated to the 125th anniversary of

Academician N.N. Semenov and the 30th anniversary of independence of the Republic of Kazakhstan. 12-13 October 2021. - P. 11-12.

151 Messerle V.E., Orynbasar M.N., Ustimenko A.B. Ecological efficiency of plasma technology for using solid fuels [Ekologicheskaya effektivnost' plazmennykh tekhnologiy ispol'zovaniya tverdogo topliva] // In the collective monograph “Some problems of decarbonization and alternative energy [Nekotoryye problemy dekarbonizatsii i al'ternativnoy energetiki]” edited by Z.A. Mansurov. – Almaty: Daryn, 2024. - P. 130–147. (in Russian)

152 Kaltay T.D., Orynbasar M.N. Utilization of plasma technology to minimize emissions of hazardous substances // XV Konferencja “Młodzi w energetyce”. - Wroclaw, 2023. – P. 101.

153 On approval of technical specific emission standards, including for mobile sources of emissions of pollutants into the atmosphere [Ob utverzhdenii tekhnicheskikh udel'nykh normativov emissiy, v tom chisle dlya peredvizhnykh istochnikov vybrosov zagryaznyayushchikh veshchestv v atmosferu] // Internet newspaper “Adilet”. - 2021. https://adilet.zan.kz/rus/docs/V2100022068. (in Russian)

APPENDIX A

An example of a listing of thermodynamic calculations of plasma ignition of thermal coal using the TERRA software

```
     Composition:  (C - 48.86) + (O - 6.56) + (H - 3.05) + (N - 0.8) +
                   (S - 0.73) + (SiO2 - 23.09) + (Al2O3 - 13.8) +
                   (Fe2O3 - 2.15) + (CaO - 0.34) + (MgO - 0.31) +
                   (K2O - 0.16) + (Na2O - 0.15) +
                   (N54.63O14.67[0,1.012] - 143)
  Formula, mol/kg:  C 16.740 O 15.395 H 12.453 N 32.387 S 0.094 Si1.581 Al1.114
                    Fe0.111 Ca0.025 Mg0.032 K 0.014 Na0.020
    1st parameter:  T =300-2000/300
    2nd parameter:  p =0.1
-------------------------------------------------------------------------------

      Equilibrium parameters at p=0.1 MPa, T=300 K   (SI units):
 p=0.1          T=300          v=0.566658     S=4.78164      I=-4890.86
 U=-4891.21     M=40.131      Cp=1.01189      k=1.22951    Cp'=1.03212
k'=1.22401     Ap=0.0033334   Bv=0.0033334   Gt=0.00001    MMg=27.5065
Rg=302.269    Cpg=1.1182      kg=1.37046   Cp'g=1.11841    k'g=1.37038
Mu=0.0000158   Lt=0.0253195  Lt'=0.0253733   Pr=0.698987   Pr'=0.697636
 A=263.362      z=0.375107
      Equilibrium concentrations  (vol.fract.):
       H2 = 0.2266e-5         H2O = 0.19296          H2S = 0.2900e-7          N2 = 0.7128
      NH3 = 0.1925e-5          CO = 0.1144e-10        CO2 = 0.0912           CH4 = 0.00304
     C2H6 = 0.3849e-11        COS = 0.7197e-13

      Equilibrium parameters at p=0.1 MPa, T=600 K   (SI units):
 p=0.1          T=600          v=1.23556      S=5.94039      I=-4404.59
 U=-4466.75     M=39.839      Cp=1.2334       k=1.20042    Cp'=1.56493
k'=1.17355     Ap=0.0017999   Bv=0.0017921   Gt=0.0000104  MMg=27.4621
Rg=302.757    Cpg=1.24136     kg=1.32256   Cp'g=1.692      k'g=1.2621
Mu=0.0000269   Lt=0.04952    Lt'=0.187333    Pr=0.674122   Pr'=0.242889
 A=379.96       z=0.31983
      Equilibrium concentrations  (vol.fract.):
         H2 = 0.01806            H2O = 0.17157           H2S = 0.7332e-4           N2 = 0.65378
        NH3 = 0.8196e-4           CO = 0.4650e-3          CO2 = 0.12519           CH4 = 0.03079
       C2H4 = 0.7146e-11        C2H6 = 0.3156e-7        C3H8 = 0.2358e-12        CH2O = 0.6916e-11
      CH2O2 = 0.8299e-9        C2H4O2 = 0.2158e-11        COS = 0.1392e-6          HCN = 0.2225e-10


      Equilibrium parameters at p=0.1 MPa, T=900 K   (SI units):
 p=0.1          T=900          v=2.1407       S=7.11172      I=-3498.68
 U=-3641.83     M=40.9299     Cp=1.38369      k=1.20758    Cp'=5.40332
k'=1.14989     Ap=0.0020333   Bv=0.0019498   Gt=0.0000113  MMg=24.9422
Rg=333.345    Cpg=1.38183     kg=1.31793   Cp'g=3.46175    k'g=1.20555
Mu=0.0000365   Lt=0.0889734  Lt'=0.0889734   Pr=0.566843   Pr'=1.42005
 A=485.848      z=0.286457
      Equilibrium concentrations  (vol.fract.):
         H = 0.4592e-10           H2 = 0.15396           H2O = 0.04858           S2 = 0.1769e-11
       SO2 = 0.2052e-12           SH = 0.1412e-9         H2S = 0.9684e-4          N2 = 0.56602
       NH3 = 0.5540e-4            CO = 0.12963           CO2 = 0.09419           CH3 = 0.3809e-10
       CH4 = 0.00747            C2H2 = 0.9704e-11       C2H4 = 0.8585e-8        C2H6 = 0.2440e-7
      C3H8 = 0.3168e-12          CHO = 0.4885e-12       CH2O = 0.1221e-7        CH2O2 = 0.1070e-7
    C2H4O2 = 0.4593e-11          CS2 = 0.1665e-10        COS = 0.3981e-5          HCN = 0.3863e-6
       FeOH = 0.2528e-11       FeO2H2 = 0.9147e-11        Na = 0.1840e-10        NaOH = 0.1044e-10
          K = 0.6723e-11          KOH = 0.1367e-9

      Equilibrium parameters at p=0.1 MPa, T=1200 K   (SI units):
 p=0.1          T=1200         v=3.2703       S=8.17957      I=-2420.91
 U=-2666.69     M=41.2745     Cp=  -          k=  -        Cp'=  -
k'=  -         Ap=  -         Bv=  -         Gt=  -        MMg=23.1996
Rg=358.384    Cpg=1.44116     kg=1.33099   Cp'g=1.54506    k'g=1.3197
Mu=0.0000441   Lt=0.116399   Lt'=0.119962    Pr=0.545948   Pr'=0.567926
 A=503.713      z=0.239572
      Equilibrium concentrations  (vol.fract.):
         H = 0.8517e-7            H2 = 0.18589           OH = 0.5560e-11          H2O = 0.00152
         S = 0.1715e-9            S2 = 0.1067e-6         S3 = 0.1312e-11           SO = 0.2474e-10
       SO2 = 0.2975e-11          S2O = 0.1830e-12        SH = 0.4738e-6          H2S = 0.00141
       SOH = 0.4062e-13           N2 = 0.49402           NO = 0.3507e-13          NH2 = 0.8840e-11
```

```
        NH3 = 0.1083e-4          NS = 0.1573e-11          CO = 0.31458          CO2 = 0.00187
       C3O2 = 0.1438e-12         CH3 = 0.5089e-8          CH4 = 0.5524e-3       C2H2 = 0.2094e-7
       C2H3 = 0.1988e-11        C2H4 = 0.4430e-7         C2H5 = 0.6616e-12      C2H6 = 0.1265e-8
       C4H2 = 0.8998e-13         CHO = 0.1939e-9         CHO2 = 0.2876e-12      CH2O = 0.2948e-7
      CH2O2 = 0.3646e-9           CS = 0.7821e-8          CS2 = 0.6997e-6       COS = 0.1037e-3
       C2N2 = 0.3243e-11         HCN = 0.3076e-4          HNC = 0.2634e-11      C3HN = 0.2170e-9
       C5HN = 0.7317e-12         N2C = 0.2177e-11         SiS = 0.7237e-11      SiS2 = 0.2251e-11
         Fe = 0.3088e-10        FeOH = 0.2722e-9        FeO2H2 = 0.2766e-11      FeS = 0.1227e-10
         Mg = 0.2413e-12          Na = 0.1989e-5          Na2 = 0.4187e-12      NaH = 0.6333e-9
       NaOH = 0.7310e-8          NaS = 0.1973e-10           K = 0.4776e-6        KH = 0.1715e-9
        KOH = 0.2853e-7           KS = 0.7427e-12         NaK = 0.1277e-12       e- = 0.4509e-12
        SH- = 0.9196e-11          CN- = 0.7141e-12         K+ = 0.1036e-10       SiO = 0.3309e-11


     Equilibrium parameters at p=0.1 MPa, T=1500 K   (SI units):
 p=0.1          T=1500         v=4.11321      S=8.53669      I=-1940.88
 U=-2270.44     M=41.3316     Cp=  -          k=  -         Cp'=  -
k'=  -         Ap=  -         Bv=  -         Gt=  -         MMg=23.1822
Rg=358.652    Cpg=1.48848     kg=1.31744   Cp'g=1.5009     k'g=1.31591
Mu=0.0000509   Lt=0.139088   Lt'=0.139997    Pr=0.544857   Pr'=0.545837
 A=565.501      z=0.235432
     Equilibrium concentrations  (vol.fract.):
        H = 0.7609e-5           H2 = 0.18652           OH = 0.1193e-9         H2O = 0.1030e-3
        S = 0.1015e-6           S2 = 0.6316e-5          S3 = 0.2232e-9          SO = 0.5716e-9
      SO2 = 0.1617e-11         S2O = 0.3316e-11         SH = 0.1646e-4        H2S = 0.00176
      SOH = 0.7578e-12           N = 0.4252e-13         N2 = 0.49079           NO = 0.2187e-11
       NH = 0.5305e-11         NH2 = 0.3600e-9         NH3 = 0.3515e-5         NS = 0.7164e-9
       CO = 0.31902            CO2 = 0.6773e-4         C2O = 0.1904e-12       C3O2 = 0.1866e-11
      CH2 = 0.2674e-11         CH3 = 0.7792e-7         CH4 = 0.9072e-4        C2H = 0.9538e-12
     C2H2 = 0.1815e-5         C2H3 = 0.2736e-9         C2H4 = 0.9128e-7       C2H5 = 0.3619e-11
     C2H6 = 0.1483e-9          C3H = 0.5332e-11        C4H2 = 0.2737e-9        CHO = 0.3956e-8
     CHO2 = 0.3664e-12        CH2O = 0.2684e-7        CH2O2 = 0.1670e-10       CS = 0.4241e-5
      CS2 = 0.3298e-4          COS = 0.1274e-3          CN = 0.6371e-10        CN2 = 0.4848e-12
     C2N2 = 0.1695e-8          HCN = 0.4100e-3         HNC = 0.1053e-8        C2HN = 0.1438e-12
     C3HN = 0.9227e-7         C5HN = 0.4634e-8         C7HN = 0.6993e-10      C9HN = 0.8911e-12
      N2C = 0.1022e-8           Si = 0.3706e-12         SiO2 = 0.7849e-11       SiH = 0.9809e-12
     SiH2 = 0.9866e-11        SiH3 = 0.3931e-13        SiH4 = 0.1157e-11       SiS = 0.7840e-4
     SiS2 = 0.7573e-5           Al = 0.5861e-12         AlH = 0.7089e-12       AlOH = 0.1899e-10
   AlO2H2 = 0.5356e-13         AlS = 0.1336e-11          Fe = 0.8382e-7        FeOH = 0.2387e-8
   FeO2H2 = 0.4647e-12         FeS = 0.1802e-7           Mg = 0.1427e-6        MgH = 0.4922e-11
     MgOH = 0.4563e-10      MgO2H2 = 0.1005e-11         MgS = 0.1244e-7         Ca = 0.1597e-11
     CaOH = 0.6642e-13      CaO2H2 = 0.3708e-13         CaS = 0.6791e-12        Na = 0.6035e-3
      Na2 = 0.8457e-8           NaH = 0.3719e-6        NaOH = 0.6392e-7        NaS = 0.4454e-7
        K = 0.3393e-3           KO = 0.1846e-12          KH = 0.2543e-6        KOH = 0.3638e-6
   K2O2H2 = 0.6918e-13          KS = 0.6017e-8          NaK = 0.7221e-8         e- = 0.1668e-8
       H- = 0.3739e-13          S- = 0.1934e-10         S2- = 0.8984e-10       S3- = 0.1244e-12
      SH- = 0.7645e-8           CN- = 0.6028e-8         Na+ = 0.5692e-10        K+ = 0.1539e-7
      K2+ = 0.3013e-11          SiO = 0.2673e-5

     Equilibrium parameters at p=0.1 MPa, T=1800 K   (SI units):
 p=0.1          T=1800         v=5.42161      S=9.3813       I=-523.483
 U=-975.844     M=39.9012     Cp=1.48071      k=1.25536     Cp'=2.01913
k'=1.20433     Ap=0.0005965   Bv=0.0005945   Gt=0.0000101  MMg=23.686
Rg=351.024    Cpg=1.49481     kg=1.3069    Cp'g=1.50886    k'g=1.3043
Mu=0.0000572   Lt=0.155218   Lt'=0.160278    Pr=0.551155   Pr'=0.538773
 A=806.636      z=0.141938
     Equilibrium concentrations  (vol.fract.):
        O = 0.7006e-12           H = 0.1481e-3          H2 = 0.17064           OH = 0.1046e-8
      H2O = 0.1839e-4            S = 0.6155e-7          S2 = 0.6998e-8          SO = 0.4731e-10
       SH = 0.1425e-5          H2S = 0.1597e-4         SOH = 0.5179e-13          N = 0.2440e-10
       N2 = 0.44596            NO = 0.3931e-10         NH = 0.4477e-9        NH2 = 0.3708e-8
      NH3 = 0.1383e-5         N2H2 = 0.5431e-13         NS = 0.3462e-9          C = 0.2524e-12
       C3 = 0.1141e-12          CO = 0.37453           CO2 = 0.1051e-4        C2O = 0.5044e-10
     C3O2 = 0.1419e-10          CH = 0.1287e-11         CH2 = 0.3945e-9        CH3 = 0.4104e-6
      CH4 = 0.2288e-4          C2H = 0.1094e-8         C2H2 = 0.3187e-4       C2H3 = 0.6210e-8
     C2H4 = 0.1220e-6         C2H5 = 0.8850e-11        C2H6 = 0.2716e-10       C3H = 0.7816e-8
     C3H4 = 0.4556e-12         C4H = 0.7221e-13        C4H2 = 0.5110e-7        CHO = 0.3294e-7
     CHO2 = 0.5832e-12        CH2O = 0.2717e-7        CH2O2 = 0.2837e-11        CS = 0.2347e-5
      CS2 = 0.3111e-7          COS = 0.1483e-5          CN = 0.2064e-7         CN2 = 0.9668e-10
      C2N = 0.1381e-10        C2N2 = 0.1003e-6         NCO = 0.9771e-12        HCN = 0.00208
      HNC = 0.5152e-7         C2HN = 0.6352e-10        C3HN = 0.4686e-5       C5HN = 0.1420e-5
     C7HN = 0.1294e-6         C9HN = 0.9824e-8          N2C = 0.5740e-7          Si = 0.8831e-7
      Si2 = 0.9140e-10         Si3 = 0.1170e-12        SiO2 = 0.1946e-8        SiH = 0.7139e-7
```

```
      SiH2 = 0.1428e-6         SiH3 = 0.3110e-9         SiH4 = 0.8469e-9          SiS = 0.00256
      SiS2 = 0.9876e-6          SiN = 0.3168e-8          SiC = 0.1879e-12        SiC2 = 0.2414e-8
      Si2C = 0.1147e-8        Si2C2 = 0.4512e-12        Si3C = 0.3003e-12         Al = 0.2099e-6
       Al2 = 0.3847e-13        Al2O = 0.3551e-7        Al2O2 = 0.5816e-12        AlH = 0.7960e-7
      AlH2 = 0.1913e-9         AlH3 = 0.1353e-12        AlOH = 0.6659e-7       HAlO2 = 0.5170e-13
    AlO2H2 = 0.7605e-11         AlS = 0.1890e-8         Al2S = 0.8134e-12         AlN = 0.2010e-11
      AlC2 = 0.1064e-12       Al2C2 = 0.3513e-13          Fe = 0.1235e-4          FeO = 0.2815e-11
      FeOH = 0.8613e-8       FeO2H2 = 0.1470e-12         FeS = 0.1476e-7          Mg = 0.8429e-3
       Mg2 = 0.1378e-9          MgO = 0.1918e-9         MgH = 0.8246e-7         MgOH = 0.2832e-7
    MgO2H2 = 0.1751e-10         MgS = 0.8253e-6          Ca = 0.5181e-6          CaO = 0.2242e-12
       CaH = 0.5725e-9         CaOH = 0.1012e-8       CaO2H2 = 0.1072e-10        CaS = 0.1431e-8
        Na = 0.5493e-3          Na2 = 0.2497e-8         NaO = 0.1337e-12         NaH = 0.5054e-6
      NaOH = 0.6292e-8          NaS = 0.1304e-8           K = 0.3851e-3          KO = 0.8395e-12
        KH = 0.4542e-6          KOH = 0.3259e-7          KS = 0.2922e-9          KN = 0.2932e-13
       NaK = 0.2993e-8           e- = 0.4425e-7          H- = 0.4628e-11          S- = 0.1345e-10
       S2- = 0.2021e-12         SH- = 0.5604e-9         CN- = 0.2375e-6         AlO- = 0.1074e-9
       Na+ = 0.2324e-8           K+ = 0.2801e-6         K2+ = 0.2115e-10         AlO = 0.1081e-9
       SiO = 0.00217

     Equilibrium parameters at p=0.1 MPa, T=2100 K   (SI units):
 p=0.1          T=2100         v=6.54657      S=9.85506      I=382.507
 U=-179.207     M=39.8964     Cp=1.48489      k=1.26573    Cp'=1.88284
k'=1.21177     Ap=0.0004905   Bv=0.0004899   Gt=0.0000101  MMg=23.9584
Rg=347.033    Cpg=1.50766     kg=1.29901   Cp'g=1.59663    k'g=1.28475
Mu=0.0000632   Lt=0.172185   Lt'=0.204523    Pr=0.553103   Pr'=0.49313
 A=890.112      z=0.101695
     Equilibrium concentrations  (vol.fract.):
       O = 0.2911e-10          H = 0.00126           H2 = 0.16206          OH = 0.5284e-8
     H2O = 0.5775e-5           S = 0.1655e-6         S2 = 0.7941e-9         SO = 0.3264e-10
      SH = 0.9533e-6         H2S = 0.2152e-5        SOH = 0.3134e-13         N = 0.2294e-8
      N2 = 0.41406            NO = 0.3299e-9         NH = 0.1068e-7        NH2 = 0.1984e-7
     NH3 = 0.7253e-6        N2H2 = 0.3622e-12       HNO = 0.4758e-13        NS = 0.7858e-9
       C = 0.2176e-9          C2 = 0.2009e-10        C3 = 0.2239e-9         C5 = 0.7093e-13
      CO = 0.40468           CO2 = 0.2903e-5        C2O = 0.2421e-8       C3O2 = 0.5244e-10
      CH = 0.3302e-9         CH2 = 0.1279e-7        CH3 = 0.1247e-5        CH4 = 0.8205e-5
     C2H = 0.1411e-6        C2H2 = 0.2096e-3       C2H3 = 0.4917e-7       C2H4 = 0.1302e-6
    C2H5 = 0.1464e-10       C2H6 = 0.7194e-11       C3H = 0.1088e-5       C3H4 = 0.3901e-11
     C4H = 0.5666e-10       C4H2 = 0.1527e-5        CHO = 0.1458e-6       CHO2 = 0.8563e-12
    CH2O = 0.2711e-7       CH2O2 = 0.8617e-12        CS = 0.5308e-5        CS2 = 0.2876e-8
     COS = 0.2306e-6          CN = 0.1159e-5        CN2 = 0.3902e-8        C2N = 0.3579e-8
    C2N2 = 0.1556e-5         NCO = 0.1717e-10       HCN = 0.0061           HNC = 0.7596e-6
    C2HN = 0.4157e-8        C3HN = 0.5990e-4       C5HN = 0.5531e-4       C7HN = 0.1538e-4
    C9HN = 0.3529e-5         N2C = 0.9419e-6         Si = 0.1301e-4         Si2 = 0.8046e-7
     Si3 = 0.4274e-9         SiO2 = 0.2439e-8        SiH = 0.4529e-5        SiH2 = 0.2907e-5
    SiH3 = 0.4166e-8        SiH4 = 0.2113e-8        SiS = 0.00249          SiS2 = 0.7193e-7
     SiN = 0.2802e-6         SiC = 0.3590e-9       SiC2 = 0.1499e-5        Si2C = 0.7159e-6
   Si2C2 = 0.1210e-8        Si3C = 0.1245e-8         Al = 0.1766e-3         Al2 = 0.5645e-8
    Al2O = 0.4315e-4       Al2O2 = 0.2159e-9        AlH = 0.2945e-4        AlH2 = 0.6609e-7
    AlH3 = 0.3269e-10       AlOH = 0.2221e-5       HAlO = 0.5468e-11      HAlO2 = 0.8034e-12
  AlO2H2 = 0.2806e-10        AlS = 0.1184e-6       AlS2 = 0.3420e-13       Al2S = 0.1752e-8
   Al2S2 = 0.1493e-12        AlN = 0.4724e-8        AlC = 0.1977e-9        AlC2 = 0.2087e-8
   Al2C2 = 0.8180e-8          Fe = 0.4344e-3        FeO = 0.8931e-10       FeOH = 0.2271e-7
  FeO2H2 = 0.7699e-13        FeS = 0.4791e-7         Mg = 0.8439e-3         Mg2 = 0.9326e-10
     MgO = 0.2742e-9         MgH = 0.1755e-6       MgOH = 0.6122e-8      MgO2H2 = 0.3259e-12
     MgS = 0.1287e-6         MgN = 0.1660e-12        Ca = 0.6639e-3         Ca2 = 0.2784e-9
      CaO = 0.2919e-9         CaH = 0.1165e-5       CaOH = 0.1576e-6      CaO2H2 = 0.1074e-9
      CaS = 0.1950e-6          Na = 0.5306e-3         Na2 = 0.1090e-8         NaO = 0.4736e-12
      NaH = 0.6570e-6        NaOH = 0.1340e-8         NaS = 0.4101e-9         NaN = 0.2144e-12
        K = 0.3697e-3           KO = 0.2325e-11        KH = 0.6098e-6         KOH = 0.5507e-8
       KS = 0.1120e-9           KN = 0.5531e-12       NaK = 0.1410e-8          e- = 0.3707e-6
       H- = 0.1117e-9         OH- = 0.8777e-13         S- = 0.3024e-10        S2- = 0.2878e-13
      SH- = 0.2527e-9         C2- = 0.7784e-11        CN- = 0.2238e-5         Al+ = 0.4851e-10
     AlO- = 0.6046e-8         Fe+ = 0.3052e-13        Mg+ = 0.2736e-12        Ca+ = 0.1029e-8
   CaOH+ = 0.5732e-11         Na+ = 0.4476e-7          K+ = 0.2570e-5         K2+ = 0.8482e-10
      AlO = 0.2694e-7         SiO = 0.00585
```

APPENDIX B

An example of a listing of kinetic calculations of heating and plasma ignition of thermal coal using the PlasmaKinTherm software

```
Без лет.=(0.000000 % C),(0.000000 % H),(0.021543 % O), (0.084482 % N)Ent=605.321472,Ent_Let=0.000000,TFRAC=0
With let=(0.000000 % C),(0.000000 % H),(0.021543 % O), (0.084482 % N)O2-6.349732
N2-28.443853
NO-0.000196
NO2-0.000028
dx=0.020000 T=868.554504 Q=0.000000,dT=0.000145,dT_SUM_Q=0.000000,dT_SUM_T=0.000163
Без лет.=(0.000000 % C),(0.000000 % H),(0.023136 % O), (0.090729 % N)Ent=976.665283,Ent_Let=0.459149,TFRAC=1
With let=(0.000168 % C),(0.000012 % H),(0.023183 % O), (0.090729 % N)O2-6.197021
OH-0.000021
H2O-0.052171
N2-28.383035
NO-0.008555
NO2-0.000111
CO2-0.122596
dx=0.020000 T=1189.470825 Q=0.000000,dT=4.909279,dT_SUM_Q=0.000000,dT_SUM_T=5.882596
Без лет.=(0.000168 % C),(0.000012 % H),(0.024833 % O), (0.097199 % N)Ent=1237.773315,Ent_Let=5.606343,TFRAC=2
With let=(0.000354 % C),(0.000030 % H),(0.024973 % O), (0.097199 % N)O-0.000065
O2-6.046035
OH-0.000515
H2O-0.121179
N2-28.290916
NO-0.040780
NO2-0.000196
CO2-0.240490
dx=0.020000 T=1450.820068 Q=0.000000,dT=5.920729,dT_SUM_Q=0.000000,dT_SUM_T=13.268563
Без лет.=(0.001297 % C),(0.000030 % H),(0.026679 % O), (0.103891 % N)Ent=1206.345093,Ent_Let=18.495270,TFRAC=3
With let=(0.001897 % C),(0.000231 % H),(0.027268 % O), (0.103891 % N)O-0.003605
O2-4.693995
H-0.000075
H2-0.000283
OH-0.018133
HO2-0.000027
H2O-0.850358
N2-27.745236
NO-0.157856
NO2-0.000267
CO-0.001659
CO2-1.183301
dx=0.020000 T=1654.825562 Q=60.419233,dT=26.775033,dT_SUM_Q=82.380602,dT_SUM_T=49.775867
Без лет.=(0.003060 % C),(0.000231 % H),(0.029031 % O), (0.110807 % N)Ent=1659.127319,Ent_Let=85.923553,TFRAC=4
With let=(0.004100 % C),(0.000397 % H),(0.029909 % O), (0.110807 % N)O-0.177676
O2-3.146607
H-0.028208
H2-0.027158
OH-0.262277
HO2-0.000192
H2O-1.183743
N-0.000012
N2-26.963286
NO-0.551621
NO2-0.000315
N2O-0.000031
CO-0.297635
CO2-2.053081
dx=0.020000 T=2332.896729 Q=45.483333,dT=23.922615,dT_SUM_Q=184.042469,dT_SUM_T=103.246398
Без лет.=(0.005988 % C),(0.000397 % H),(0.031729 % O), (0.117945 % N)Ent=1665.916626,Ent_Let=148.774628,TFRAC=5
With let=(0.006496 % C),(0.000855 % H),(0.032721 % O), (0.117945 % N)O-0.352866
O2-1.817858
H-0.165130
H2-0.166971
OH-0.565201
HO2-0.000278
H2O-2.151902
N-0.000072
N2-26.354083
NO-0.580755
```

```
NO-0.580755
NO2-0.000204
N2O-0.000032
HNO-0.000017
CO-1.190257
CO2-2.232401
dx=0.020000 T=2613.709229 Q=34.275947,dT=16.955975,dT_SUM_Q=301.905375,dT_SUM_T=161.552016
Без лет.=(0.007587 % C),(0.000855 % H),(0.034598 % O), (0.125306 % N)Ent=2449.312500,Ent_Let=125.886765,TFRAC=6
With let=(0.007963 % C),(0.001278 % H),(0.035672 % O), (0.125306 % N)O-0.779974
O2-1.422655
H-0.658815
H2-0.514052
OH-0.994092
HO2-0.000381
H2O-2.383813
N-0.000390
N2-25.928311
NO-0.699339
NO2-0.000177
N2O-0.000037
NH-0.000048
HNO-0.000037
CO-2.395094
CO2-1.499745
dx=0.020000 T=2931.934326 Q=14.539987,dT=7.042891,dT_SUM_Q=369.997125,dT_SUM_T=194.534359
Без лет.=(0.008817 % C),(0.001278 % H),(0.037605 % O), (0.132890 % N)Ent=2046.922485,Ent_Let=75.062767,TFRAC=7
With let=(0.009102 % C),(0.001551 % H),(0.038336 % O), (0.132890 % N)O-0.522129
O2-1.131817
H-0.524354
H2-0.544490
OH-0.877001
HO2-0.000311
H2O-2.985038
N-0.000227
N2-25.800687
NO-0.562512
NO2-0.000135
N2O-0.000030
NH-0.000034
HNO-0.000030
CO-2.370266
CO2-1.796265
dx=0.020000 T=2870.198975 Q=11.817902,dT=4.856169,dT_SUM_Q=423.285719,dT_SUM_T=216.431500
Без лет.=(0.009781 % C),(0.001551 % H),(0.040327 % O), (0.140696 % N)Ent=1569.792969,Ent_Let=49.463043,TFRAC=8
With let=(0.010034 % C),(0.001738 % H),(0.040860 % O), (0.140696 % N)O-0.308819
O2-0.893701
H-0.340884
H2-0.477162
OH-0.689644
HO2-0.000229
H2O-3.467147
N-0.000106
N2-25.762184
NO-0.433196
NO2-0.000101
N2O-0.000023
NH-0.000018
HNO-0.000021
CO-2.119333
CO2-2.201824
dx=0.020000 T=2772.069580 Q=10.286373,dT=3.991514,dT_SUM_Q=465.680375,dT_SUM_T=232.882281
Без лет.=(0.010570 % C),(0.001738 % H),(0.042908 % O), (0.148726 % N)Ent=1101.042236,Ent_Let=28.102055,TFRAC=9
With let=(0.010776 % C),(0.001859 % H),(0.043269 % O), (0.148726 % N)O-0.162524
O2-0.687403
H-0.187866
H2-0.361570
OH-0.490448
HO2-0.000152
H2O-3.805923
N-0.000041
N2-25.785900
NO-0.317812
NO2-0.000072
```

N2O-0.000017
HNO-0.000013
CO-1.704681
CO2-2.679714
dx=0.020000 T=2656.818604 Q=9.214295,dT=3.087380,dT_SUM_Q=499.155875,dT_SUM_T=244.098719
Без лет.=(0.011189 % C),(0.001859 % H),(0.045374 % O), (0.156978 % N)Ent=669.716431,Ent_Let=18.273882,TFRAC=10
With let=(0.011353 % C),(0.001951 % H),(0.045644 % O), (0.156978 % N)O-0.076851
O2-0.512751
H-0.090303
H2-0.245286
OH-0.320654
HO2-0.000093
H2O-4.031524
N-0.000013
N2-25.840656
NO-0.222263
NO2-0.000050
N2O-0.000012
CO-1.219924
CO2-3.157581
dx=0.020000 T=2527.886719 Q=8.239184,dT=2.799680,dT_SUM_Q=524.904000,dT_SUM_T=252.847953
Без лет.=(0.011661 % C),(0.001951 % H),(0.047805 % O), (0.165453 % N)Ent=315.816559,Ent_Let=12.240371,TFRAC=11
With let=(0.011800 % C),(0.002022 % H),(0.048024 % O), (0.165453 % N)O-0.034900
O2-0.396923
H-0.039063
H2-0.149529
OH-0.200630
HO2-0.000056
H2O-4.143614
N2-25.906807
NO-0.154961
NO2-0.000035
CO-0.766993
CO2-3.555214
dx=0.020000 T=2398.126953 Q=7.216073,dT=2.760706,dT_SUM_Q=544.110188,dT_SUM_T=260.195812
Без лет.=(0.012038 % C),(0.002022 % H),(0.050242 % O), (0.174151 % N)Ent=41.937195,Ent_Let=10.444525,TFRAC=12
With let=(0.012130 % C),(0.002097 % H),(0.050428 % O), (0.174151 % N)O-0.016352
O2-0.348398
H-0.015583
H2-0.081890
OH-0.126030
HO2-0.000036
H2O-4.203461
N2-25.975601
NO-0.113642
NO2-0.000028
CO-0.415966
CO2-3.813029
dx=0.020000 T=2271.802490 Q=6.562328,dT=3.376892,dT_SUM_Q=558.977813,dT_SUM_T=267.846500
Без лет.=(0.012339 % C),(0.002097 % H),(0.052703 % O), (0.183071 % N)Ent=-148.925186,Ent_Let=8.414528,TFRAC=13
With let=(0.012439 % C),(0.002182 % H),(0.052928 % O), (0.183071 % N)O-0.008592
O2-0.362168
H-0.006192
H2-0.042121
OH-0.083800
HO2-0.000026
H2O-4.231953
N2-26.030022
NO-0.091567
NO2-0.000027
CO-0.205186
CO2-3.927108
dx=0.020000 T=2158.479492 Q=6.672137,dT=4.716860,dT_SUM_Q=572.027812,dT_SUM_T=277.072187
Без лет.=(0.012657 % C),(0.002182 % H),(0.055259 % O), (0.192215 % N)Ent=-277.244385,Ent_Let=7.439779,TFRAC=14
With let=(0.012764 % C),(0.002266 % H),(0.055487 % O), (0.192215 % N)O-0.005041
O2-0.419852
H-0.002577
H2-0.021492
OH-0.059049
HO2-0.000022

APPENDIX C

Act on the use of work results

ОТРАСЛЕВОЙ ЦЕНТР ПЛАЗМЕННО-ЭНЕРГЕТИЧЕСКИХ ТЕХНОЛОГИЙ
РАО «ЕЭС РОССИИ»

671160, Бурятия, г. Гусиноозерск
ул. Пушкина, 33, ОЦ ПЭТ

Сибирское ОВК, г. Улан-Удэ, р/с 40702810881360000052,
р/с 30101810100000000797, БИК 048142797, ИНН 0318001983,
ОКОНХ 95120, ОКПО 00118977, СОАТО 1181405000

Тел: 8(30145) 43-4-41, факс 8(30145) 42-6-49 E-mail: k-ura@mail.ru

« 10 » октября 2024 г.

№ 01-10-2024

АКТ

об использовании результатов диссертационной работы Орынбасар Мағжана Нұрланұлы «Энергетическая и экологическая эффективность плазменно-угольных горелок: численное моделирование и эксперимент», представленной на соискание степени доктора философии (PhD) по образовательной программе «8D07106 – Теплоэнергетика», научный руководитель – д.т.н., профессор Мессерле В.Е.

Настоящий Акт составлен о том, что выполненные в диссертационной работе Орынбасар М.Н. исследования по компьютерному моделированию и экспериментальному исследованию процессов плазменного воспламенения и стабилизации горения пылеугольного факела использованы при принятии технических решений для разработки плазменно-угольной горелки на котле ТПЕ-215 Гусиноозерской ГРЭС, г. Гусиноозерск, Республика Бурятия, Российская Федерация.

Генеральный Директор Отраслевого Центра

Плазменно-Энергетических Технологий РАО «ЕЭС России»

Доктор технических наук Ю.Е. Карпенко